

Dissertation

**Characterization of aminergic neurons
controlling behavioral persistence and
motivation in *Drosophila melanogaster***

Sercan Sayin

Zur Erlangung des akademischen Grades
Doktor der Naturwissenschaften
Dr. rer. nat.

Fakultät für Biologie
Ludwigs-Maximilians-Universität München

14/01/2019

Erstgutachter: Prof. Dr. Nicolas Gompel
Zweitgutachter: Prof. Dr. Hans Straka

Eingereicht am: 14/01/2019
Tag der mündlichen Prüfung: 16/05/2019

Diese Dissertation wurde unter der Leitung von Prof. Dr. Ilona Grunwald Kadow angefertigt.

KURZFASSUNG

Mangelzustände stehen im Widerspruch zum Überleben. Tiere nehmen daher enorme Risiken wie z.B. eine beschwerliche Futtersuche auf sich, um ihren Hunger zu stillen. Eine erfolgreiche Futtersuche erfordert zudem die unaufhörliche Integration von externer sensorischer Information und internen Stoffwechselmonitoren. Es überrascht nicht, dass solche zentralen Bedürfnisse zu starken Verhaltensimpulsen führen. Ungeprüft kann Impulsivität jedoch nachteilig sein und Tiere daran hindern, andere wertvolle Möglichkeiten zu nutzen oder ihre Energie zu konservieren.

Grundsätzlich wurde Motivation als derjenige Mechanismus vorgeschlagen, mittels dessen einer Reaktion auf einen starken Impuls entweder nachgegeben oder sie abgelehnt wird. So entpuppt sich die Motivation als kritische Determinante für die beobachtete Verhaltensvariabilität der Tiere zu einem bestimmten Zeitpunkt. Obwohl Pläne neuronaler Schaltkreise trügerisch statisch sein können, kann Neuromodulation Verhaltensvariabilität im Nervensystem realisieren. Bioamine wie Dopamin und Noradrenalin wirken modulierend auf intrinsische Motivationsschaltkreise, die Ernährung und Belohnung steuern. Über alle Modellorganismen hinweg ist jedoch nach wie vor sowohl auf der molekularen als auch auf Schaltkreisebene unklar, wie Tiere die Entscheidungsfindung auf Grundlage ihrer aktuellen Motivation und ihrer inneren Zustände integrieren und aktualisieren. Aufgrund des umfangreichen methodischen Werkzeugkastens und des leicht zugänglichen, übersichtlichen Nervensystems bietet sich *Drosophila melanogaster* als Modellorganismus an, unsere gegenwärtige Sichtweise auf diese Konzepte zu erweitern.

Für *Drosophila melanogaster* sind bestimmte Gerüche wichtige Signale für die Futtersuche über lange Strecken. Um zu erforschen, wie hungrige Fliegen zielgerichtete Entscheidungen treffen, habe ich ein neuartiges kugelförmiges Laufband-Paradigma entwickelt. Durch den Einsatz von hochauflösenden Verhaltensanalysen und die genaue Kontrolle der ansonsten stark wirbelnden

Geruchsabgabe fand ich heraus, dass Fliegen unter Nahrungsentzug Essigduft auch bei wiederholter Abwesenheit einer Belohnung dauerhaft verfolgen. Die Kombination dieses Verhaltensparadigmas mit unmittelbaren neuronalen Manipulationen zeigte, dass diese angeborene Hartnäckigkeit Schaltkreise rekrutierte, die traditionell in einer vom inneren Zustand abhängigen Weise mit Lernen und Gedächtnis in Verbindung gebracht werden. Dopaminerge Neurone des TH+ Clusters, Operatoren des Strafenlernens und *DopR2*-Signale ermöglichten diese olfaktorische Hartnäckigkeit. Diesen dopaminergen Neuronen nachgeschaltet war MVP2, ein einzelnes Pilzkörper-Ausgangsneuron, entscheidend für die Hartnäckigkeit. MVP2 war notwendig und ausreichend, um den Hungerzustand als zugrundeliegenden Antrieb für die Hartnäckigkeit bei der Nahrungssuche zu integrieren.

Außerdem habe ich untersucht, wie diesem starken Impuls entgegengewirkt wird, wenn eine Fliege ihr Ziel, das nahrhafte Futter, erreicht. Ein Wechsel von der Verfolgung des Geruchs zum Verzehr der Nahrung erfordert die Koordination verschiedener sensorischer Systeme und motorischer Steuerungseinheiten. Bei derartigen globalen Umstellungen wie z.B. Kampf-oder-Flucht-Übergängen wird Noradrenalin eingesetzt. Mit optogenetischer Manipulation zeigte ich, dass der Antrieb zur Nahrungsmittelsuche durch ein Insekten-Norepinephrin-Analogon, einen oktopaminergen Input, über VPM4-Neurone unterdrückt wurde. VPM4-Neurone, die synaptisch mit MVP2 verbunden sind, was wir durch hochauflösenden Tracingtechniken und einen Fütterungsersatz auf neuronaler Ebene gezeigt haben, fungierten als Bremse der beharrlichen Verfolgung des Geruchs, um fütterungsähnliches Verhalten zu ermöglichen.

Als Ergebnis aus der Entwicklung neuartiger Paradigmen, thermo- und optogenetischer neuronaler Manipulationen und Connectomics stellt diese Arbeit einen neuronalen Mikroschaltkreis vor, der die Veränderungen des Verhaltens von der Verfolgung des Geruchs bis zur Unterdrückung des Geruchs während der Nahrungsaufnahme genau zusammenfasst. Spezifische Untergruppen dopaminerger und oktopaminerger Neurone gelten als Vermittler motivationsgesteuerter Ereignisse. Meine Ergebnisse liefern neue mechanistische Erkenntnisse darüber, wie multimodale Integration im Gehirn stattfinden kann, wie

solche Systeme zu den inneren Zuständen stehen und bieten mehrere plausible Erklärungen, wie Hartnäckigkeit entsteht. Schließlich könnte diese Arbeit als Vorlage dienen, um die Rollen und die funktionelle Vielfalt der aminergen Neuronen von Säugetieren besser verstehen zu können.

ABSTRACT

Deprivation is at odds with survival. To obliterate their condition of hunger animals engage in costly foraging behavior. This conundrum demands unceasing integration of external sensory processing and internal metabolic monitors. Unsurprisingly, such critical behaviors are translated to strong impulses. If unchecked, however, impulsivity can trap animals in unfavorable behavioral states and prevent them from exploiting other valuable opportunities.

Categorically, motivational mechanisms have been proposed as the conduit to comply with or decline a response to a strong impulse. Thus, motivation emerges as a critical determinant for observed animal behavioral variability at a given time. Although neuronal circuit diagrams may be deceptively static, neuromodulation can implement behavioral variability in the nervous systems. Bioamines, such as dopamine and norepinephrine, mediate modulatory impact on intrinsic motivational circuits that govern feeding and reward. Across model organisms, however, how animals integrate and update decision-making based on the current motivational and internal states are still poorly understood at the molecular and circuitry levels. Due to its extensive toolbox and amenable miniature nervous systems, *Drosophila melanogaster* is poised to enrich the current perspective for these concepts.

For *Drosophila melanogaster*, certain odors are salient cues for long distance foraging events. To explore how starved flies make goal-directed decisions, I developed a novel spherical treadmill paradigm. Through the utilization of high-resolution behavioral analyses and tight control of, otherwise highly turbulent, odor delivery, I found that food-deprived flies tracked vinegar persistently even in the repeated absence of a food reward. Combining this behavioral paradigm with immediate neuronal manipulations revealed that this innate persistence recruited circuits that are traditionally linked with learning and memory in an internal state-dependent manner. TH⁺ cluster dopaminergic neurons, operators of punishment learning, and *Dop1R2* signaling enabled this olfactory-driven persistence. Downstream of these dopaminergic neurons, a single mushroom body

output neuron, MVP2 was crucial for persistence. MVP2 was necessary and sufficient to integrate hunger state as the underlying motivational drive for food-seeking persistence.

Furthermore, I investigated how this strong impulse is counteracted when a fly reaches its goal, nutritious food. A change from odor tracking to food consumption demands the coordination of different sensory systems and motor control subunits. Norepinephrine is implemented in such global switches; such as fight or flight transitions. Using optogenetic manipulation, I demonstrated that the food-seeking drive was suppressed by, an insect norepinephrine analog, octopaminergic input, via VPM4 neurons. Being connected to MVP2 synaptically, which we showed using high-resolution tracing techniques, and a surrogate for feeding at the neuronal level, VPM4 neurons acted as the inhibitory brake on persistent odor tracking to allow feeding related behavior.

As a culmination of novel paradigm development, thermo/optogenetic neuronal manipulations and connectomics, this work presents a neuronal microcircuit that recapitulates the alterations of animal behavior faithfully from odor tracking to olfactory suppression during feeding. Specific subsets of dopaminergic and octopaminergic neurons are found to be mediators of motivationally driven events. My findings provide fresh mechanistic insights on how multimodal integration can occur in the brain, how such systems are prone to the internal states, and offers several plausible explanations on how persistence emerges. Finally, this work might serve as a template to better understand the roles and the functional diversity of mammalian aminergic neurons.

CONTRIBUTIONS & PUBLICATIONS

The results from the doctoral thesis are presented in the biology preprint server bioRxiv (February 2018). The manuscript is currently under revision for a peer-reviewed journal submission.

A neural circuit arbitrates between perseverance and withdrawal in hungry *Drosophila*

Sercan Sayin, Jean-Francois De Backer, Marina E Wosniack, Laurence Lewis, K.P. Siju, Lisa-Marie Frisch, Philipp Schlegel, A. Edmondson-Stait, N. Sharifi, C.B. Fisher, S. Calle-Schuler, Scott Lauritzen, Davi Bock, Marta Costa, Gregory S.X.E. Jefferis, Julijana Gjorgjieva, Ilona Grunwald Kadow
bioRxiv 259119; doi.org/10.1101/259119

Contributions:

Conceptualization by **SS**, IGK. **SS** designed the spherical treadmill, performed and analyzed the behavioral experiments. LMF collected and analyzed the 4-arm arena data. JFDB and KPS conducted the imaging and electrophysiological work. Anja Friedrich carried out immunohistochemistry. EM data acquisition and analyses were executed by PS, AES, CBNF, SCS, SL, DB, MC, and GSXEJ.

Further publications produced:

Internal state dependent odor processing and perception — The role of neuromodulation in the Fly olfactory system

Sercan Sayin[†], Ariane C. Boehm[†], Johanna M. Kobler[†], Jean-François De Backer and Ilona C. Grunwald Kadow

Front. Cell. Neurosci., 30 January 2018, doi.org/10.3389/fncel.2018.00011

[†] Equal Contribution

ACKNOWLEDGMENTS

I would like express my deepest gratitude to my supervisor Ilona Grunwald Kadow for the opportunity of taking on a project as ambitious as my aspirations. Without her patience and continued support, this project would have never seen the finish line.

I am grateful to Nicolas Gompel and Hans Straka for the time dedicated and the valuable feedback on this thesis. I would also like to thank the other thesis defense members Herwig Baier and Peter Geigenberger. I am glad for the comments of my thesis advisory committee during the earlier phases of my PhD: Björn Brembs, Andreas Herz and Alexander Borst. I would like to also thank Julijana Gjorgjieva for the fruitful conversations and collaboration we had. Gregory Jefferis and Davi Bock also deserve recognition for their data contributions to this dissertation.

I would like to thank all the principal investigators of the Marie Curie Initial Training Program “FLiACT”. Their efforts culminated into this unique experience that gave me the chance to participate in several exciting workshops and meetings over Europe, the USA, and Africa. Especially Matthieu Louis deserves a special mention as the spearhead of FLiACT, for his persistent dedication and motivation. Furthermore, I wish to thank Silke Sachse and Vivek Jayaraman for granting me the possibility to visit their labs to learn new techniques.

During my long track in the lab, I had the pleasure of meeting and working with excellent colleagues, good friends, delightful companions and partners in crime. I thank you all! Although each of you deserves more than a simple mention, shamefully, I pooled your names here in alphabetical order. I hope you will forgive my insolence: Ariane Boehm, Jean-Francois De Backer, Ugur Dag, Ajinkya Deogade, Valentina Ferlito, Elie Fink, Anja Friedrich, Ashiq Hussain, Martianthi Karageorgi, Johanna Kobler, Ivan Larderet, Laurence Lewis, Ahmed Mohamed, Siju Kunhi Purayil, Sayanne Soselisa, Vladimiro Thoma, Daniel Turner-Evans, Samuel J. Walker, Marina Elaine Wosniack. Nothing breaks the monotony of daily

life in abroad, but few words spoken in mother-tongue. Teşekkürler: Hakan Kucukdereli, Habibe Ucpunar, Inci Temizer, Tugce Yildizoglu. Last but not least, Ibrahim Tastekin for 15 years spent side by side on benches and desks!

I am thankful to Armin Bahl, Stephan Prech, Tabea Schilling, the crew of fine-mechanic and electronic Werkstatt at the Max Planck Institute of Neurobiology for sharing resources with me during the early phases of the treadmill.

I also appreciate the work put by Lasse Bräcker and Jörg Henninger into the treadmill prototype. Just let me remind them to check their codes better next time!

CONTENTS

1	INTRODUCTION	1
1.1	Motivation	1
1.2	Olfaction: Smells like Food	2
1.2.1	Olfactory Maps in Fly Brain	3
1.2.2	Olfactory Tracking.....	5
1.3	Mushroom Bodies: Center of Learning, and More	5
1.3.1	Mushroom Body Anatomy	6
1.3.2	Role of Mushroom Bodies in Associative Learning.....	6
1.3.3	Mushroom Bodies Modulates Innate Behaviors	8
1.4	Hunger Governs Olfaction	9
1.4.1	Modulation at Periphery.....	9
1.4.2	Central Modulation by Starvation	10
1.5	Drosophila Gustatory System.....	12
1.5.1	Gr43a as an Internal Sensor	12
1.5.2	Subesophageal Zone: CNS Taste Relay	13
1.5.3	Gustation as a Sequence	14
1.6	Octopamine: A Bridge Between Action and Expenditure.....	14
1.6.1	Octopaminergic Neurons in SEZ.....	16
1.7	Drosophila, A Systems Neuroscience Model	17
2	THESIS OBJECTIVES	21
3	MATERIAL AND METHODS.....	22
3.1	Fly Husbandry and Fly Lines Used in the Study	22
3.2	Spherical Treadmill Setup and Analyses.....	22
3.2.1	Olfactory Delivery	22
3.2.2	Treadmill and Data Acquisition	23
3.2.3	Preparation for Behavioral Experiments on the Treadmill.....	24
3.2.4	Data Analyses of the Treadmill and Statistics	25
3.3	Behavioral Arena	26
3.4	T-Maze.....	26
3.5	Immunohistochemistry.....	27
3.6	Calcium Imaging.....	27
3.7	Connectomics	28

4	RESULTS	29
4.1	Repeated Food Odor Exposure Underlies Persistent Tracking	29
4.1.1	Wild-type <i>Drosophila</i> Responses to Vinegar.....	29
4.1.2	Flies do not track CO ₂	31
4.1.3	Vinegar Tracking is Olfaction Dependent.....	32
4.1.4	Characterization of Persistence	34
4.2	Starvation Drives Odor-Guided Locomotion.....	36
4.3	Dopaminergic Input is Required for Persistence	40
4.4	Mushroom Body Output is Crucial for Innate Odor Attraction	44
4.5	Octopamine Underlies Transition from Olfaction to Exploitation.....	49
4.5.1	Activation of Taste Neurons Counteracts Olfaction	49
4.5.2	Octopaminergic Neurons Control the Transition	52
4.5.3	Octopaminergic Neurons are Modulators of Odor Responses	58
4.5.4	Octopamine and NPF as Possible Partners.....	60
4.6	Specific OANs Suppress Olfaction.....	63
4.6.1	Characterization of VPM3 and VPM4 neurons	63
4.6.2	VPMs Phenocopy Tdc2 Activation	64
4.6.3	VPMs are not Necessary for Olfaction	68
4.6.4	Manipulations of other OA+ SEZ neurons	69
4.6.5	MVP2 and VPMs are connected	70
4.6.5	VPMs mediated suppression of MVP2.....	73
5	DISCUSSION	76
5.1	Flies Engage with Vinegar Persistently	77
5.2	Flies Avoid Repellent Odors on the Treadmill.....	78
5.3	The Mushroom Body Processes Innate Olfactory Attraction	79
5.4	Persistence is not a By-Product.	80
5.5	Persistence Generators.....	81
5.6	MB Dependent Mechanistic Descriptions of Persistence.....	83
5.7	Sequence Transitions are Flexible	84
5.8	VPMs Exert Control on Behavioral Transitions	85
5.9	Mechanisms of OAN Mediated Inhibition of MVP2 activity	86
5.10	VPM Post-Synaptic Targets are Diverse.....	87
5.11	VPM4 Might Receive Tarsal Input.....	88
5.12	VPMs Do Not Regulate Olfactory Learning.....	89
5.13	Broad Manipulations of Tdc2+ OANs Have Opposite Effects.....	89
5.14	OAN Diversity in SEZ	90
5.15	Possible Tdc2 and NPF Signaling Convergence	91

6	CONCLUSIONS AND FUTURE DIRECTIONS	92
7	REFERENCES	94
8	APPENDIX	110

LIST OF FIGURES

Figure 1 The Fly Olfactory Map	4
Figure 2 Mushroom Body Architecture	7
Figure 3 Summary of Starvation Induced Changes in Olfaction	11
Figure 4 Gal4-UAS system	18
Figure 5 Spherical Treadmill Schematic and Odor Delivery Dynamics	29
Figure 6 Odor tracking at room temperature for starved wild-type CS	30
Figure 7 Odor tracking at 30°C for starved wild-type CS	30
Figure 8 Odor tracking for 60 sec long vinegar simulation of starved wild-type CS	31
Figure 9 Carbon dioxide aversion of starved wild-type CS on the spherical treadmill	32
Figure 10 Olfactory input dependency of odor tracking on the treadmill	33
Figure 11 Repeated appetitive odor exposure driven persistence	34
Figure 12 Running activity over repeated vinegar exposures for starved wild-type CS flies	35
Figure 13 Running bout times over repeated vinegar exposures for starved wild-type CS flies	36
Figure 14 Effects of starvation on persistent odor tracking of wild-type CS flies	37
Figure 15 Closed-loop assay for vinegar odor tracking on the treadmill for wild-type CS flies	38
Figure 16 Calcium Imaging in projection neurons under repeated odor exposure	39
Figure 17 Requirement of TH+ dopaminergic input in forward running during persistence	41
Figure 18 Turning bias in manipulation of TH+ dopaminergic input on the treadmill	42
Figure 19 Running performance in the absence of dopaminergic input at 35°C	42
Figure 20 Vinegar response of <i>Dop1R1</i> mutants	43
Figure 21 Vinegar response of <i>Dop1R2</i> mutants	44
Figure 22 Mushroom body output neuron necessity screen for vinegar attraction in T-maze	45
Figure 23 Thermogenetic block of MB γ Kenyon cell and MVP2 synaptic output in starved flies ..	46
Figure 24 Optogenetic activation of MVP2 neurons activity while odor tracking in fed flies	47
Figure 25 Optogenetic activation of MVP2 neurons activity while odor tracking in starved flies ..	48
Figure 26 Optogenetic only activation of MVP2 neurons	48
Figure 27 Chronic activation of MVP2 neurons activity during vinegar exposure in fed flies	49
Figure 28 Optogenetic activation of gustatory receptors during vinegar approach	50
Figure 29 Calcium imaging of Gr43a neurons in SEZ <i>ex vivo</i>	51
Figure 30 Acute activation of Tdc2+ octopaminergic neurons in vinegar tracking of starved flies ..	53
Figure 31 Chronic activation of Tdc2+ neurons in vinegar tracking of starved flies	54
Figure 32 Chronic activation of Tdc2+ neurons in vinegar tracking of fed flies	55
Figure 33 Chronic activation of Tdc2+ neurons in lower concentration tracking of starved flies ..	55
Figure 34 Chronic activation of Tdc2+ neurons during air stimulation of starved flies	56
Figure 35 Optogenetic activation of Tdc2+ neurons in the arena assay	56
Figure 36 Calcium imaging of Tdc2 neurons in SEZ <i>in vivo</i>	57

Figure 37 Tyramine β hydroxylase mutants during persistent odor tracking	58
Figure 38 Blocking synaptic release from Tdc2+ neurons in vinegar approach	59
Figure 39 Knockdown of <i>sNPF-R</i> and <i>NPF-R</i> receptors in Tdc2+ neurons during persistence	61
Figure 40 Blocking synaptic output from <i>NPF</i> neurons in vinegar tracking in starved flies	62
Figure 41 Artificial activation of <i>NPF</i> neurons during vinegar tracking	62
Figure 42 Morphological immunohistochemistry analyses of VPM neurons.....	63
Figure 43 Octopamine and tyramine stainings of VPM4 neuron.....	64
Figure 44 Acute activation of OA+ MB split-Gal4 lines	65
Figure 45 CsChrimson expressing OA+ MB split-Gal4 flies in vinegar only approach	66
Figure 46 Chronic activation of VPM3 and VPM4 neurons in starved flies.....	67
Figure 47 Chronic activation of only VPM4	67
Figure 48 Blocking VPM activity in starved and fed flies.....	68
Figure 49 Acute and chronic activation of OA+ VUMa2 for starved flies	69
Figure 50 Blocking VUMa2 output during vinegar approach.....	70
Figure 51 Double-labeling of VPM4 and MVP2 neurons	71
Figure 52 Connectome analyses of VPM and MVP2 neurons in MB peduncle.....	72
Figure 53 Functional connectivity between MVP2 and VPM4 in vivo	73
Figure 54 Epistasis analysis of MB112C and MB113C activation in fed flies	74
Figure 55 Epistasis analysis of MB112C and MB113C activation in starved flies	74
Figure 56 Summary	93
Figure 57 Common starved Gal4 controls used in the study	112
Figure 58 Unilateral odor presentation for wild-type flies	112

LIST OF TABLES

Table 1 Fly Lines 110

Table 2 List of antibodies..... 111

ABBREVIATIONS

olfactory sensory neuron	OSN
activation domain	AD
antennal lobe	AL
antennal mechanosensory and motor center	AMMC
DNA-binding domain	DBD
dopamine	DOPA
dopaminergic neuron	DAN
gustatory receptor	GR
ionotropic receptor	IR
Kenyon cell	KC
lateral horn	LH
local neuron	LN
pedunculus-medial lobe and vertical lobe arborizing neuron 2	MVP2
mushroom body	MB
mushroom body output neuron	MBON
octopamine	OA
octopaminergic neuron	OAN
odor receptor	OR
olfactory co-receptor	ORCO
projection neuron	PN
protocerebral anterior medial	PAM
protocerebral posterior lateral 1	PPL1
subesophageal zone	SEZ
ventral nerve chord	VNC
ventral paired median neuron	VPM

1 INTRODUCTION

1.1 Motivation

Most animal bodies are comprised of a similar, elementary architecture. Sensory organs, motor units, digestive tracks are housed into a unified organization. Such systems are, however, not self-sufficient. To fulfill the most basic functions of life, survival, and reproduction, most animals unceasingly interact with their environment to incorporate nutrients or seek partners. However, they are not simply reactionary machines. Salient objects, goals, and needs can be present at any given time; an animal can choose to act upon an option or decline. Motivation has been offered as an umbrella term aimed at providing causality for this behavioral contingency (Berridge, 2004).

This definition posits motivation as a behavioral threshold. One of the earliest mechanisms offered to explain how motivational systems work is the psychohydraulic model. As an animal's need grows over time, the pressure to execute a relevant set of behaviors accumulates. When the critical level is reached, a behavior is executed to release this pressure. When the strength of external stimuli is more potent, behavioral thresholds could be lower (Lorenz and Leyhausen, 1973). Decades-long research in behavior supplemented or refuted the linear psychohydraulic model, via expanding it with feed-forward, feedback mechanisms (Mason and Bateson, 2009).

One of the central functions of motivational mechanisms is to maintain homeostasis. Lack of food or water results in motivational drives to ameliorate this lack. Such drives might function as an error signal from an ideal physiological reference point. Also, likely, motivation can emerge from a 'settling point of counteracting mechanisms (competition of hunger and satiety signals) that promote or oppose a particular behavior. Regardless, motivational drives command several motor programs. For example, hunger can be manifested in exploration or lowered acceptance of less desirable foods (Berridge, 2004). In theory, motivational drives

would be able also to organize the hierarchy of behaviors that are promoted by them.

Unraveling neuronal correlates of motivation is an ongoing effort. In the case of hunger, decades of work in humans and other mammals revealed a distributed network spanning several regions in the brain, centered around the mesocorticolimbic system (Ferrario et al., 2016). The ventral tegmental area and the nigrostriatal pathway are sources of the neurotransmitter dopamine, which is thought to be essential for motivation (Ferrario et al., 2016; Ikemoto et al., 2015).

1.2 Olfaction: Smells like Food

Odors are long-distance messengers. These airborne cues could mediate various signals. For a hungry animal, certain odors would convey an eventual encounter with its goal, the food. As a highlight to the significance of olfaction, hunter-gather human societies expanded capabilities in odor recognition (Majid and Kruspe, 2018).

Motivation and homeostasis are intertwined concepts. Hunger as a motivational drive is expected to shape olfaction. To study the neurobiology of olfaction and motivation, the reduced complexity of *Drosophila melanogaster* nervous system offers a numerical advantage. Before venturing forth to ask questions on mechanisms of motivation, first, one has to incorporate two concepts: the challenges of fly navigation and the neuronal circuitry of *Drosophila*.

In the desert, *Drosophila melanogaster* could travel over immense distances to find food sources (Coyne et al., 1987). Surrounded by this hospitable environment, these flies highly possibly relied on odor cues during foraging. However, olfaction, as a sensory guide, is tricky. To reach the oasis too far, flies should overcome several obstacles: the chaotic nature of air plumes that carry olfactory cues, the complexity of the olfactory space, habituation-prone noisy olfactory circuitry.

1.2.1 Olfactory Maps in Fly Brain

Olfactory sensory neurons (OSNs) reside in the fly olfactory organs, a pair of antennae and maxillary palps. OSNs are comprised of three types of receptor classes: OR (odor receptor), IR (ionotropic receptor), and GR (gustatory receptor). OR and IR receptor families form the major basis of olfactory input, they constitute more than hundred receptors for flies (Benton et al., 2009; Clyne et al., 1999; Vosshall et al., 1999). In addition to these, two odd gustatory receptors were found to facilitate olfactory responses (Jones et al., 2007). Olfactory receptor function depends on the presence of co-receptors; for example, the absence of the universal fly OR co-receptor ORCO renders flies almost smell-blind (Larsson et al., 2004). With the exception of few, most OSNs harbor a single olfactory receptor in addition to their co-receptor(s) (Goldman et al., 2005; Vosshall et al., 2000). With this limited receptor library, fly brains have to decode and encode a vast chemical space. Despite the fact that specific mode of recognition is not yet unraveled fully (Block et al., 2015; Turin, 1996), it is not surprising that olfactory coding is combinatorial in an odor concentration-dependent manner (Hallem and Carlson, 2006; Wang et al., 2003). High concentration of appetitive odors can recruit 'aversive' channels (Semmelhack and Wang, 2009). Some chemical compounds can suppress OSN activity in an antagonistic manner (Turner and Ray, 2009). Furthermore, OSNs are housed in several morphologically distinct sensilla, in which OSNs can suppress each other's activity (Su et al., 2012).

From the receptors, in a simplified scheme, olfactory information flows in one direction towards the protocerebrum (Figure 1) (Galizia, 2014). Firstly, OSNs that express the same receptor project to the antennal lobe (AL) and form a unit called glomerulus (Fishilevich and Vosshall, 2005; Vosshall et al., 2000). AL is the relay point where olfactory information is processed mostly through the actions of local neurons (LNs). In addition to some excitatory neurons, most LNs are inhibitory and release GABA (Olsen et al., 2010; Shang et al., 2007; Yaksi and Wilson, 2010). While LNs have different innervation patterns in AL, global LNs mediate uniform inhibition throughout AL (Hong and Wilson, 2015). This inhibition scales with olfactory input to prevent saturation of the efferent neurons (called projection

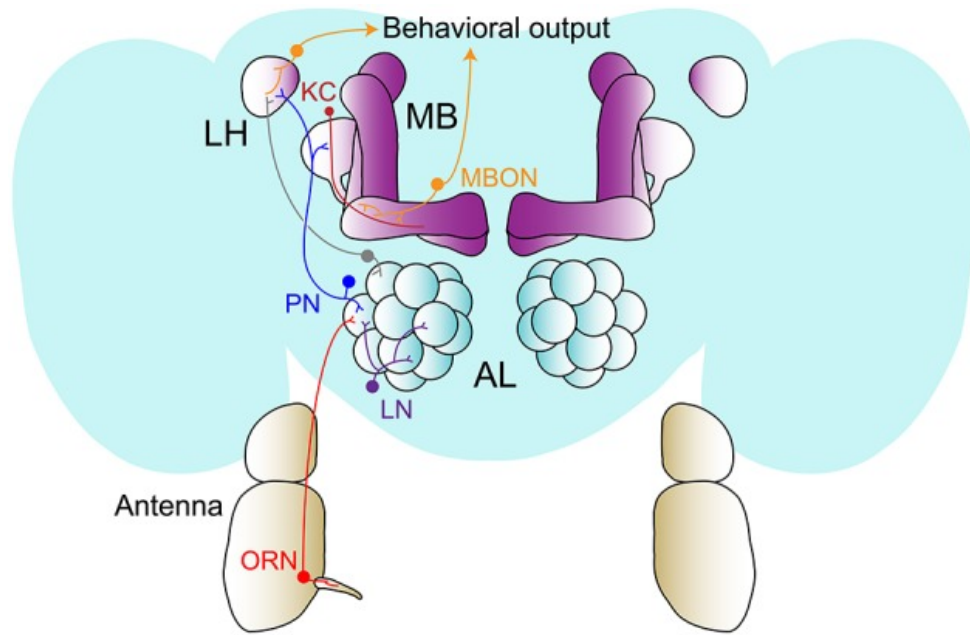


Figure 1 The Fly Olfactory Map

Olfactory sensory neurons (OSNs), distributed across several sensilla in antennae and maxillary palp, collect the odor input in the environment. This information is then relayed to antennal lobe (AL) for processing. Then olfactory pathway diverges into two centers in the higher brain lateral horn (LH) and the mushroom body (MB) (Image from Sayin et al., 2018).

neurons - PNs), the so-called “divisive normalization” (Olsen et al., 2010). PNs can talk to a single or multiple glomerular channels (Liang et al., 2013; Stocker et al., 1990). While inhibitory PNs enhance odor decoding to feed-forward olfactory signal, excitatory cholinergic PNs innervate lateral horn (LH) and mushroom body (MB) (Liang et al., 2013; Marin et al., 2002; Parnas et al., 2013; Wong et al., 2002).

Traditionally, MB is the associative learning center (Heisenberg, 2003). Since earlier MB chemical ablation experiments did not alter innate olfactory choice, LH alone was long considered to carry out innate olfaction (de Belle and Heisenberg, 1994). Newer work, however, showed that the MB is important for context- and state-dependent olfactory behavior (Grunwald Kadow, 2019). The exact role of the LH is therefore not fully understood. Very recent experiments show that PNs show stereotyped odor responses and tailor the LH into domains that segregate according to categories (Frechter et al., 2018; Jeanne et al., 2018; Jefferis et al., 2007; Strutz et al., 2014).

1.2.2 Olfactory Tracking

During flight, simple motor reflexes and bilateral olfactory input are sufficient to maintain plume tracking (van Breugel and Dickinson, 2014; Duistermars et al., 2009). Walking adult *Drosophila melanogaster* also relies on bilateral olfactory input (Borst and Heisenberg, 1982). Concentration differences between the two antennae result in neurotransmitter release disparities (Gaudry et al., 2012; Rodrigues, 1988). However, during walking, odor concentrations are expected to vary less close to the source. This invariance might be problematic for prolonged odor searches due to olfactory habituation. In this regard, olfactory behavior of walking *Drosophila melanogaster* is less explored, in comparison to “in flight”. OSNs and PNs fire less under sustained odor exposure and better suited to monitor fast changes in odor concentration (de Bruyne et al., 1999; Kazama and Wilson, 2008; Schulze et al., 2015). OSNs can resolve plume frequencies at 10 Hz, or even higher frequency fluctuations (Nagel and Wilson, 2011; Szyszka et al., 2014). In addition, effects of immediate and developmental habituation have been reported and attributed mostly to LN activity at antennal lobe (Cho et al., 2004; Das et al., 2011; Sachse et al., 2007; Twick et al., 2014). Regardless, walking flies were able to respond to unilateral odor application for extended periods, although this experiment did not document the exact dynamics of this behavior (Borst and Heisenberg, 1982). Furthermore, previous exposure to a specific odor shapes further responses to subsequent odors, suggesting a working memory or arousal component in olfactory decision making (Badel et al., 2016). How adaptation alters olfactory information in the higher olfactory circuits and how this information is transformed into motor behavior need further examination. For example, LNs are heterogeneous in their temporal dynamics, which might help to perceive prolonged odor exposure (Nagel and Wilson, 2016).

1.3 Mushroom Bodies: Center of Learning, and More

The Mushroom body (MB) is a highly compartmentalized neuropil in the fly protocerebrum. MB is one of the two recipients of secondary level neurons, PNs, in the olfactory hierarchy. MB harbors intrinsic input neurons called Kenyon cells

(KCs) and output neurons (MBONs). The distinctiveness of MB anatomy and PN to KCs connections present MB as a significant center of association in the fly brain. Furthermore, MB receives substantial neuromodulatory input.

1.3.1 Mushroom Body Anatomy

Of the ~2000 Kenyon cells, each receives very few, randomized synaptic inputs from PNs in the dendritic claws of MB input region, calyx (Butcher et al., 2012; Caron et al., 2013). KC are excitatory cholinergic neurons, and their axons constitute the MB lobes (α/β , α'/β' , γ) (Barnstedt et al., 2016; Crittenden et al.; Gu and O'Dowd, 2006). These MB lobes are partitioned by efferent 34 MBONs (with 21 distinct subtypes) and 20 dopaminergic neurons (DANs) (Aso et al., 2014a; Tanaka et al., 2008). Kenyon cells exhibit sparse activity under olfactory input and require combinatorial PN input, yet 25 KCs were found to be sufficient to carry odor discrimination (Campbell et al., 2013; Gruntman and Turner, 2013; Honegger et al., 2011; Ito et al., 2008). Without KC activity, dependent on *FoxP* expression, flies took longer to differentiate odor pairs (DasGupta et al., 2014; Groschner et al., 2018). This sparse coding strategy aided by GABAergic anterior paired lateral (APL) neuron. APL forms an inhibitory feedback loop with KCs. Strong global increases in KC population activity is counter-balanced by APL (Lin et al., 2014a). The numerical compression in neuronal numbers manifest in MBON responses to odors; in comparison to KCs, MBON responses are highly correlated. For a particular odor, the divergence and convergence of olfactory information are thought to enable unique combinations of representations at the level of the synapses between KCs and MBONs (Galizia, 2014).

1.3.2 Role of Mushroom Bodies in Associative Learning

KC-MBON synapses are, indeed, the loci of associative learning. In associative learning, KC-MBON synapses in the relevant compartment are dampened in a sustained manner due to the dopaminergic activity of DANs, promoted by dopamine receptor *Dop1R1* and extinguished by *Dop1R2* (Berry et al., 2012; Hige et al., 2015a; Kim et al., 2007). In an artificial activation paradigm, the activity of MBONs biased fly behavior towards either attraction or aversion,

indicating MBONs fall into broadly two categories that influence valence (Aso et al., 2014b). Surprisingly, these two categories map onto distinct lobes of MB: Attraction driving MBONs reside in vertical lobes, whereas aversion promoting MBONs can be found in horizontal lobes (Figure 2) (Aso et al., 2014b, 2014a). Concerning valence, DAN innervation pattern is complementary and opposite to MBON topography (Aso et al., 2014a). Protocerebral posterior lateral 1 (PPL1) sub-cluster of DANs, also labeled by TH-Gal4, has been implicated in aversive learning and target lobes with appetitive MBONs (Aso et al., 2014a; Claridge-Chang et al., 2009; Riemensperger et al., 2005). On the other hand, protocerebral anterior medial (PAM) sub-cluster were shown to be responsible for instructing appetitive learning through aversive MBONs (Burke et al., 2012; Liu et al., 2012). Moreover, during learning MBON activity can be altered a bidirectional manner (Bouzaiane et al., 2015; Oswald et al., 2015). While neuronal mechanisms for the enhancement is lacking, recent larval and partial adult MB connectomes exposed that DAN can bypass KCs and directly synapse onto MBON in their respective compartment (Eichler et al., 2017; Takemura et al., 2017). Interestingly, under pharmacological

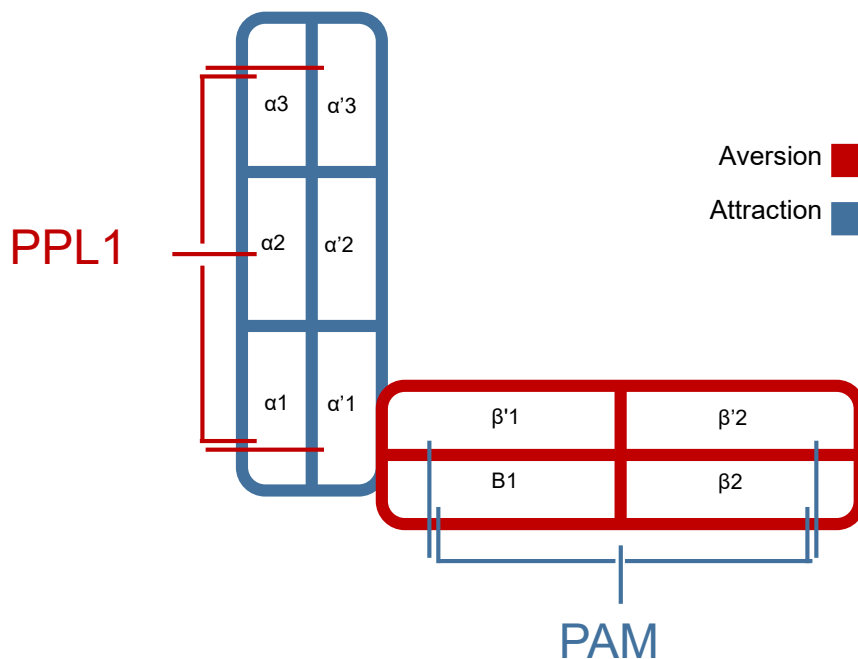


Figure 2 Mushroom Body Architecture

MB compartments are roughly divided into two groups. Vertical lobes bias animal behavior towards attraction and receives negatively reinforcing dopamine input. Horizontal lobes drive aversion and are innervated by positively reinforcing dopamine input. For simplification, γ lobes are omitted.

ablation of KC activity, artificial induction of DAN activity resulted in depolarization of the corresponding MBON (Takemura et al., 2017). The larval and adult electron microscopy traces revealed further reciprocal connections within each neuron belonging to same MB tile and extensive crosstalk across these compartments (Eichler et al., 2017; Takemura et al., 2017). As a showcase for both cases, olfactory learning depends on both the maintenance of a positive feedback loop from KCs to DANs within the same compartment and the hierarchy between an MBON and DANs of the several vertical MB compartments (Cervantes-Sandoval et al., 2017; Ueoka et al., 2017). Furthermore, during learning, DAN activity can be subject to lateral-inhibition from adjacent dopaminergic neurons (Cohn et al., 2015).

1.3.3 Mushroom Bodies Modulates Innate Behaviors

Within the frame of learning, dopaminergic input can represent pleasant and repulsive events for the animal. Caloric / sweet taste information of ingested food, water as well as heat, electric shock, bitter compounds, and outcomes of failed reproductive attempts can be encoded in DAN network (Galili et al., 2014; Huetteroth et al., 2015; Keleman et al., 2012; Kirkhart and Scott, 2015; Lin et al., 2014b). Despite earlier contrary evidence, MB has been shown to be required for visual learning (Vogt et al., 2014, 2016; Wolf et al., 1998). Along with this established critical role, the growing evidence suggests MB is involved in processing of several innate behaviors available to the flies, in particular during adaptive sequences. Flies rely on the mushroom body to overcome their aversion to offensive odors and water vapor during food-foraging, and water consumption (Lewis et al., 2015; Lin et al., 2014b). Sleep promotion and inhibition is underlined via distinct MB circuits (Joiner et al., 2006; Pitman et al., 2006; Sitaraman et al., 2015). Innate temperature preference and aversive odor valence are also reliant on MB (Frank et al., 2015; Perisse et al., 2016; Tomchik, 2013). Modulation of innate behaviors, as well as associative learning, by MB is highly likely altered by the current behavioral state of the animal (Berry et al., 2015; Cohn et al., 2015).

1.4 Hunger Governs Olfaction

Nervous systems are far from static maps. Information flow is continuously subject to short- and long-term alterations by modulatory agents (Bargmann, 2012). Internal states are representations of an animal's global conditions critical for its survival, and internal states can be potent agitators for various animal behaviors to preserve homeostasis (Berridge, 2004). As a part of the foraging behavior to find food and suppress the negative drive against starvation, olfaction is heavily modulated by a particular internal state, hunger.

1.4.1 Modulation at Periphery

Modifications by hunger state can be traced at most, if not all, known stages of olfactory processing and behavioral execution in *Drosophila* (Figure 3) (Sayin et al., 2018). Consequent to food deprivation flies increase their basal locomotor activity to improve the likelihood of food-encounter (Yang et al., 2015; Yu et al., 2016). To capitalize such encounters, flies, furthermore, change their odor detection dynamics and valence computations. Global changes can be observed in the olfactory center antennal lobe (AL), and both so-called innate and learning higher centers, lateral horn (LH) and mushroom body (MB) (Knaden et al., 2012; Strutz et al., 2014; Tsao et al., 2018). Not surprisingly, such changes are found as early as the olfactory receptor neuron (OSN) level. Food odors, such as vinegar, according to their available concentration at a given time, could elicit attraction and aversion driving channels in the AL (Semmelhack and Wang, 2009). Upon starvation, positive valence glomeruli (DM1, DM2, DM4) were strengthened and negative valence glomerulus (DM5) was dampened for their neuronal response during vinegar exposure. This facilitation and depression occurred in respective Or42b and Or85a OSNs via two distinct neuromodulators. short neuropeptide F receptor (*sNPFR*) molecule in Or42b OSNs was observed to accumulate within 4 hours of food deprivation and acted as an autocrine to boost Or42b activity. Whereas local neurons released tachykinin (*DTK*) onto Or85a, which harbored higher tachykinin receptor (*DTKR*) under starvation, and led to the suppression of aversive DM5 channel. Ultimately, the availability of *sNPFR* and *DTKR* were dependent on the insulin signaling and tightly linked to the metabolic state of the animal (Ko et al.,

2015; Root et al., 2011). While ablation of *sNPF-R* and *DTKR* alone in the relevant OSNs were to sufficient to confer fed state in starved animals, a plethora of potential neuromodulators exists: in antenna alone, 45 G-protein coupled receptors were found to be differentially expressed due to fasting, while 200 proteins were upregulated in a later expression analyses (Farhan et al., 2013; Ko et al., 2015). *CCHamide* was required at the level of OSNs for mediating attraction for several odors, while *SIFamide* modulated secondary order projections neurons arising from DM3 glomerulus (Farhan et al., 2013; Martelli et al., 2017). Furthermore, OSNs that are tuned for aversive odors are subject to modulation as well. Upon satiation, Or7a responses to benzaldehyde were amplified. Such a shift in tuning would increase the likelihood of triggering aversion in low benzaldehyde concentrations, which is otherwise an attractive signal for starved flies (Farhan et al., 2013).

1.4.2 Central Modulation by Starvation

Neuromodulatory mechanisms how starvation exerts control on olfaction in higher brain centers have also been unraveled. Analogous to broadening of OSN detection, motivational thresholds were found to be altered via signaling through unpaired (*upd*) - neuropeptide F (*NPF*) signaling. While direct functional connectivity remains to be unearthed, series of studies implied that *upd1*, as a functional homolog of mammalian leptin, disinhibits dopaminergic PPL1 activity to prevent food-seeking and appetitive associative learning in satiated animals (Beshel and Zhong, 2013; Beshel et al., 2017; Krashes et al., 2009). *upd1* mutant fed flies phenocopied starvation induced behaviors. The interference against *upd1* receptor dome in *NPF* positive neurons was sufficient to promote odor-search in fed flies. In return, artificial activation of a narrow subset of *NPF* neurons in the fly brain generated odor attraction in satiated flies. The *NPF* activity induced approach was extended to non-food odors, suggesting *NPF* mediates broader motivational drive (Beshel and Zhong, 2013; Beshel et al., 2017). Previous studies in learning and memory also suggested a role of *NPF* for olfactory motivation control. The absence on *NPF* receptor (NFPR) in PPL1- γ 1 peduncle DAN neuron repressed appetitive learning in starved flies, due to the increased inhibition over the mushroom body output (MBON- γ 1 pedc> α/β) (Aso et al., 2014a; Krashes et al.,

patches which does confound any “olfactory-only” explanations for the contribution of neuromodulation due to the gustatory and ingestion feedback presence.

1.5 *Drosophila* Gustatory System

The ultimate goal of the majority of starvation-induced olfactory behaviors is locating the relevant and sufficient nutrient sources and their subsequent exploitation. However, food consumption is far from a straightforward execution of various reflex sequences. Feeding involves the continuation of further evaluation of food sources, during gustation and later in ingestion. Furthermore, food is a potent reward. Equally crucial is its absence. As a highly salient object, food acts as a strong reinforcer for incorporation of past experiences in appetitive or aversive learning.

Taste detection of non-volatile compounds in *Drosophila* relies on several different classes of gustatory receptors, most notably seven-transmembrane chemoreceptor GRs and ionotropic receptors (IRs), pickpocket and transient receptor potential (TRP) families. Gustatory receptors can be housed in external sensilla distributed in several extremities such as leg tarsi, wings, the ovipositor, and internal organs, labella and gustatory tract (Joseph and Carlson, 2015; Liman et al., 2014). Neurons in the fly central nervous system were also reported to monitor sugar concentrations (Miyamoto et al., 2012). In the case of external taste sensation, akin to olfaction, each sensillum can harbor several gustatory receptor neurons (GRNs) which contains several and differentially tuned gustatory receptors. Particularly for Grs, GRNs might express a highly variable number of receptors across several locations throughout the fly anatomy (Fujii et al., 2015; Thorne et al., 2004).

1.5.1 Gr43a as an Internal Sensor

Maintaining a steady level of sugar in hemolymph is essential for survival (Lee and Park, 2004; Matsuda et al., 2015). Regardless of sugar types given as a food source, fructose levels were the sole indicator of feeding state. Fructose

hemolymph concentrations followed feeding bouts. While Gr43a+ GRNs in fly legs were expansive sugar sensors, Gr43 was exclusively activated by fructose and functioned as an ion channel (Miyamoto et al., 2012; Sato et al., 2011). Thus Gr43a neurons were indeed in a position to act as sensors for the metabolic state of the animal. Fly protocerebrum contained neurons that expressed only Gr43a receptors as Grs. Activation of these neurons conferred fed-like state and promoted associative olfactory learning in deprived flies. Surprisingly, in fed animals, activation of Gr43a assigned negative valence to the conditioned stimulus (Miyamoto et al., 2012). Corazonin was found to be co-expressed in these neurons and were postulated to be the mode of modulation (Miyamoto and Amrein, 2014). In addition to Gr43a, further nutrient sensors hint multiple levels of nutritional monitoring in the central nervous system (Dus et al., 2013).

In contrast to Gr43a, other fly sweet taste receptors are broadly tuned. To abolish most, if not all, sweet gustation, it was necessary to ablate both Gr5a and Gr64a receptor activity (Dahanukar et al., 2007). Later, Gr64f was proposed to be a necessary coreceptor for other sweet Grs (Jiao et al., 2008). Tarsal sugar sensation was further dependent on Gr61a (Thoma et al., 2016). Similarly, bitter taste relied on more than 30 GRs and 2 TRPs (Liman et al., 2014).

1.5.2 Subesophageal Zone: CNS Taste Relay

Highly distributed nature of taste receptors do not necessarily indicate a decentralized nervous system for gustation. Depending on the locality of a gustatory neuron, its projections can innervate ventral nerve chord (VNC). For the case of ascending tarsal GRNs, they project directly to the central nervous system, a brain-stem like a region called the subesophageal zone (SEZ) (Thoma et al., 2016). GRN synapses arising from the fly pharynx are also located in SEZ (Dahanukar et al., 2007). SEZ harbor motor neurons required for feeding, and commands abundant neuromodulation (Busch et al., 2009; Gordon and Scott, 2009; Kim et al., 2017; Manzo et al., 2012; Marella et al., 2012). Conditional to the internal state, direct control of feeding cessation or prolongation occurs within SEZ, or is ensured by SEZ - antennal mechanosensory and motor center (AMMC) axis (Joseph et al., 2017; Kain and Dahanukar, 2015; Pool et al., 2014; Yapici et al., 2016). AMMC is

not the only zone that receives gustatory input from SEZ: taste projection neurons (TPNs) were described to convey taste coding to ventral nerve cord and higher brain centers. So far, morphologically and functionally identified TPNs carried exclusively either positive and negative valence (Kim et al., 2017). At the global scale, in the fly protocerebrum, bitter and sweet taste information was mapped to distinct regions (Harris et al., 2015). Indeed dopaminergic PPL1 cluster was postsynaptic to TPNs: positive valence TPN2 depressed PPL1 DANs while negative valence TPN3 potentiated (Kim et al., 2017).

1.5.3 Gustation as a Sequence

Whether reliant on short microcircuits or long projections neurons, the gustatory system is in interaction with other behavioral modes. Brief activation of taste sensation results in enhanced locomotion (Murata et al., 2017). Upon finding of a food patch, a well-described ‘dance’ phenotype, local search, is evolutionarily conserved across several insects, including *Drosophila melanogaster* (Kim and Dickinson, 2017). However, locomotion and feeding behaviors can be antagonistic. A local circuit in VNC inhibited feeding start (Mann et al., 2013). In contrast, segmental tarsal GRNs that project to VNC were crucial for feeding induced suppression of locomotion. Indeed, Dethier pointed out early on that hungry flies ceased walking behavior upon contacting food (Dethier, 1976; Thoma et al., 2017). It is highly probable that food source quality and eventual successful acquisition of nutrient ultimately determines how gustation and related behaviors, locomotion, and olfaction, are coordinated.

1.6 Octopamine: A Bridge Between Action and Expenditure

Internal states and energy expenditure are tightly linked. A neuromodulator that presides over this interaction must talk both to nutrient sensors and action selection/generation agents. In insect brains, as an analog of mammalian norepinephrine, octopamine (OA) is one of the important molecules to take such a role.

Octopamine is expressed in more than 100 neurons within the central nervous system of the fly brain, labeled by *Tdc2-Gal4* and *NP7088-Gal4* (Busch et al., 2009; Cole et al., 2005). Some of the OA positive neurons have extensive, global arborizations that connect two or more central nodes in the brain (Busch et al., 2009). Analogously, mammalian norepinephrinergic neurons located in locus coeruleus (LC) engage in similar central extensive branching (Sara and Bouret, 2012). Octopamine can be found in other cell types, including glia (Cole et al., 2005; Ma et al., 2016). Octopamine is synthesized in a cascade starting from tyrosine, in which tyramine- β -hydroxylase (*T β h*) converts another neuromodulator, tyramine (*Tyr*), to OA (Monastirioti et al., 1996). This conversion implies that OA and *Tyr* can drive a wide variety of behaviors through a single molecular switch. Indeed, octopamine and tyramine might have an antagonistic influence on the organism (Fox et al., 2006; Li et al., 2016; Ormerod et al., 2013; Ryglewski et al., 2017; Saraswati et al., 2004; Selcho et al., 2012). In addition to the four known dedicated G-coupled receptors for octopamine, interestingly, octopamine and tyramine share a receptor (El-Kholy et al., 2015; Evans and Maqueira, 2005; Ohhara et al., 2012). Another common receptor was recently described for octopamine and serotonin (Qi et al., 2017).

Starved animals engage in energy-intensive food-seeking foraging behavior. Foraging strategies were modulated by octopamine (Corrales-Carvajal et al., 2016). The increased locomotion upon starvation was also dependent on OA, which is promoted via adipokinetic hormone and counteracted by insulin signaling (Yang et al., 2015; Yu et al., 2016). The neuromuscular junction is a target of octopamine during this high arousal state (Koon et al., 2011; Ormerod et al., 2013). Further studies reflect a more profound, complex integration of octopamine modulation to the metabolic state. Octopamine in flies controls body lipid accumulation, glucose, and insulin concentration maintenance. Insulin-producing neurons were found to be under the regulation of octopamine. Devoid of octopamine signaling, survival rates were affected both positively and negatively, depending on the OA receptor perturbation (Li et al., 2017, 2016; Luo et al., 2014). In return, induction of fasting state via nutrient-deficient sucralose feeding required insulin receptor presence in octopaminergic cells (Wang et al., 2016). Induction of thoracic *Tdc2*⁺ neurons promoted the feeding reflex (Keene and Masek, 2012). Further contrasting effects

of octopamine on food-intake can be observed depending on the internal state and food-type (Zhang et al., 2013). Sugar-sensitive gustatory receptors Gr5a and Gr64f were strengthened via octopamine, whereas bitter taste responsive Gr66a neurons were dampened in starved animals via Oct-TyrR receptor (LeDue et al., 2016; Youn et al., 2018). Akin to starvation-induced locomotion, octopamine also gated arousal levels to stimulate waking-state via insulin-producing neurons (Crocker et al., 2010). The activity of octopamine modulates further energy intensive behaviors, such as flight, aggression and reproduction (Andrews et al., 2014; Brembs et al., 2007; Rezával et al., 2014; Zhou et al., 2008).

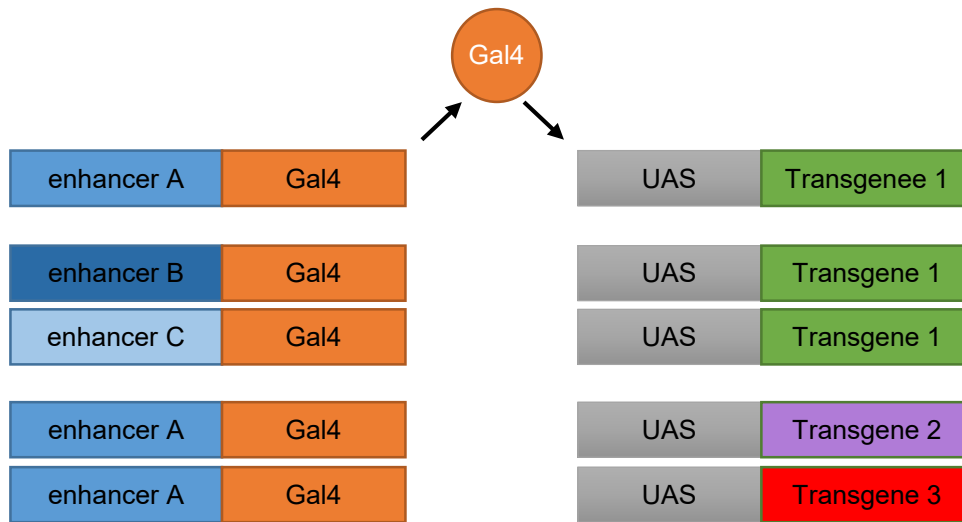
1.6.1 Octopaminergic Neurons in SEZ

In addition to direct modulation of gustatory receptors, the high density and morphological variety of octopaminergic neurons in the primary taste center subesophageal zone (SEZ) suggests a broader role of OA in taste guided behaviors (Busch et al., 2009). In *Apis mellifera*, OA-VUMmx1 neuron represented the unconditioned stimulus, the reward, in appetitive learning (Hammer and Menzel, 1998). Initially, non-overlapping roles for dopamine and octopamine in the formation of, respectively, aversive and appetitive learning was posited (Schwaerzel et al., 2003). Later studies expanded these findings: artificial octopamine activation was sufficient to mediate short-term sugar reward. However, OAMB receptor in dopaminergic $\beta'2$ and $\gamma4$ DAN neurons were also necessary for memory formation, suggesting a feedforward mechanism (Burke et al., 2012; Huetteroth et al., 2015). Octopamine is also critical for the mediation of ethanol reward. In visual assays, flies accumulated in the area where OA-Tdc2⁺ neurons depolarized by optogenetics (Kaun et al., 2011; Schneider et al., 2012; Schroll et al., 2006). Comparable to feeding, octopamine might have an opposite role for reward substitution. *Oct β 2R* lacking flies were deficient in aversive learning (Wu et al., 2013). In contrast, knockdown of *Oct β 2R* in PPL1 clusters impaired appetitive associations (Burke et al., 2012). Gustatory and visual learning is not affected by manipulation of Tdc2⁺ neurons (Kirkhart and Scott, 2015; Vogt et al., 2014).

1.7 *Drosophila*, A Systems Neuroscience Model

Since the discovery of the first mutant *Drosophila melanogaster*, a series of discoveries culminated to the point where this miniature fly has become a cornerstone of systems neuroscience. The roots of *Drosophila* as a neuroscience model organism lies in its history as a genetic model. The discovery of ‘white’ gene, subsequent genetic mapping and robust systematic efforts to create mutants via X-rays, chemical mutagens and later various transposable elements, created a wealth of interventionist tools for necessity studies. For gain-of-function analyses, as well as loss-of-function, p-element transgenesis and, later, site-specific recombination made possible of introducing any desired sequence element in a genetically stable manner across generations (Bachmann and Knust, 2008; Bischof et al., 2007; Stephenson and Metcalfe, 2013). The balancer chromosomes, a catalog of ‘highly modified chromosomes’ with easily identifiable markers, were utilized to prevent spontaneous crossing-over and enabled tracking desired transgenes and mutations (Lindsley and Zimm, 1992). Ultimately, the wide-spread adoption and collaborative effort to expand the drivers of the Gal4-UAS system has been critical for the fly genetics community.

Gal4-UAS system is an exogenous binary system adopted from *Saccharomyces cerevisiae*. Gal4 is a transcription factor, majorly composed of activation (AD) and DNA-binding (DBD) domains, and recognizes specifically a cis-regulatory UAS (upstream activating sequence) to drive downstream transcription (Figure 4) (Brand and Perrimon, 1993). As in so-called enhancer trap screens, Gal4 insertions coupled to an enhancer can confer spatiotemporal specificity to any transgenic expression (Mlodzik and Hiromi, 1992). In other words, these ‘Gal4 driver’ libraries are used to determine when and in which particular tissue a UAS linked protein (‘UAS effector lines’) would be expressed. Through random p-element transgenesis and att-based targeted site-specific recombination, a plethora of Gal4 driver and UAS lines, which a parent fly harbors either of those, has been established. Any combination of parents, one for Gal4 and one UAS, achieves transgenic protein expression and eliminates the need for creating dedicated lines for every desired protein and cell combination (Figure 4).



3 Gal4 + 3 UAS Transgenics = 9 Unique Expression Pattern

Figure 4 Gal4-UAS system

Gal4 lines generated by enhancer-trap screens or transgenic insertions dictate tissue-specific expression of Gal4 protein, which in turn locate and bind to UAS sequences and thus enabling downstream gene transcription. Binary systems allows the use of fewer transgenic constructs. Otherwise, in an enhancer-target gene direct fusion scenario, a library of nine unique transgenic constructs has to be created.

Historically, enhancer trap lines were broad, labeling a high number of cells at a given driver. Further expansions of the Gal4-UAS system reveal that even narrower, tighter control of binary expression systems is possible. Gal80, as a repressor of Gal4, can restrict UAS-Gal4 expression in a tissue-specific and time-dependent fashion (Suster et al., 2004). Through the flip-frt system, an analog of mammalian Cre-lox, mosaic clones, and single-cell expressions can be accomplished (Theodosiou and Xu, 1998). Recent effort to emphasize intersectional genetics, by the generation of split-Gal4 libraries, however, made such efforts less stochastic and straight-forward. Gal4 can be split into its AD and DBD subunits under the control of two different enhancers. Then successful induction of the Gal4-UAS system is only plausible where AD and DBD expression overlaps narrowly, and two subunits form a functional dimer (Luan et al., 2006; Pfeiffer et al., 2010). Therefore, high-throughput production of stable transgenic lines that target a single cell has become a reality. Moreover, in parallel to the Gal4-UAS system, similar binary expression modes such as LexA-lexAop and QF-QUAS

exists to enable multiple manipulations without interference between these systems (Lai and Lee, 2006; Potter and Luo, 2011).

To be able to effortlessly target, monitor and manipulate one neuron, or a narrow subset of neurons, is immensely valuable for systems neuroscience approach. Gal4-UAS system provides expression of several commonly used effectors. Neuronal activity can be silenced by overexpression of inward potassium channels (Kir2.1), tetanus toxin light chain (TNT) and high-temperature activated dominant negative dynamin mutant shibire^{ts1} (Baines et al., 2001; Kitamoto, 2001; Sweeney et al., 1995). A novel set of channelrhodopsins, algal *Guillardia theta* anion channelrhodopsins (GtACRs) can mediate high temporal scale inhibition of neuronal activity (Mohammad et al., 2017). Similarly, artificial activation can be achieved by temperature dependent transient receptor potential cation channel A1 (TrpA1) or red-shifted channelrhodopsins CsChrimson and red-activable channelrhodopsin (ReaChr) (Hamada et al., 2008; Inagaki et al., 2014; Klapoetke et al., 2014). Neurons can be biased towards excitation via NaChBac expression at the target neuron (Nitabach et al., 2006). Neuronal activity can also be explicitly regulated by altering gene expression. Binary gene expression systems can provide knockdown of neurotransmitter release via RNA interference, or the receptor for a particular neuromodulator can be overexpressed at the postsynaptic neuron (Clemens et al., 2000).

For such a small brain size, fly brain harbors more than hundred thousand neurons in its nervous system. Prior to the emergence of holistic neuronal models, in this cacophony of cells, it is imperative to flesh out micro-units of neuronal computation. Various fluorescent proteins are undoubtedly useful to visualize neuronal morphology. The larval connectome is an immensely useful tool as a guideline to flesh out neuronal roadmaps (Berck et al., 2016; Eichler et al., 2017; Larderet et al., 2017). The adult connectome is also partially completed (Takemura et al., 2017). These static maps need to be validated for functional connectivity and neuronal identity. Single cell transcriptomics would help to identify cell profiles (Karaikos et al., 2017). The state-of-the-art trans-synaptic tracers are now available to the fly community (Talay et al., 2017). Furthermore, depolarization of the presynaptic neuron, with tools such as P2X2, and simultaneous monitoring of

the candidate postsynaptic neuron's activity is achievable (Yao et al., 2012). To monitor neurons in real time, genetically encoded calcium indicators can be used (Fiala et al., 2002). While still electrophysiology is somewhat technically challenging in flies, its application is prevailing (Wilson, 2005). Furthermore, genetically encoded voltage indicators are promising to provide higher temporal and faithful recordings (Cao et al., 2013). While single neuronal activity can be read out in such assay, through volumetric imaging, it is now feasible to achieve recordings of whole nervous systems (Mann et al., 2017).

2 THESIS OBJECTIVES

In this study, I aimed to contribute to unraveling one of the fundamental questions of neuroscience: how do nervous systems generate and control behavior? More specifically, how do animals utilize motivational mechanisms and integrate internal states to execute and control effortful behaviors?

Through utilization of toolbox made available by the *Drosophila* neuroscience community and by developing a new behavioral paradigm, in particular, I focused on high-resolution analyses of olfactory odor tracking for walking *Drosophila melanogaster* and how this behavior is interacting with other modalities and the internal state in question, hunger.

How do energy deprived animals face the drive to forage, an energy-demanding task? Internal states shape behavior, and in particular, hunger modulates olfaction in several levels in the nervous system (Sayin et al., 2018). What are the implications of hunger levels on responses to repeated odor stimuli?

What are the mechanisms of multisensory reconciliation? Foraging is a composite behavior. Tracking commences via long distance engagement, yet the ultimate goal is finding nutritious food sources. Therefore, it is conceivable olfaction would eventually engage with gustatory and post-digestive feedback. Understanding the nature of such multisensory integrations poses challenges; therefore I aimed at clear separation of sensory modality presentation.

3 MATERIAL AND METHODS

3.1 Fly Husbandry and Fly Lines Used in the Study

Flies were raised on standard cornmeal recipe in chambers at 25°C room temperature (for Shi^{ts1} experiments 18°C until hatching) and 60% humidity. Before the behavioral or physiological experiments, depending on the internal state in question, the flies were also raised in starvation bottles (for wet starvation, wet tissue paper was placed in empty bottles). For optogenetic experiments, recently eclosed flies were reared in all-trans-retinal fortified food (1:250) under dim blue light (470nm, 0,05 $\mu\text{W}/\text{mm}^2$).

Fly stocks are introduced in Table 1 at the appendix section.

3.2 Spherical Treadmill Setup and Analyses

Bilateral olfactory treadmill paradigm consists of a custom-built olfactory system and a spherical treadmill similar to a previously described setup for visually guided behaviors (Seelig et al., 2010).

3.2.1 Olfactory Delivery

In the olfactory delivery system, the odor application was accomplished via the collection of the odor headspace. Odor delivery was driven by a NATEC mass flow controller (maximum air flow 500 ml / min), which enabled high temporal control, and compressed air was used as background air flow. The air speed was adjusted to 100 ml / min via a mass flow controller. PTFE tubing was used throughout the odor delivery to minimize contamination from sticky compounds. After the mass flow controller, air stream reached a 100 ml Schott bottle with Festo PTFE caps for headspace collection. The Schott bottle was placed in the behavioral chamber to equalize odor temperature and ambient temperature. For the majority

of the experiments, 20 ml 10% vinegar solution was used. The vinegar solution was prepared with refrigerated Aceto Balsamico (Alnatura) with Milli-Q (Millipore) once, daily. For carbon dioxide experiments, a custom-made injection module was employed. Into the air pathway, a PTFE Gauge 16 needle was inserted before the odor outlet and connected to a second NATEC mass flow controller. This second flow controller was set to 50 ml / min. The odor delivery was finalized at the custom-made PTFE odor outlet. This odor outlet was 4 mm in diameter, which resulted in comparably very low air speeds and facilitated volumetric odor mixtures. The odor outlet placed to the anterior position of the flies and terminated 3 mm away from the fly head.

For vinegar concentration calculations, a photoionization detector (Aurora Scientific, 200B miniPID) was employed. PID detects volatile ionizable organic compounds at 1 kHz and converts 10 V, which was read by an Arduino Uno via analog read. A custom made Python software was written to read Arduino input. Using the PID, odor input was calibrated to 3 parts per million at 20% 10 ml / min of vinegar solution via a known ethyl-butyrate concentration previously published (Semmelhack and Wang, 2009). The PID traces were smoothened with Butterworth filter for visualization.

The Schott bottles containing the odor solution, the odor outlet, and the recipient fly, in addition to data acquisition systems, were housed in a 16 liter enclosed chamber that prevented visual and external olfactory environmental contamination. Furthermore, the chamber was covered in thick Styrofoam to reduce auditory pollution from outside as well.

3.2.2 Treadmill and Data Acquisition

The ball used in the treadmill assay, a gift from Alexander Borst's lab, was hand-carved with a fine-manufactured blade into 6 mm, 35 mg sphere of polyurethane (Last-A-Foam; General Plastics Manufacturing Company) in a similar fashion to previous designs (Seelig et al., 2010). The ball was seated on air

cushion through a custom-made ball holder. The air cushion was provided a NATEC mass flow controller (100-300 ml / min air speed).

Two acquisition cameras were positioned perpendicularly against each other and focused on the equator of the treadmill. The treadmill was illuminated with two 800 nm LEDs (Roithner JET-800-10). These two cameras were assembled from optical mouse sensors (ADNS-6090). The cameras fed into a single μ -controller ATmega644p, which sent the online data via USB serial connection to a master in-house developed Python software. The treadmill acquisition was accomplished at an initial 4 kHz in two cardinal directions for each camera (Seelig et al., 2010). These data were post-processed and down-sampled at 200 Hz, later to 10 Hz during the final analyses by summation of respective data bins.

3.2.3 Preparation for Behavioral Experiments on the Treadmill

Due to their bigger body size, 3-4 days old (after eclosion) adult female flies were selected via suction, placed into a plastic vial on the ice, and then transferred onto a commercial cooling pad (Bioquip). Fly wings were clipped with a pair of forceps. A micro-manipulator (Narishige) was used to direct a custom-made pin holder with an attached insect pin (Austerlitz, 0.15 mm) under a microscope. A drop of dental glue was placed on to the pin which was directed towards the fly's thorax. Later the dental glue was hardened by 10 s of light application (M+W Superlite 1100). In the second round, the fly head was also immobilized by gluing to the fly thorax. The pin holder was then detached from the micromanipulator, transferred to the behavioral chamber where a second micromanipulator (Narishige) was present. The tethered fly was carefully and quickly positioned on the treadmill. A third camera (Point Grey Firefly MV Mono USB 2.0) was available to assist correct fly positioning. The chamber was closed and, subsequently, the fly was left to acclimatize for 3 minutes. Those flies that failed to recover from anesthesia were discarded.

The enclosed behavioral chamber was kept at 30°C to achieve higher arousal and permitting thermogenetic experiments. For optogenetics, a single high-

power LED (617 nm max intensity, 30 μ W/mm² M617, Thorlabs) was positioned overhead of the tethered fly.

3.2.4 Data Analyses of the Treadmill and Statistics

A custom-written Python software collected data coming from the μ -controller and saved as forward, rotational, sideslip speeds for later analyses. Forward running corresponds to displacement over time in the direction towards the odor source (ahead), whereas rotational displacements were computed as turning of the ball in either direction over time. Sideslip speeds were calculated as lateral displacements. Due to the anterior position of the bilateral odor delivery and lack of positional information, absolute values of rotational speed data were used to compute absolute turning over time. For the construction of 2D trajectories, all forward, rotational, sideslip speeds at a given time were used as previously described and later filtered with Butterworth filter for visualization (Seelig et al., 2010). Average running and absolute turning speeds were calculated by taking averages of 100 msec data bins in their respective pre-, during and post-stimulation periods. Average running time was measured as the first 100 msec data bin where a given fly exhibited 0 mm / s forward running speed after an odor or optogenetic stimuli. Average running activity was calculated from a fraction of 100 msec data bins where fly forward speed was higher than 0 mm / sec in a given time period. For constructing plots of averages over time and over a given period, the average of ten trials for a fly was determined at first, and this representative average was utilized to compute for the average of a given genotype or an experimental group. All analyzes for the treadmill were performed in Python 2.7, numpy 1.8, scipy.stats (0.14) and pyvtbl (0.5.2.2). All treadmill data were visualized by matplotlib (1.4.2). All pairwise comparisons were handled as unpaired T-test. If it was possible to compare a particular fly's behavior under two different conditions, paired T-tests were employed. In the case of comparing three or more genotypes, one-way analysis of variance (ANOVA) was utilized. Multiple comparisons were handled via Tukey's HSD post hoc test. Statistical denominations were as followed conventionally: “-” $p < 0.05$, “*” $p \leq 0.05$, “**” $p \leq 0.01$, “***” $P \leq 0.001$.

3.3 Behavioral Arena

Behavioral arena enables concurrent, independently controlled odor and optogenetic stimulation in each quadrant by a script governed by MATLAB. Based on an expansion of the previously published olfactory only design (Aso et al., 2014b), the 4-arena includes a custom-made LED array panel (Amber SMD PLCC2, 617 nm) placed beneath the arena. The odor delivery relied on passive suction created by a rotary pump (Thomas G12/01-4 EB, 200 ml / min), connected to the center of the arena. Negative pressure drove odor input from corners of each quadrant where PTFE tubings connected to 4 pairs of Schott bottles (20% Aceto Balsamico, Alnatura, solution or Milli-Q water, Millipore) in each corner. Festo MFH-3-MFs solenoid valves executed the odor and blank water switch.

Infrared LEDs provided the background illumination of the arena. A camera placed above the setup recorded 3-4 days old, mixed gender flies' behavior (FLIR Flea3 MP Mono). The post-analyses were done via custom-written MATLAB code that extracted fly position over time from the recorded videos. The preference indices were calculated “(# flies in stimulation quadrant - # flies in non-stimulation quadrant) / # of total flies in the arena”.

3.4 T-Maze

For the two-choice assay, 3-4 days old flies (after eclosion) were collected into groups of 40-60 and transferred to tubes with wet tissue paper. After acclimatization in the behavioral chamber (60% humidity, only red light illumination and permissive temperature of 25°C or non-permissive temperature of 32°C) for 20 minutes, flies were loaded into the T-maze elevator. Subsequently, the elevator pushed down, and flies were transferred to the choice point. During the time window (1 min), flies were presented with two choices, a blank and an experimental tube. The blank tube contained a small Whatman filter paper with Milli-Q water. The experimental tube contained either Whatman filter paper with 40 µl 10% Aceto Balsamico, Alnatura or 1% CO₂ mixture. CO₂ mixture was previously prepared using NATEC mass flow controllers to mix pure CO₂ and compressed air. In the

next step, flies were collected and counted under anesthesia. The preference indices were calculated “(# flies in odor tube - # flies in blank tube) / # of total flies collected”.

3.5 Immunohistochemistry

Using standard protocols, adult fly brains (4-7 days old after eclosion) were dissected, fixed and stained (Bräcker et al., 2013). The visualization was realized by using a Leica SP8 confocal microscope, the image processing with ImageJ and Photoshop. The primary antibodies used in the study are available in Table 2 of the appendix section.

3.6 Calcium Imaging

Data acquisition was carried out with a 40X water immersion lens in a fluorescent microscope (Leica DM6000FS, in junction with Leica LAS AF E6000 acquisition software for ROI drawing and raw data analyses). Calcium activity was computed as $\Delta F/F = 100 \cdot (F - F_0)/F_0$, F_0 as the baseline fluorescence and F as the fluorescence at a given time.

For *in vivo* calcium experiments, a window opened in the fly cranium as previously described (Bräcker et al., 2013). Of those experiments with vinegar (20 frames / sec for 75 sec, 4x4 binning, baseline recording for 15 frames), an internally developed odor delivery system (Smartec, Martinsried) was used to apply 1 l / min humidified stream through PTFE tubing (8 mm in diameter). Vinegar delivery was achieved via a set of valves (FESTO) and NATEC mass flow controllers (Bräcker et al., 2013; Lewis et al., 2015). The odor delivery protocol followed the experimental procedure of spherical treadmill for vinegar. The gustatory stimuli presentation (recording: 20 frames / sec for 75 sec, 4x4 binning, baseline recording for 15 frames) involved a micromanipulator (Narishige) controlled syringe needle (MicroFil) (Hussain et al., 2016). The syringe carried fructose (1 M) to the tethered fly proboscis with visual guidance. The stimuli duration was 10 seconds. During

functional connectivity experiments, an ATP solution (2 mM, final concentration) was applied to the AHL buffer to activate P2X2 receptors (20 frames per seconds for 75 seconds, 4x4 binning, baseline recording for 15 frames). *Ex vivo* gustatory experiments (1 frame per second, 10 minutes, no binning, baseline recording for 60 frames) used a custom-made grid to immobilize a dissected adult brain (3-4 days old after eclosion) in perfusion of in AHL solution (500 μ L). The fructose stimulus (50 μ L, 1 M) was added directly to the perfusion.

3.7 Connectomics

During serial section transmission electron microscope reconstruction of MB peduncle region (Zheng et al., 2017), MB pedunculus-medial lobe and vertical lobe arborizing neuron 2 (MVP2) upstream synaptic partners were revealed to ventral paired median neuron 3 and 4 (VPM3-4). Using CATMAID, neurons were reconstructed and validated (Aso et al., 2014a; Busch et al., 2009). Data preparation and representation were conducted with custom R and Python libraries.

4 RESULTS

4.1 Repeated Food Odor Exposure Underlies Persistent Tracking

4.1.1 Wild-type *Drosophila* Responses to Vinegar

With the aim of establishing the paradigm to describe wild-type behavior and use the results as a reference for future experiments with thermo/optogenetic manipulations, I commenced with testing wild-type behavior under different conditions. The *Drosophila melanogaster* strain used in these experiments was Canton S.

In the first set of experiments, I observed wild-type CS behavior at room temperature. After their eclosion, 3-4 old flies were starved for 24 hours. Then CS flies were subjected to the open-loop protocol described in Figure 5.A with 3 ppm vinegar stimuli over ten trials. This concentration was proposed an optimum for starved flies (Semmelhack and Wang, 2009).

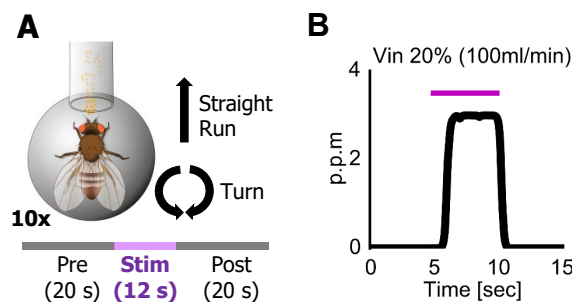


Figure 5 Spherical Treadmill Schematic and Odor Delivery Dynamics

(A) The schematic for the spherical treadmill assay for bilateral olfaction. A single pseudo-randomized trial consisted 52 sec with 12 sec of vinegar stimuli. Odor stimuli were repeated for 10 times. The behavior was analyzed in two cardinal directions (forward runs and turns). (B) Representative vinegar concentration for a single trial. The signals recorded from the photoionization detector were normalized and smoothened with a Butterworth filter.

On average, CS flies were able to increase their forward running speed to 3.81 mm / sec upon bilateral appetitive odor stimulation (Figure 6).

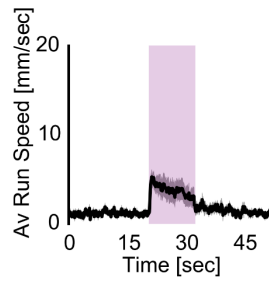


Figure 6 Odor tracking at room temperature for starved wild-type CS

Average running speeds for ten trials of 10 CS flies at 25°C.

Since arousal levels were found to be critical in previous spherical treadmill analyses previously (Bahl et al., 2013), we decided to repeat the experiment in a higher ambient temperature of 30°C (Figure 7). In this condition, flies executed odor tracking at much higher speeds (Figure 7.A). When the flies were presented with vinegar cue, they started to run in the direction of odor with a sharp increase in velocity at the odor onset and sustained it (at an average of 12.4 mm / sec) throughout the odor exposure until the odor offset, where they slowed down. On average over ten trials, flies were faster than before and after odor stimulation. At the same time, flies suppressed turning execution (Figure 7.B). Flies did show basal turning levels in left and right, which were suppressed with the odor onset. At the offset, a burst of turning was observed, where flies switched to a local search. Figure 6 and 7 together showed that flies perceived the odor at the front and were able to track it.

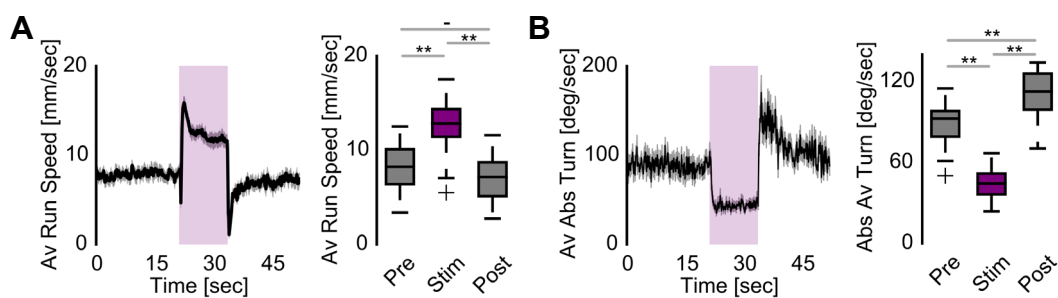


Figure 7 Odor tracking at 30°C for starved wild-type CS

(A) Left. Average running speeds for ten trials of 18 CS flies over timeframe of a single trial. Right. Boxplot for average running speeds for ten trials of 18 CS flies over pre-, during and post-stimulation periods. (B) Left. Average absolute turning speeds for ten trials of 18 CS flies over timeframe of a single trial. Right. Boxplot for average absolute turning speeds for ten trials of 18 CS flies over pre-, during and post-stimulation periods.

Longer vinegar exposures (60 seconds) also led to odor tracking as flies showed similar odor onset and offset behavior (Figure 8). However, as the trial progressed running speed in average dropped around the 50th second.

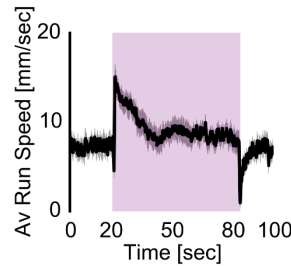


Figure 8 Odor tracking for 60 sec long vinegar simulation of starved wild-type CS

Average running speeds for ten trials of 10 CS flies over timeframe of a single trial with constant 60 seconds long vinegar exposures.

Thus, I have established the spherical treadmill with frontal vinegar presentation and showed that flies were able to respond to prolonged odor exposures. For subsequent experiments, the ambient temperature was set at 30°C, because flies showed a more reliable and consistent running behavior. Furthermore, since very long odor exposures resulted in a lower signal-to-noise ratio, medium length stimulations (12 seconds) were maintained.

4.1.2 Flies do not track CO₂

Could the observed behavior so far be just a by-product of enhanced arousal through higher ambient temperature or a more general negative state? In order to establish firmly that vinegar approach is a goal-directed behavior of the flies in this paradigm, we asked how flies behave under aversive odors.

In contrast, on the spherical treadmill, CS flies avoided potent aversive CO₂ (Figure 9). We presented six consecutive pairs of CO₂ (50 ml / min injected to 100 ml / min) or only air (150 ml / min). Confronted with an aversive CO₂, flies slowed down significantly (Figure 9.B). Meanwhile, they increased their turning, regardless of direction, presumably trying to escape aversive cue (Figure 9.C).

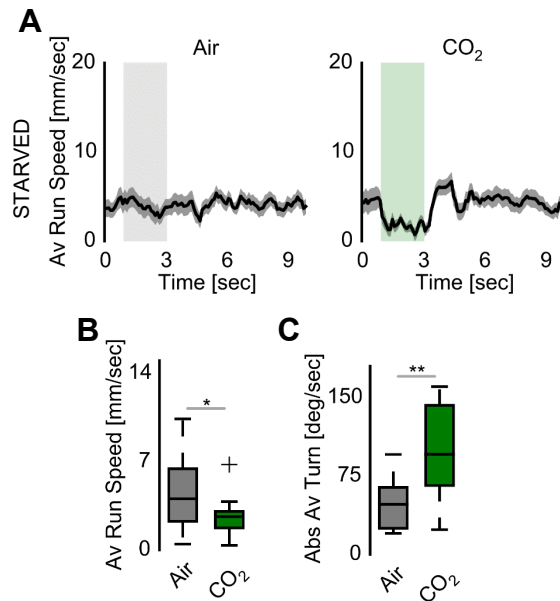


Figure 9 Carbon dioxide aversion of starved wild-type CS on the spherical treadmill

(A) Average running speeds for six trials of 10 CS flies over time under alternating air (left) and CO₂ (right) stimulation. (B) Boxplot for average running speeds during the first second recorded of stimulation periods under air and CO₂. (C) Boxplot for average absolute turning speeds during stimulation periods under air and CO₂.

This experiment revealed that CO₂ is a repellent for the walking fly, and did not induce forward running even in the presence of hunger. This conclusion reinforces the observation that vinegar was indeed tracked actively by the flies.

4.1.3. Vinegar Tracking is Olfaction Dependent

What's the contribution of olfactory input in the odor-tracking behavior on the treadmill? Were the olfactory cues within the vinegar plume directly responsible for promoting attraction? As results in Figure 9.A indicated, indeed, it was so: air itself did not elicit any forward acceleration in hungry flies.

With the aim of assessing this question with more certainty, I tested olfactory co-receptor *ORCO* heterozygous and null mutants for ten trial 10 seconds procedure (Figure 10). *ORCO* null mutants still have functional ionotropic receptors that respond to vinegar (Gaudry et al., 2012). However, their forward running speeds were significantly lower than the heterozygous controls (Figure 10.A). I also replicated the *ORCO* loss-of-function assay in a thermogenetic silencing paradigm

(Figure 10.C). By inhibiting synaptic vesicle recycling through the expression of a dominant negative version of dynamin in a temperature-sensitive manner, I blocked synaptic release from starved *ORCO-Gal4>UAS-Shi^{ts1}* flies. These flies were significantly slower than the Gal4 controls (*ORCO-Gal4>-*) after the outlier removal from the experimental group (Figure 10.C).

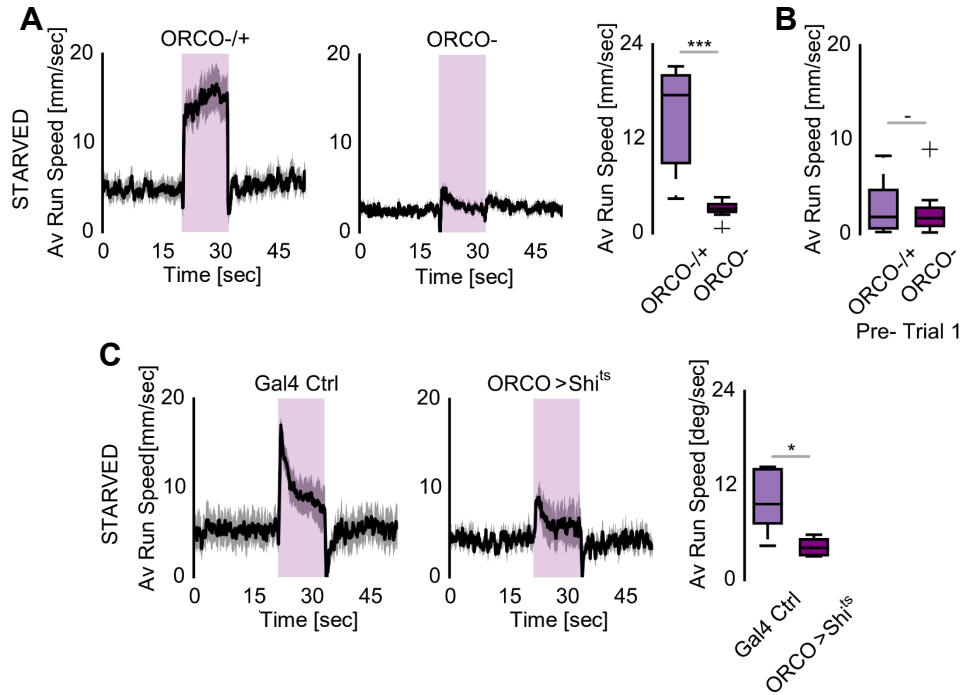


Figure 10 Olfactory input dependency of odor tracking on the treadmill.

(A) Left. Average running speeds for ten trials of 10 *ORCO* heterozygous (left) and null (right) mutant flies over time during vinegar stimulation. Right. Boxplot for average running speeds during the stimulation periods for *ORCO* mutants. (B) Boxplot for average running speeds in pre-stimulation periods for *ORCO* mutants only in the first trial. (C) Left. Boxplot for average running speeds for ten trials of Gal4 control (*ORCO-Gal4>-*, 5 flies) and *ORCO-Gal4>UAS-Shi^{ts1}*, 5 flies) during vinegar stimulation under non-permissive temperature after outlier removal (30°C). The outlier was removed according to Iglewicz and Hoaglin's robust test for multiple outliers to ensure normal statistical distribution (modified Z score threshold was 3.5).

ORCO null mutant flies were comparable in average speed to their respective controls before any odor exposure during the pre-stimulation period of the first trial (Figure 10.B). This suggests the effects observed were not due to motor defects that might have arisen by transgenic manipulations. Therefore, odor tracking depends on olfactory input, which is mostly encoded by OR receptor family.

Figure 9 and 10 results conclusively showed that the approach behavior observed in the treadmill was dependent on the attractive olfactory cues.

4.1.4. Characterization of Persistence

So far, I analyzed several conditions in the treadmill by looking at the averages of all ten trials collectively. Were the olfactory behaviors in these experiments stable, or did they show any dynamic properties? In one scenario, due to olfactory habituation or lack of reward, the performance of these flies would degrade over time.

Consequently, I re-analyzed the food-deprived wild-type fly vinegar approach. As an example from a single fly for 2d trajectory, in the

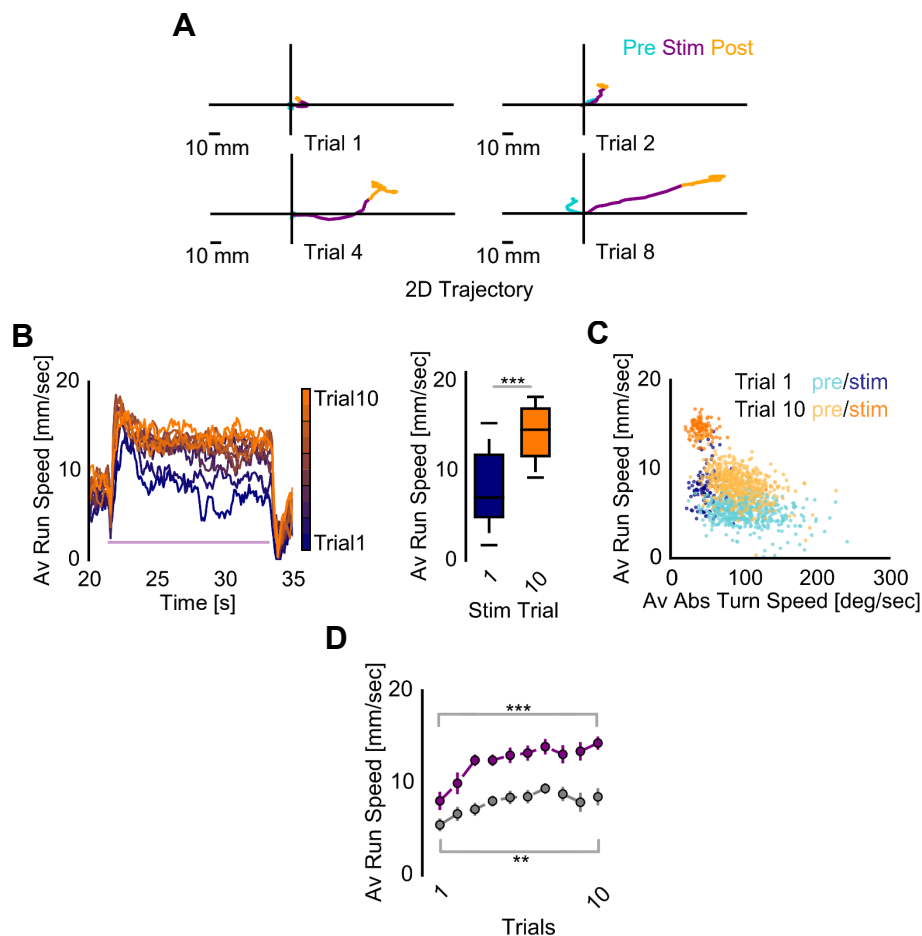


Figure 11 Repeated appetitive odor exposure driven persistence

(A) Representative 2-D reconstructed trajectories for one wild-type CS under repeated vinegar exposure. Trajectories were smoothened with Butterworth filter. (B) Left. Average running speeds of each ten trials of 18 wild-type CS flies over timeframe of a single trial. Right. Boxplot comparison for average running speeds for trial 1 and 10 of 18 CS flies over odor stimulation periods (Data from Figure 3). (C) Scatter plot for running and absolute average speed bins recorded for 100 msec in trial 1 and 10. (D) Evolution of average running speeds in pre- (grey) and during (purple) vinegar stimulation for each trial. Comparison of trial 1 and 10 average running speeds for pre- and stimulation time points.

first trial, I observed that the fly did engage with the odor initially (Figure 11.A). With odor onset, the fly ran forward, however immediately turned in the opposite direction. Interestingly, over the trials, the fly showed even more persistent tracking, exemplified its commitment to odor hunting. Importantly, the increase in persistence was also evident when I looked at all flies in averages, and there was a statistically significant difference between forward running averages of trial 1 and trial 10 during pre- and stimulation phases (Figure 11.B,D). This increase in runs was accompanied by a decrease in turns as visualized in the analysis of average run and turn speed 100-millisecond bins (Figure 11.C). As a result, flies showed higher persistence over time, without any signs of habituation.

Were the speed increments over trials the only parameter changed? To expand my analyses and extract information independent of speed, I decided to execute further investigations.

How long did the activity change over time (Figure 12)? I analyzed the fraction of stimulus time where flies were running before and then compared this to the fraction of time they were active before the odor stimuli (100 msec data bins, threshold 0 mm/s). In the first trial, flies were less active before the odor encounter (Figure 12). Over time, flies became more active in the odor direction during odor stimulation and, overall, this was statistically significant.

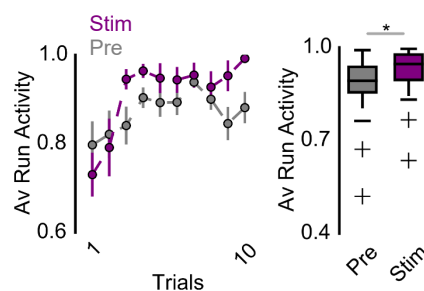


Figure 12 Running activity over repeated vinegar exposures for starved wild-type CS flies

Left. Evolution of running activity over ten trials for 18 CS flies (Data from Figure 3). Right. Boxplot comparison of pre- and stimulation average running activity under vinegar.

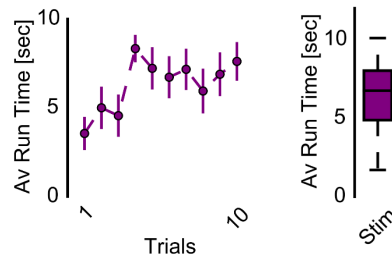


Figure 13 Running bout times over repeated vinegar exposures for starved wild-type CS flies

Left. Evolution of initial running bout times upon odor contact over ten trials for 18 CS flies (Data from Figure 3). Right. Boxplot for average running bout times after vinegar contact.

How long did flies run after encountering an odor plume? I defined running time as the time of a first stop (or turning away) behavioral event recorded within a trial after odor plume encounter. The data were analyzed in 100 msec data chunks, and a 0 mm / sec forward speed threshold designated the stop event. Similar to Figure 12, the average running time within trials was increased monotonically (Figure 13). These two results showed that persistence in odor tracking could be explained as increased engagement in locomotion activity as well.

All data taken together, I concluded that starved flies tracked food odors persistently over time, even in the absence of the reward presentation. This persistence was olfactory dependent. Loss of olfactory input translated into reduced odor approach. Furthermore, neither aversive odors nor baseline air caused attraction.

4.2 Starvation Drives Odor-Guided Locomotion

Since vinegar is a proxy for food for flies, it is possible to postulate hunger as the crucial driving force for persistent odor tracking. Internal states govern animal behavior, and hunger is one of the most robust motivational drives that alter decision making (Sayin et al., 2018).

To evaluate the role of hunger in our paradigm, I tested three groups of wild-type CS flies that were starved for different durations (Figure 14). '0h' describes the flies raised in fresh food daily and kept on food until the start of an experiment. '24 hours' and '48 hours' flies were starved accordingly. Fed flies did not accelerate as

in the other groups despite engaging the plume in the onset and offset (Figure 14.A). Fed flies were slower in average (Figure 14.B), ran shorter in their first bout after odor contact (Figure 14.C). Absolute turning averages were comparable across all three groups (Figure 14.D).

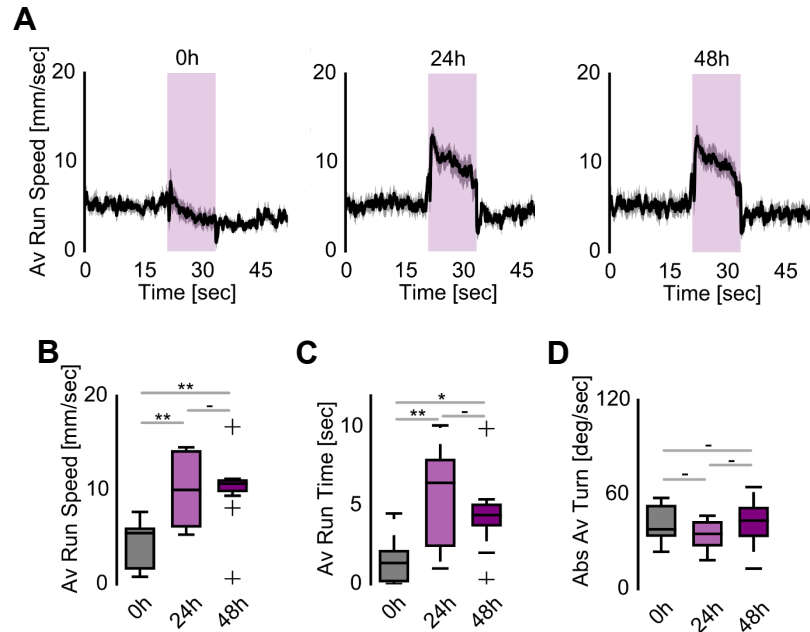


Figure 14 Effects of starvation on persistent odor tracking of wild-type CS flies

(A) Average running speeds over time for wild-type CS flies that are differentially starved (N=10). (B) Boxplot comparison of average running speeds under vinegar exposure during all trials of fed and starved CS flies. (C) Boxplot comparison of average running initial bouts under vinegar contact for all trials of CS flies. (D) Boxplot comparison of average absolute turning speeds for all trials during vinegar exposure for fed and starved CS flies.

Hunger provided a most crucial switch in appetitive behavior and induced odor tracking. However, 24 hours and 48 hours starved flies were similar in their odor approach dynamics. To test whether hunger act as just a switch or a gradient, I devised a closed-loop experiment for the olfactory spherical treadmill (Figure 15). These experiments were executed in ten trials, composed of two phases: open- and closed-loop (Figure 15.A, left). Each stimulation period commenced with the 2-sec vinegar delivery (open-loop). Later, the odor channel was kept on if forward running speed was bigger than the threshold (0 mm/sec, closed-loop). In an analysis for how long flies kept running during the closed-loop, we found that the hungrier flies were running longer over trials (Figure 15.A, right). Run times in closed-loop produced high variation between flies and trials; as a result, I summed up the run times for all trials of a single fly and tested the variance among three

starvation groups. Fed flies failed goodness-of-fit tests (data not shown). Therefore outliers were removed. In average total individual run times, each group was significantly different from each other (Figure 15.B). Flies peaked their run times in different trials, especially some of the 48 hours starved flies generated their maximum as early as the second trial (Figure 15.C). As a result, it was possible to refute that persistence is a by-product of time-spent on the treadmill, in other words,

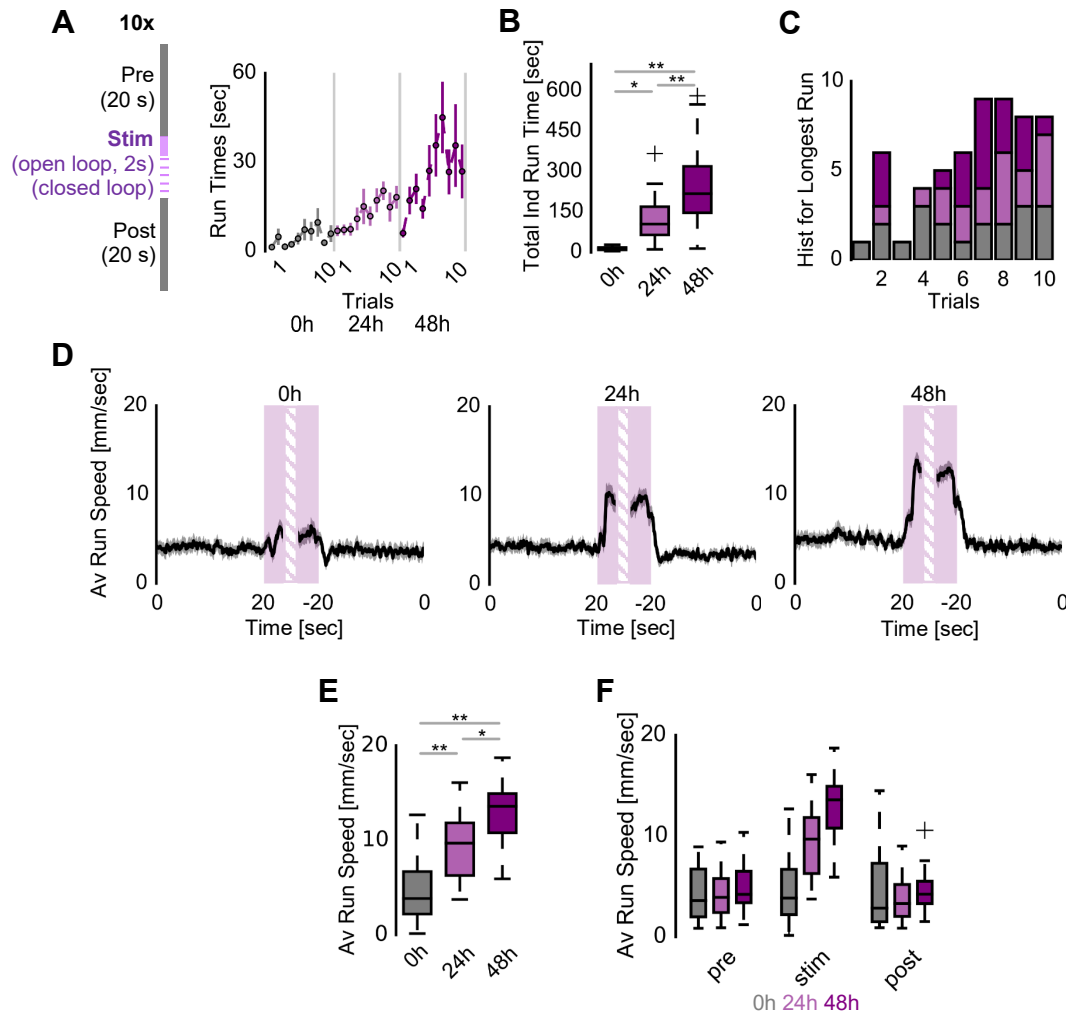


Figure 15 Closed-loop assay for vinegar odor tracking on the treadmill for wild-type CS flies

(A) Left. Schematic of the closed-loop assay. For ten trials, each flies received 2 seconds of odor delivery. This open-loop phase was followed by a closed-loop period, where odor switch-off threshold was 0 mm / sec forward running speed. Right. Evolution of running times only under the closed-loop assay for differentially starved CS flies (N=20/18/19). (B) Boxplot comparison of average summed running times for each CS starvation group. To preserve normal distribution, outliers were removed. (C) Histogram of the longest run performed during the closed-loop phase by a fly within ten trials. (D) Average running speeds over time in open- and closed-loop phases. Speed traces were aligned at the stimulation onset and offset. (E) Boxplot comparison of average running speeds during closed-loop during all trials of fed and starved CS flies. (F) Expanded boxplot comparison of average running speeds for all trials during pre-, post-stimulation and closed-loop phases.

a training effect. While flies were running longer, their average stimulation speeds were higher as well (Figure 15.D). These run speeds during closed-loop application were longer than pre- and post-stimulation speeds for 24 hours and 48 hours starved flies (Figure 15.E).

Hunger can modulate olfactory activity at the periphery and central brain centers. One of the possible explanations for hunger dependent modulation of persistence is increased vinegar-responsive olfactory receptor activity (Root et al., 2011; Semmelhack and Wang, 2009). To reveal how persistence alters and

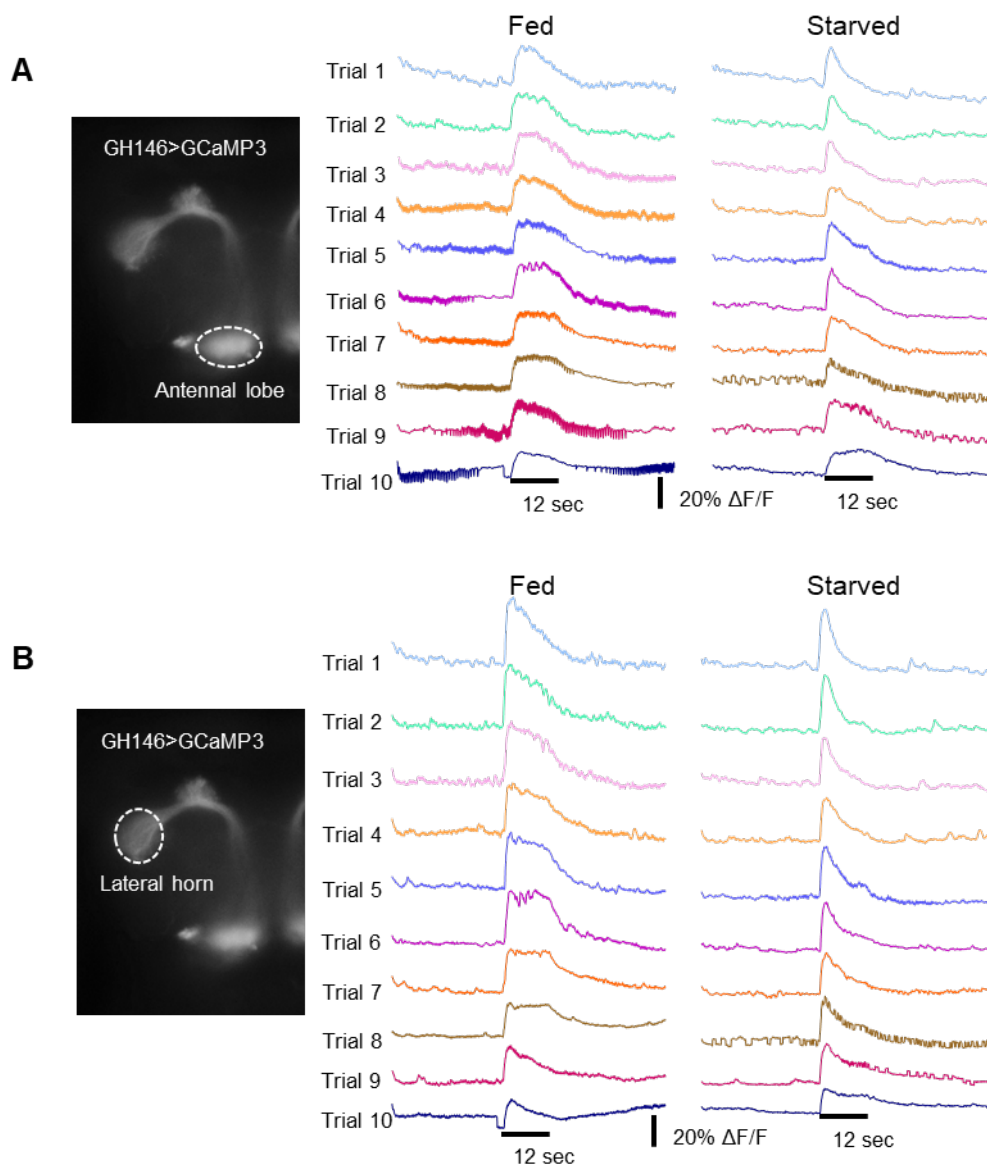


Figure 16 Calcium Imaging in projection neurons under repeated odor exposure

Representative cases for fed and starved flies (*GH146>UAS-GCaMP3*) in the projection neuron calcium responses to repeated vinegar exposures. Repeated 12 sec odor protocol followed the behavioral paradigm. Imaging planes were the antennal lobe (A) and lateral horn (B). Data were generated by Dr. K.P. Siju.

whether hunger would impact the projection neurons (the secondary neurons in the olfactory pathway), Siju Purayil, a postdoctoral research assistant in the laboratory, monitored the neuronal activity of PNs with the calcium indicator, GCaMP (Figure 16). We found no apparent difference between trials and starvation levels at antennal lobe and lateral horn.

In summary, these data suggest hunger acts as the primary motivational force in generating persistent odor tracking in our assay. Furthermore, representative analyses of calcium activity at second-order neurons pointed out any crucial signaling difference arises later in the olfactory circuitry.

4.3 Dopaminergic Input is Required for Persistence

In associative learning, dopaminergic circuits are potent modulators of olfaction and innervate the mushroom body. Since PN imaging (Figure 16) hinted at a role of persistence in the tertiary neurons, we decided to block synaptic output of dopaminergic neurons in our paradigm (Figure 17). In addition, previous data in the laboratory has implicated the mushroom body in hunger state-dependent olfactory decisions (Bräcker et al., 2013; Lewis et al., 2015).

Since neuromodulation can be a potent force in altering circuit dynamics and behavior, we looked for known neuromodulators in the third order neurons. MB receives strong dopaminergic input (Aso et al., 2014a; Oswald and Waddell, 2015). GMR58E02 and TH Gal4 lines label two major distinct *DOPA*⁺ subsets that innervate the adaptive center mushroom body (MB), PAM and PPL1 respectively. Blocking PAM *DOPA*⁺ output did not change vinegar approach from the UAS control flies (Figure 17.B,C,E,F). On the other hand, without TH⁺ *DOPA* activity, flies significantly reduced their odor tracking (Figure 17.A). Over trials, while control and *GMR58E02-Gal4>UAS-Shi^{ts1}* flies increased their runs over trials, TH⁺ *DOPA* blocked flies barely changed their run speeds from trial to trial (Figure 17.B), and consequently, had a lower average running speed (Figure 17.C). Average running activity was comparable for all groups (Figure 17.E), suggesting TH⁺ *DOPA* blocked flies were not stopping under vinegar (Figure 17.F).

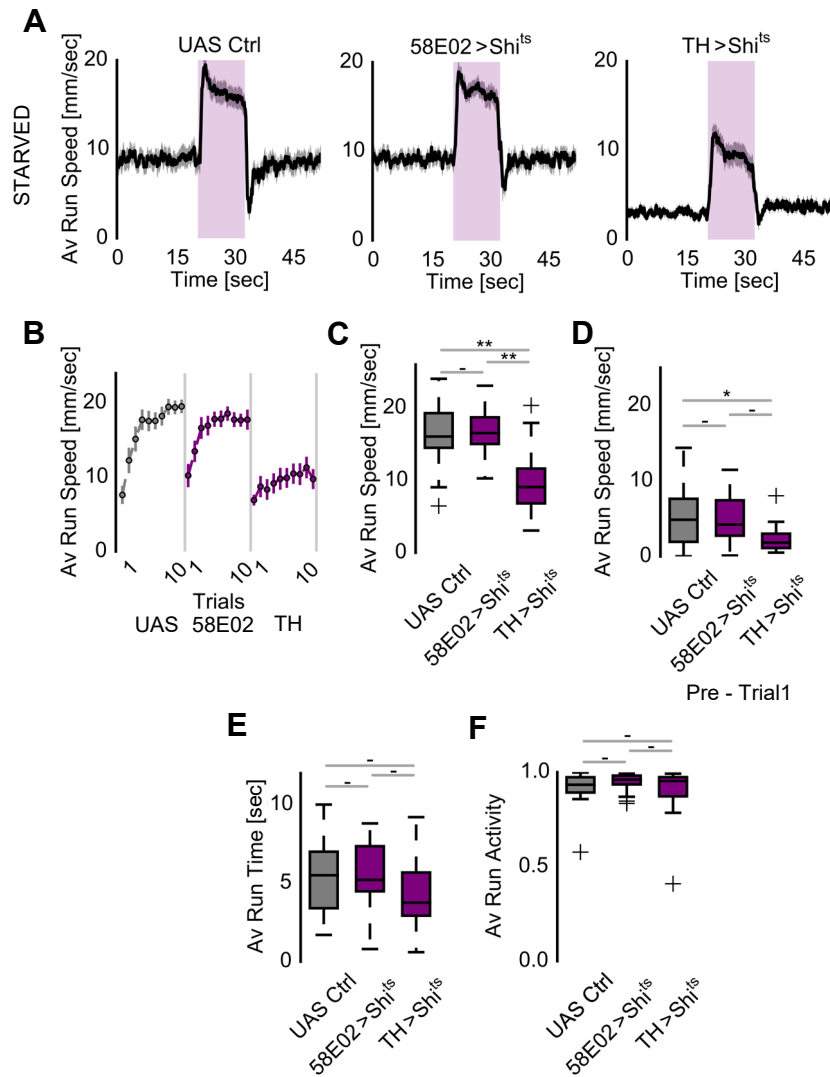


Figure 17 Requirement of TH+ dopaminergic input in forward running during persistence

(A) Average running speeds of UAS control flies (\rightarrow UAS-*Shi^{ts1}*), flies with synaptically blocked subsets of dopaminergic neurons including PAM (*GMR58E02-Gal4*>UAS-*Shi^{ts1}*) and PPL1 (*TH-Gal4*>UAS-*Shi^{ts1}*) clusters over time during vinegar stimulation for ten trials at the non-permissive temperature (N=18). (B) Evolution of running speeds during vinegar exposure over ten trials for each genotype. (C) Boxplot for average running speeds during the stimulation periods of UAS control and *DOPA*+ subset neurons blocked flies. (D) Boxplot for average running speeds in trial 1 pre-stimulation periods of UAS control and *DOPA*+ subset neurons blocked flies. (E) Boxplot for average initial running bouts upon vinegar encounter of UAS control and *DOPA*+ subset neurons blocked flies. (F) Boxplot for average running activity during odor stimulation period of UAS control and *DOPA*+ subset neurons blocked flies.

In absolute turning speeds, TH+ *DOPA* blocked flies were more likely to engage in turns in both pre- and stimulus phases (Figures 18.A-C). Is the lack of persistence an artifact in TH+ flies due to an increased tendency to turn?

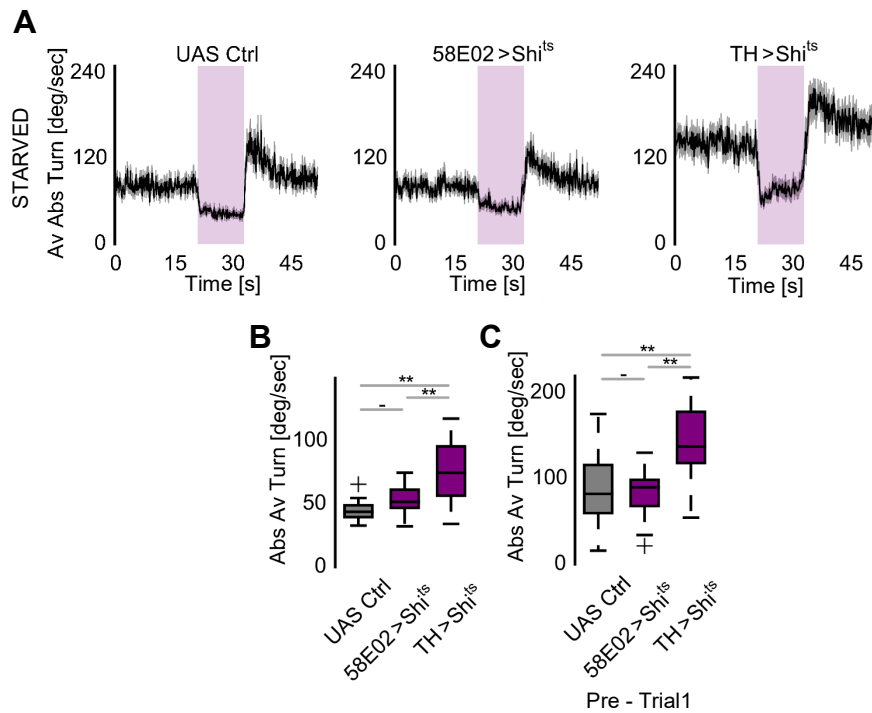


Figure 18 Turning bias in manipulation of TH+ dopaminergic input on the treadmill.

(A) Average absolute turning speeds of UAS control flies (\rightarrow UAS-*Shi^{ts1}*), flies with synaptically blocked subsets of dopaminergic neurons including PAM (*GMR58E02-Gal4*>UAS-*Shi^{ts1}*) and PPL1 (*TH-Gal4*>UAS-*Shi^{ts1}*) clusters over time during vinegar stimulation for ten trials at the non-permissive temperature (Data from Figure 17, N=18). (B) Boxplot for average absolute turning speeds during the stimulation periods of UAS control and *DOPA*+ subset neurons blocked flies. (C) Boxplot for average absolute turning speeds in trial 1 pre-stimulation periods of UAS control and *DOPA*+ subset neurons blocked flies.

To further investigate whether the lack of persistence in the absence of dopamine release from TH+ neurons was due to motor deficits or any biases, I shifted the ambient temperature from 30°C to 35°C with the expectation for higher basal arousal. Indeed, the genetic control (UAS Ctrl group) had a basal running

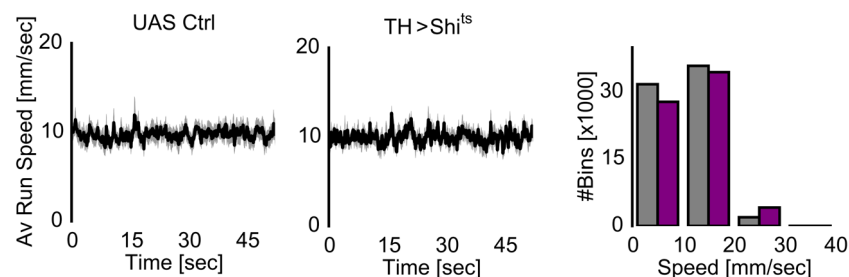


Figure 19 Running performance in the absence of dopaminergic input at 35°C

Left. Average running speeds of UAS control flies (\rightarrow UAS-*Shi^{ts1}*), flies with synaptically blocked dopaminergic neuron PPL1 (*TH-Gal4*>UAS-*Shi^{ts1}*) subtype for ten trials at 35°C (N=10). Right. Histogram for 100 msec data bins of running speed for the control and experimental group.

speed of ~10 mm / sec and TH+ *DOPA* blocked flies showed this same higher speed (Figure 19.A). Furthermore, the detailed analyses of speed distribution revealed that TH+ *DOPA* blocked flies were able to reach speeds as high as 30 mm / sec in 100 msec time frames (Figure 19.B).

Therefore, I can conclude that dopaminergic synaptic release from TH+ neurons is required to generate persistence in hungry flies. Since TH+ *DOPA* blocked flies were able to execute effortful, high speed running at 35°C, the observed phenotypes can be only explained by the necessity of *DOPA* for persistence.

As a next question, I examined the targets of *DOPA*. In associative olfactory learning, dopamine receptors *Dop1R1* and *Dop1R2* fulfill opposite roles: memory formation and active forgetting (Berry et al., 2012). I tested the available mutants for these lines and compared their performance under repeated odor exposure. Removal of *Dop1R1* did not have any noticeable influence in starved flies compared to heterozygous controls (Figure 20).

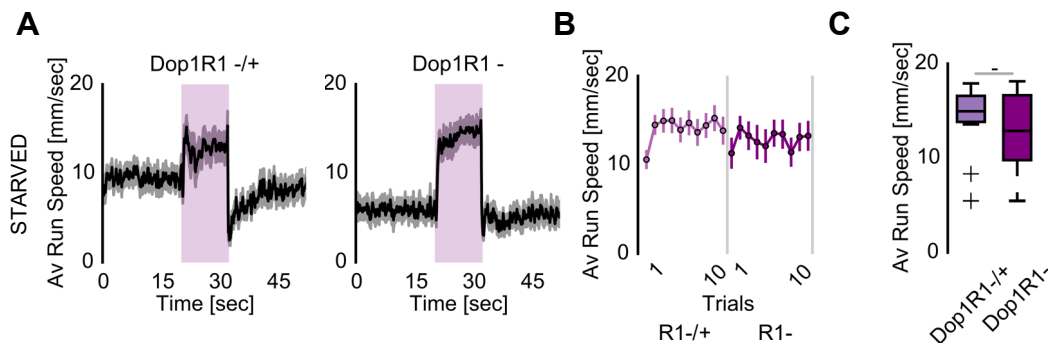


Figure 20 Vinegar response of *Dop1R1* mutants

(A) Average running speeds for dopamine receptor *Dop1R1* heterozygous (*Dop1R1 +/-*) and null mutants (*Dop1R1 -/-*) (N=10). (B) Trial by trial average running speeds for dopamine receptor 1 mutants. (C) Boxplot presentation for *Dop1R1 +/-* and *Dop1R1 -/-*.

On the other hand, while *Dop1R2* heterozygous mutants performed well, the null *R2* mutants had a significant reduction in vinegar tracking (Figure 21). Interestingly, *Dop1R2* mutants progressively responded in slower speeds to odor exposure; the difference between null and heterozygous mutants emerged in the later trials (Figure 21.B).

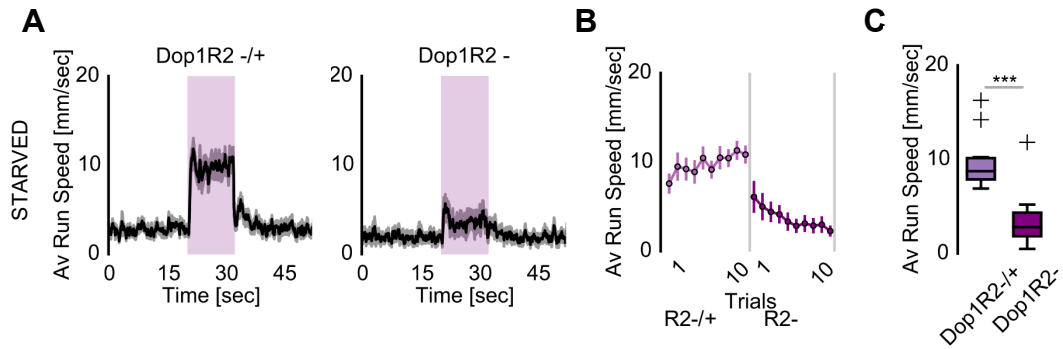


Figure 21 Vinegar response of *Dop1R2* mutants

(A) Average running speeds for dopamine receptor *Dop1R2* heterozygous (*Dop1R2* ^{-/+}) and null mutants (*Dop1R2* ⁻) (N=10). (B) Trial by trial average running speeds for *Dop1R2* mutants. (C) Boxplot presentation for *Dop1R2* ^{-/+} and *Dop1R2* ⁻.

Analyses of *Dop1R* mutants exposed *Dop1R2* as a crucial component of the persistence circuitry. Flies lacking *Dop1R2* not only could not commit more effort in odor tracking over successive trials but also failed to maintain their behavior. Highly possibly, *Dop1R2* receptors are at the receiving end for dopamine released by neurons labeled by TH-Gal4.

4.4 Mushroom Body Output is Crucial for Innate Odor Attraction

Learning and memory center, mushroom body (MB) is tiled by dense dopaminergic input. (Aso et al., 2014a; Heisenberg, 2003). The previous section established *DOPA* as the driving force behind persistence; therefore MB would be an ideal mediator for this motivational phenomenon. Moreover, MB consists of recurrent circuits: an ideal architectural feature for persistence (Major and Tank, 2004). Lastly, previous works suggest MB was essential for integrating hunger state in the suppression of innate aversion (Bräcker et al., 2013; Lewis et al., 2015). Could MB also have a role in supporting innate odor attraction?

To answer these questions, we employed a high-throughput method to screen all transgenically available mushroom body output neurons. In the primary screen, Laurence Lewis, also a graduate student in the laboratory, tested 25 lines in the T-maze at non-permissive temperature while using *UAS-Shi^{ts1}* as an effector (Figure 22.A). Removing synaptic output of horizontal lobe MBONs in the T-maze

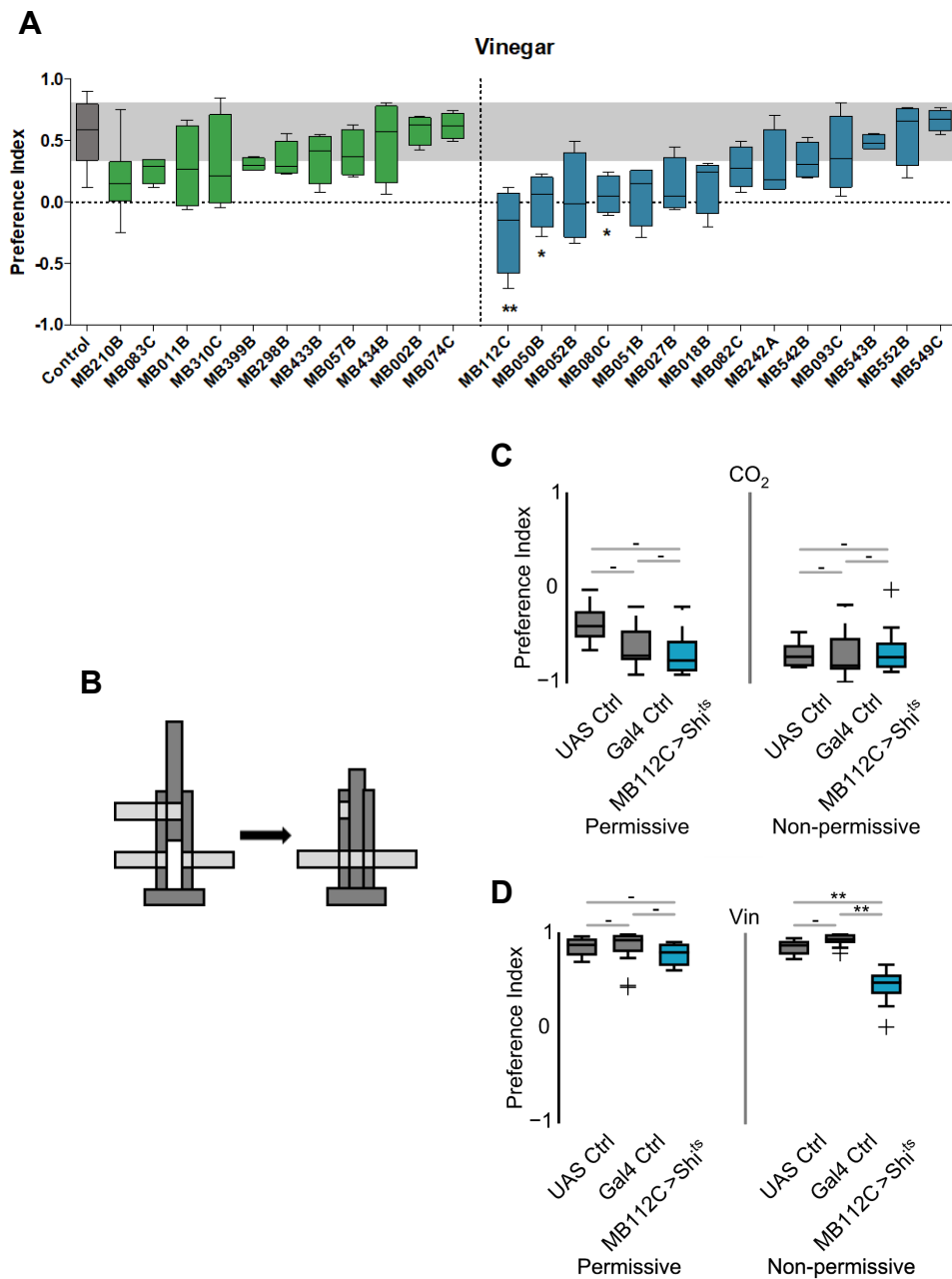


Figure 22 Mushroom body output neuron necessity screen for vinegar attraction in T-maze

(A) T-maze screen results for MBON split-Gal4 lines of starved flies in vinegar attraction at non-permissive temperature where MBON activities were blocked. Preference index for control (*pBDP-Gal4U>UAS-Shi^{ts1}*, pooled from N=46-48) and MB split lines (*MB>UAS-Shi^{ts1}*, N=4-8) were calculated after a decision window of 1 minute (Kruskal-Wallis ANOVA with Dunn's post-hoc test). (B) Schematic of T-maze. Flies were loaded into an elevator and then lowered to the decision point. In the decision point, flies were given the choice of exploring two tubes (odor vs blank). (C) Confirmation experiments for MVP2 (*MB112C>UAS-Shi^{ts1}*) under permissive (MVP2 synaptic activity unperturbed) and non-permissive (MVP2 output blocked) temperatures in comparison to UAS and Gal4 controls for CO₂ (N=16/8/16). (D) Confirmation experiments for MVP2 (*MB112C>UAS-Shi^{ts1}*) under permissive and non-permissive temperatures in comparison to UAS and Gal4 controls for CO₂ (N=16/8/16). Performed by Laurence Lewis.

did not abolish preference for vinegar. On the other hand, several lines gave a loss-of-function phenotype (MB112C: MVP2 / MBON- γ 1pedc> α/β : MB50B: MBON- α '1, MBON- α 2sc; MB080C: MBON- α 2sc). Since silencing MVP2 (MBON- γ 1pedc> α/β) showed the strongest perturbation and its prominent role in integrating hunger state during learning (Perisse et al., 2016), Laurence Lewis focused on this neuron in the confirmation experiments (Lewis et al., 2015). Loss of MVP2 activity did not alter fly aversive odor responses (Figure 22.C), while the vinegar attraction was significantly reduced only for the experimental group flies (*MB112C>UAS-Shi^{ts1}*) in the non-permissive temperature (Figure 22.D). At the permissive temperature where dominant negative impact of mutant dynamin was absent, vinegar attraction was restored in all genotypes. On the spherical treadmill, blocking MVP2 generated a similar phenotype without altering turning behavior or baseline running (Figure 23).

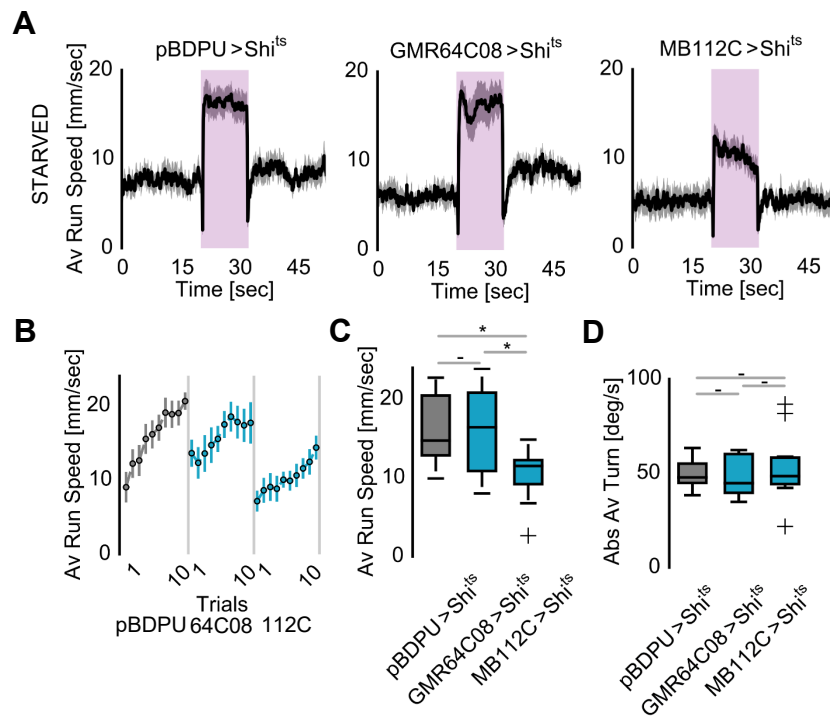


Figure 23 Thermogenetic block of MB γ Kenyon cell and MVP2 synaptic output in starved flies

(A) Average running speeds of UAS control (*pBDP-Gal4U>Shi^{ts1}*) and MB γ KC (*GMR64C08-Gal4>Shi^{ts1}*) and MVP2 (*MB112C>Shi^{ts1}*) blocked flies over time during vinegar presentation over ten trials (N=10). (B) Evolution of running speeds during vinegar presentation over ten trials for each genotype. (C) Boxplot for average running speeds during the stimulation periods of UAS control and γ KC and MVP2 blocked flies. (D) Boxplot for average running speeds in pre-stimulation periods of UAS control and γ KC and MVP2 blocked flies. (E) Boxplot for average absolute turning speeds during the stimulation periods of UAS control and γ KC and MVP2 blocked flies.

Due to the critical role of MVP2 presence for vinegar approach we postulated that it would also be sufficient to promote internal state integration. To test this idea, we decided to employ optogenetics in high temporal control of MVP2 activation (Figure 24). In the optogenetic protocol, flies would receive ten trials of concurrent odor and LED (617 nm, ~30 $\mu\text{W} / \text{mm}^2$) stimulation. The odor onset command preceded optogenetic onset by 2 seconds. This window was used as an internal control to assess flies odor responses in the absent of optogenetic stimulation. Subsequently, I tested fed flies' odor response upon MVP2 depolarization (Figure 24). To reduce visual artifacts, I introduced a constant basal LED light at very low intensity, which would be insufficient to drive CsChrimson. Acute activation of MVP2 (*MB112C>UAS-CsChr*) led to increased running over trials in comparison to controls (Figure 22.B,C). The running bouts were also longer; however, it was only statistically significant against the Gal4 control genotype (Figure 24.D). Regardless, flies were more active when MVP2 neurons were depolarizing (Figure 24.F).

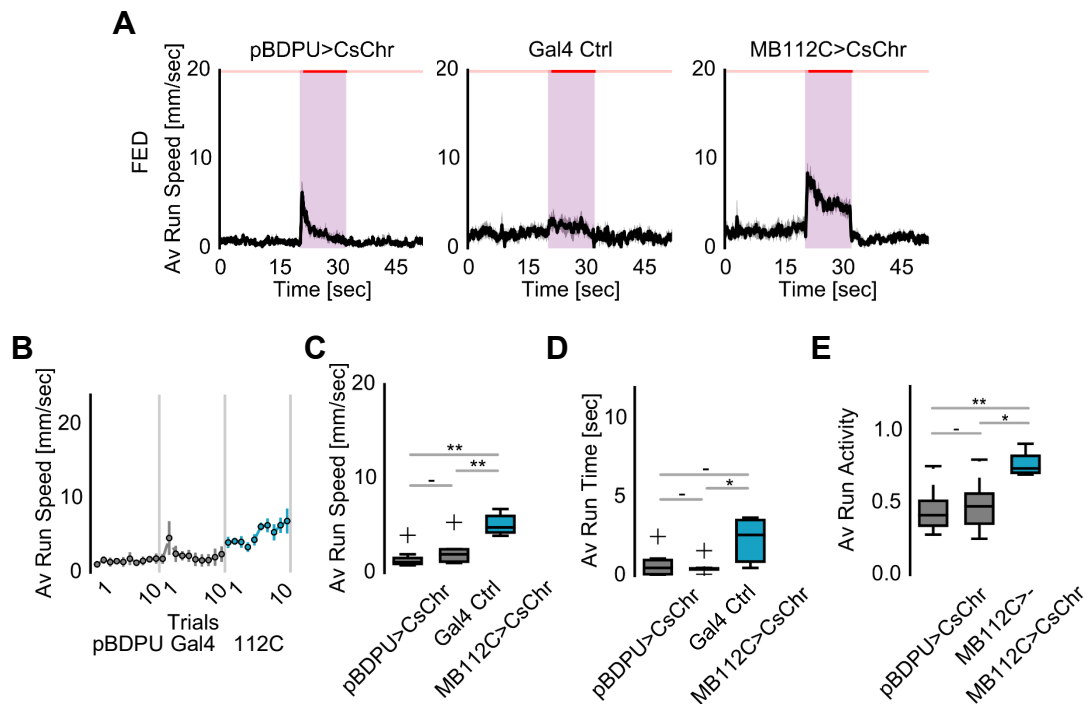


Figure 24 Optogenetic activation of MVP2 neurons activity while odor tracking in fed flies

(A) Average running speeds of UAS (*pBDP-Gal4U>UAS-CsChr*) and Gal4 (*MB112C>-*) control and MVP2 targeted (*MB10B>UAS-CsChr*) fed flies during optogenetic activation experiment for ten trials (N=10). To reduce light onset artifact, low intensity LED light was present throughout the trials. (B) Evolution of running speeds during concurrent vinegar exposure and optogenetic manipulation over ten trials for each genotype in fed flies. (C) Boxplot comparison for average running speeds during the stimulation periods of controls and MVP2 activated fed flies. (D) Boxplot for average running speeds in pre-stimulation periods of controls and MVP2 activated fed flies. (E) Boxplot comparison for average running bout times after optogenetic of controls and MVP2 activated fed flies. (F) Boxplot comparison of average running activity during times optogenetic onset of controls and MVP2 activated fed flies.

Depolarizing MVP2 optogenetically in 24 hours starved flies did not further increase locomotion in the absence or presence of odors (Figure 25, 26). Under starvation, it is probable that MVP2 neurons were already saturated with odor only stimulation and optogenetic activation did not further increase MVP2 activity.

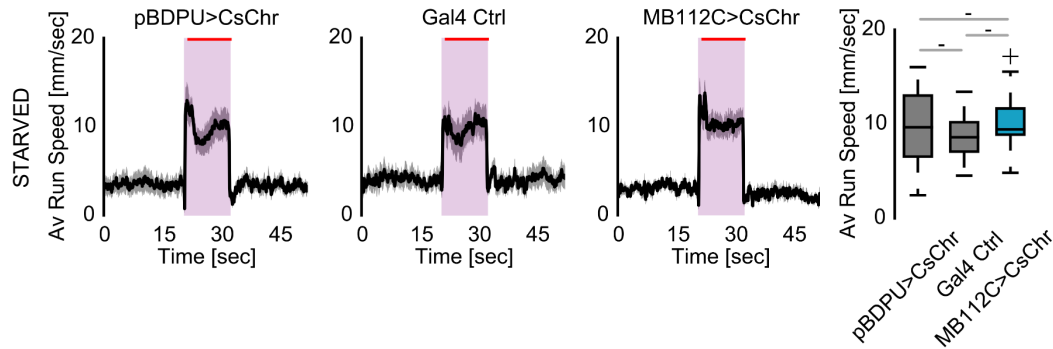


Figure 25 Optogenetic activation of MVP2 neurons activity while odor tracking in starved flies

Left. Average running speeds of UAS (*pBDP-Gal4U>UAS-CsChr*) and Gal4 (*MB112C>-*) control and MVP2 targeted (*MB112C>UAS-CsChr*) 24 hour starved flies during optogenetic activation experiment for ten trials (N=10). Right. Boxplot comparison for average running speeds during the stimulation periods of controls and MVP2 activated starved flies.

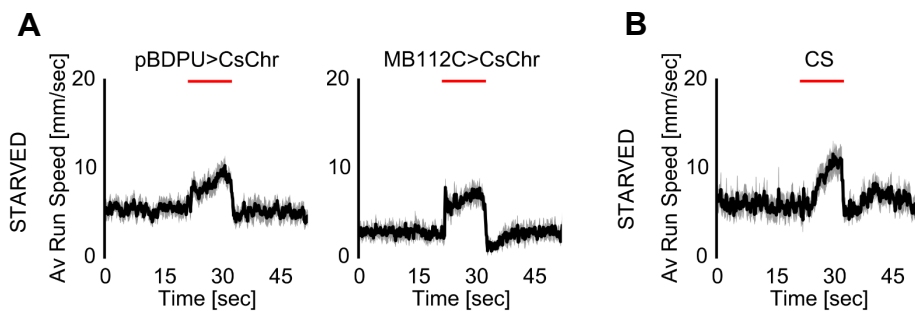


Figure 26 Optogenetic only activation of MVP2 neurons

(A) Average running speeds of UAS control (*pBDP-Gal4U>UAS-CsChr*) and experimental group (*MB112C>UAS-CsChr*) starved flies for ten trials without odor presentation (N=10). (B) 24h starved wild-type CS behavior in “optogenetic only” experiment (N=10).

Interestingly, ~30 min long chronic activation of MVP2 in fed flies via thermogenetics did not recapitulate acute MVP2 activation (Figure 27). All of these results advocate that MVP2 neurons were sufficient to integrate hunger state in a temporally restricted, dynamic mode.

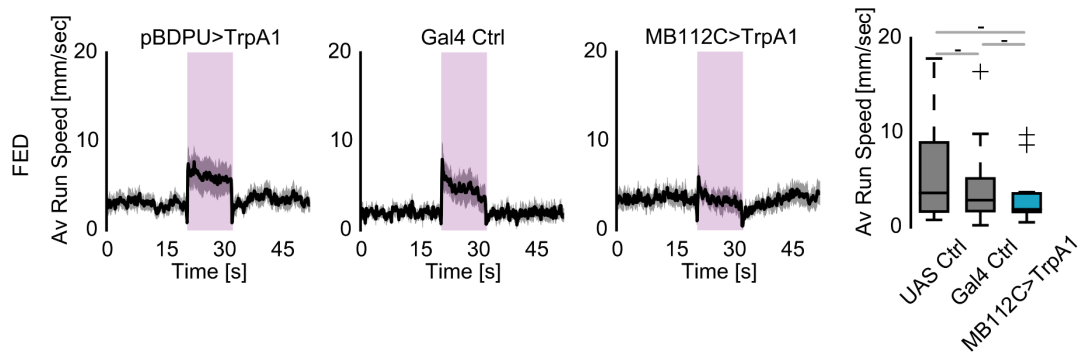


Figure 27 Chronic activation of MVP2 neurons activity during vinegar exposure in red flies

Left. Average running speeds of UAS (*pBDP-Gal4U>UAS-TrpA1*) and Gal4 (*MB112C>-*) control and thermogenetically activated MVP2 (*MB112C>UAS-TrpA1*) fed flies during ten trials (N=10). Right. Boxplot comparison for average running speeds during vinegar input for controls and MVP2 activated fed flies.

Taken together, these results firmly establish mushroom body output neurons as processors of innate olfactory attraction. They also support the claim the MB is more than learning and memory center. Furthermore, MVP2, in particular, is shown here to provide the motivational switch dynamically for hunger state.

4.5 Octopamine Underlies Transition from Olfaction to Exploitation

4.5.1 Activation of Taste Neurons Counteracts Olfaction

As explored in the previous part, hunger drove a strong impulse on behavior. Kept unchecked, uncontrolled impulses result in behavioral inflexibility, which may be detrimental to survival. So then next, we asked how this impulse is controlled? Odor tracking is not the end goal. It is just one of the sequential behaviors that are part of feeding. Animals first track odor plumes, then evaluate a food patch and lastly ingest. For successful execution of feeding, it is possible that the following sequence could inhibit the previous one for successful sequence transition (Seeds et al., 2014).

To test this hypothesis, we artificially activated two gustatory receptors while presenting vinegar to the flies (Figure 28). Gr5a conveys only sweet taste from the periphery and would be activated when a fly encounters a sweet food patch. In addition to the periphery, the other receptor Gr43a which is present both in pharynx

and brain, so it is active during ingestion and post-ingestion. Activation of both sweet taste receptors led to immediate but transient stop (Figure 28.A). The Gr5a activated flies immediately reverted back to follow the odor cue while activating Gr43a neurons resulted in a sustained reduction. In average, for both genotypes, reduced odor tracking was observed upon Gr activation (Figure 28.B, C). However,

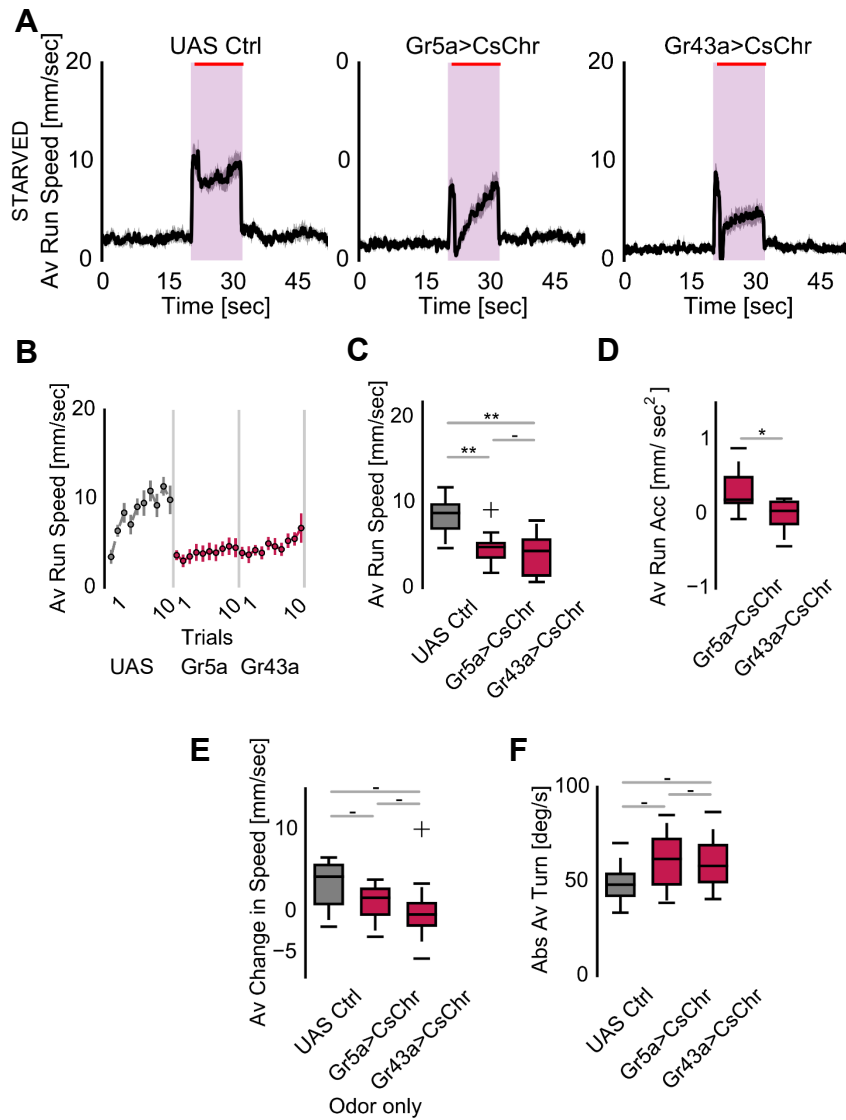


Figure 28 Optogenetic activation of gustatory receptors during vinegar approach

(A) Average running speeds of UAS control (*pBDP-Gal4U>UAS-CsChr*) and Gr activation groups (*Gr5a>UAS-CsChr* and *Gr43a>UAS-CsChr*) for ten trials in simultaneous odor presentation and optogenetic manipulation under starvation conditions (N=10). (B) Evolution of running speeds during concurrent vinegar exposure and optogenetic manipulation. (C) Boxplot comparison for average running speeds during optogenetic activation for control and Gr activated starved flies. (D) Boxplot comparison for average running acceleration from optogenetic onset to offset for Gr5a and Gr43a activated starved flies. (E) Boxplot for average change in running speeds during odor only phase. Odor only phase has been calculated by normalization to the average speed in the first trial. (F) Boxplot for average absolute turning speeds during the simultaneous stimulation periods.

due to the continuous suspension of running by Gr43a activation, there was a critical difference in acceleration between two experimental groups (Figure 28.D). Since odors and sugar sensation can be paired during learning, we also asked whether previous simultaneous presentation would alter subsequent vinegar approach behavior. For this, I normalized average run speeds in odor only phase (trial 2 to trial 10) to the average run speed of the first trial (before optogenetic manipulation) and compared within three groups. While Gr activation in the first trial caused a reduced odor tracking when compared to UAS control flies, this was not significant (Figure 28.E). Artificial sugar taste did not lead to a change in turning behavior (Figure 28.F). To recapitulate, reward presentation temporarily suppressed persistent odor tracking.

Previously, it has been shown that Gr43a⁺ neurons in the protocerebrum acts an internal nutrient sensor and modulate odor valence during learning in a bidirectional manner dependent on the current hunger state (Miyamoto et al., 2012). During ingestion, Gr43a neurons might take over the immediate nutrient sensors. Jean-Francis de Backer, a postdoctoral fellow in the laboratory, performed *ex vivo*

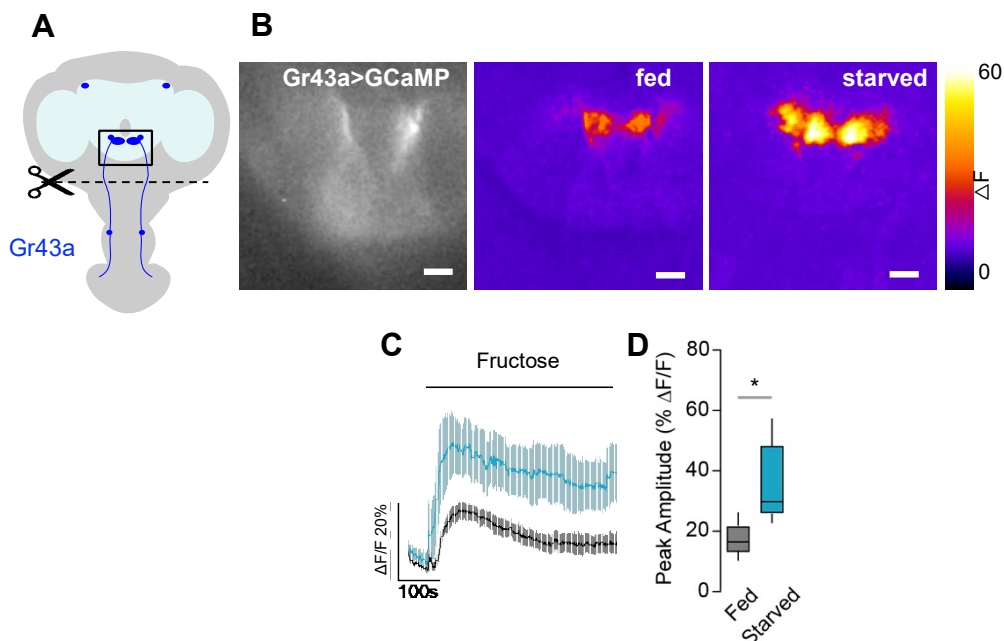


Figure 29 Calcium imaging of Gr43a neurons in SEZ *ex vivo*

(A) Schematics of *ex vivo* SEZ imaging. (B) Representative true baseline and pseudocolored GCaMP signal images recorded in fed and starved flies. (C) Calcium signal of *Gr43a>UAS-GCaMP6f* monitored in Gr43a neuron axon terminals upon fructose bath application *ex vivo*. (D) Comparison of GCaMP activity in fed and starved flies (N=8/5). Performed by Jean-Francois De Backer.

calcium imaging on Gr43a neurons. These neurons responded to continuous bath application (Figure 29.A) in a state-dependent manner (Figure 29.B). The sustained activity of Gr43a in the periphery suggests that indeed Gr43a neuronal activity recapitulates the dynamics observed during the behavior in Figure 28. Furthermore, since we ablated pharyngeal input to Gr43a neurons, only fructose information received by them was internal sugar. This proves that Gr43a in SEZ can also function as internal sugar sensors as Gr43a neurons in the protocerebrum.

To sum up, I was able to exhibit that concurrent activation of gustatory neurons reduced olfactory tracking to enable a successful transition from exploration to exploitation. Since feeding starts with gustation and then proceeds with ingestion, Gr43a neurons represented the latter stages of feeding (ingestion and post-ingestion); thus activation of Gr43a neurons induced a more potent, sustained brake on olfaction.

4.5.2 Octopaminergic Neurons Control the Transition

The SEZ harbors a high number of octopaminergic (OA) neurons; therefore OA+ neurons are suited to carry gustatory information to higher centers (Burke et al., 2012; Busch et al., 2009). Furthermore, OA has been implicated in feeding regulation (Zhang et al., 2013). I repeated the previous gustatory neuron activation assay for acute depolarization of octopaminergic neurons (Figure 30).

In starved flies, activation of OA+ neurons arrested odor tracking immediately (Figure 30.A-C,E.). The observed effect was stronger than Gr activation (Figure 28). *Tdc2-Gal4>UAS-CsChr* flies did not have a motor defect, and slightly reduced turning as well (Figure 30.D,F). Furthermore, *Tdc2-Gal4>UAS-CsChr* flies were able to respond to odor clearly in the absence of optogenetic manipulation (Figure 30.G,H). Since the *Tdc2-Gal4* transgenic line has expression in both the fly brain and ventral nerve chord, we asked whether OA modulation of appetitive odor approach occurs in the central or peripheral nervous system. *Tsh-gal80* abolishes Gal4 activity in ventral nerve chord (Clyne et al., 1999). The preliminary experiments showed that OA+ VNC neurons were disposable and

activation of only *OA+* neurons in the brain was sufficient to stop odor tracking (Figure 30.I).

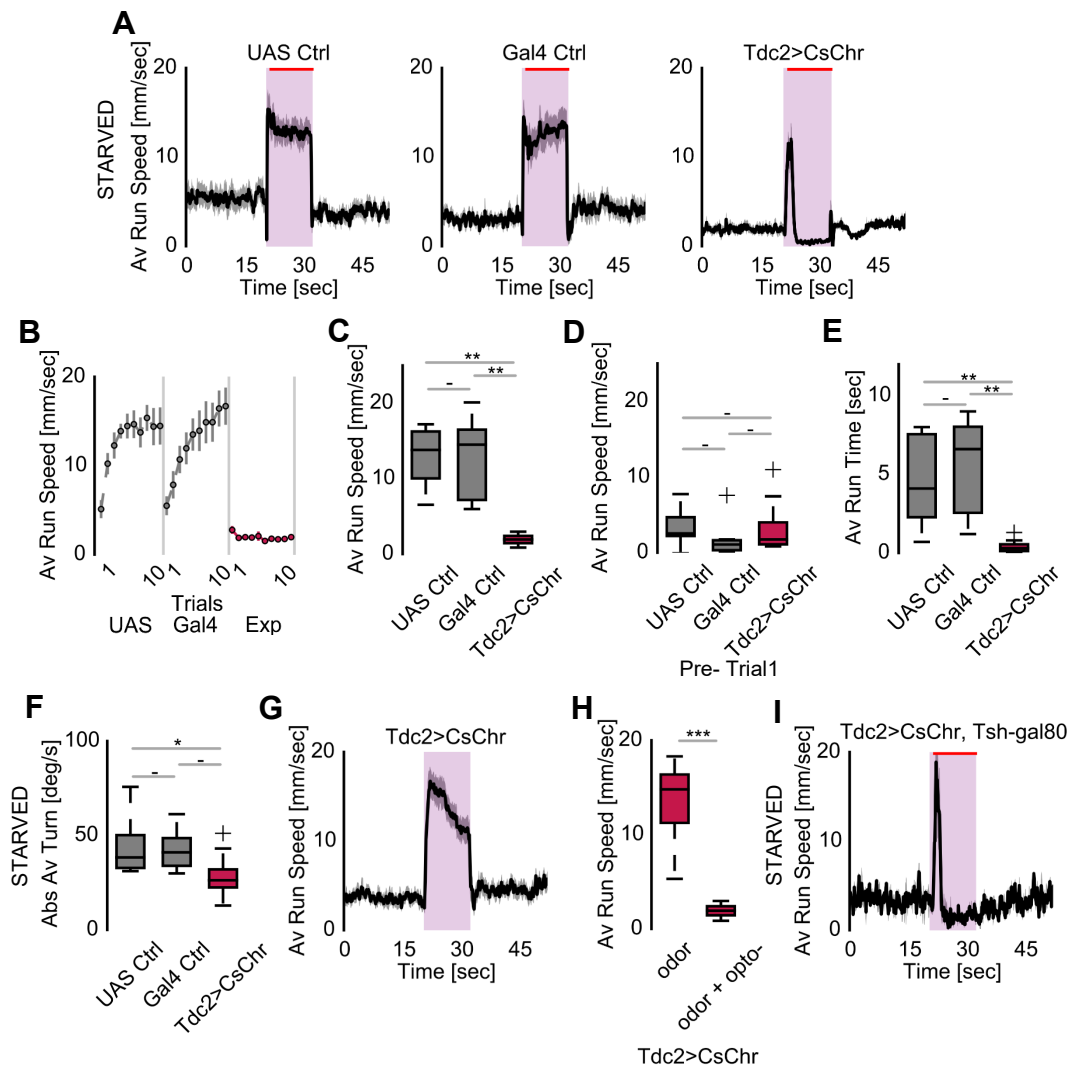


Figure 30 Acute activation of *Tdc2+* octopaminergic neurons in vinegar tracking of starved flies

(A) Average running speeds of UAS (\rightarrow UAS-*CsChr*) and Gal4 (*Tdc2-Gal4* \rightarrow) control flies in comparison to flies with optogenetically activated *Tdc2+* octopaminergic neurons (*Tdc2-Gal4* \rightarrow UAS-*CsChr*) under starvation (N=10). (B) Evolution of running speeds during vinegar and optogenetic stimulation over ten trials for controls and the experimental group. (C) Boxplot comparison for average running speeds during optogenetic stimulation for controls and *Tdc2+* activated starved flies. (D) Boxplot comparison for average running speeds in the first trial prior to odor presentation and optogenetic manipulation for controls and *Tdc2+* activated starved flies. (E) Boxplot comparison for average first running bout times after optogenetic onset of controls and experimental *Tdc2-Gal4* \rightarrow UAS-*CsChr* flies. (F) Boxplot for average absolute turning speeds during the stimulation periods of controls and experimental *Tdc2-Gal4* \rightarrow UAS-*CsChr* flies. (G) Average running speeds of experimental flies expressing *CsChrimson* in *Tdc2+* octopaminergic neurons (*Tdc2-Gal4* \rightarrow UAS-*CsChr*) under starvation in the absence of optogenetic manipulation (N=10). (H) Boxplot comparison for average running speeds of flies expressing *CsChrimson* in *Tdc2+* octopaminergic neurons (*Tdc2-Gal4* \rightarrow UAS-*CsChr*) in the presence or absence of optogenetic stimulation under starvation (Data from Figure 31.A and G). (I) Average running speeds flies expressing *CsChrimson* exclusively in central *OA* neurons (*Tdc2-Gal4* \rightarrow UAS-*CsChr*, *Tsh-gal80*) (N=10).

Chronic activation of OA+ neurons recapitulated the acute activation with immediate stop, reduced average speed and run times (Figure 31.A-C,D). Chronic and acute gain-of-function experiments highlight that the phenotypes I observed were odor-induced. Activation of *Tdc2+* did not halt the flies before or after odor exposure (Figure 31.A,E). Turns were also comparable to the controls (Figure 31.F).

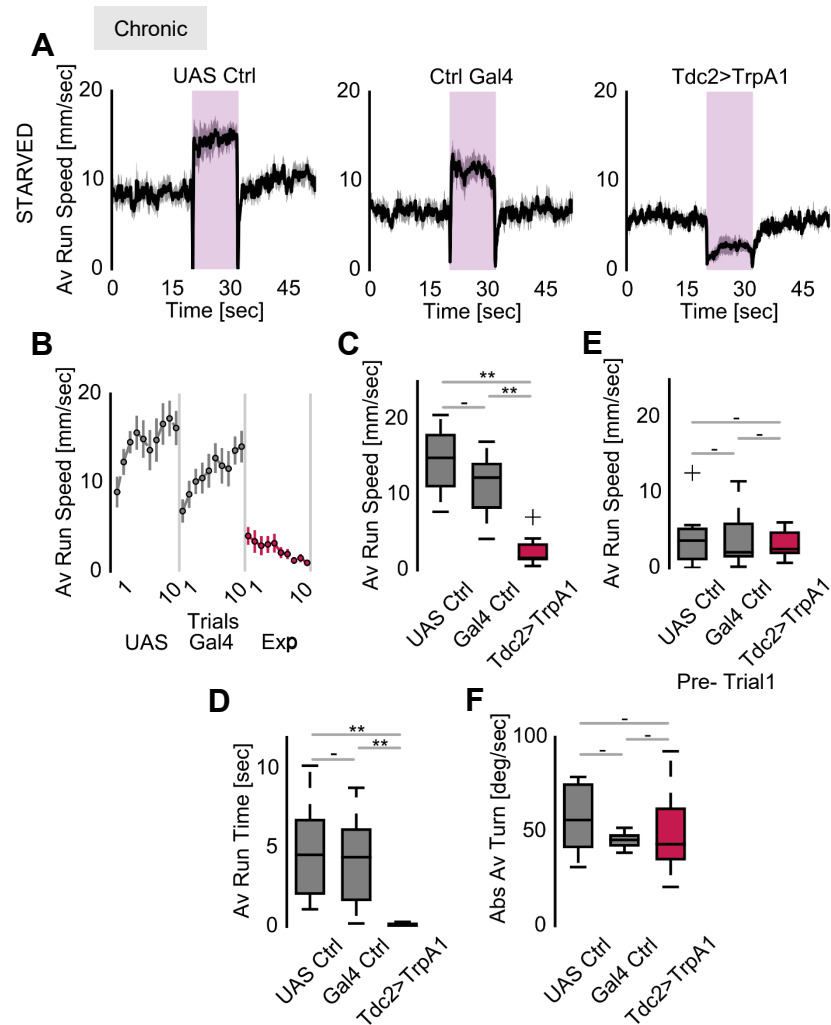


Figure 31 Chronic activation of *Tdc2+* neurons in vinegar tracking of starved flies

(A) Average running speeds of UAS (\rightarrow UAS-*TrpA1*) and Gal4 (*Tdc2-Gal4* \rightarrow) control flies in comparison to flies with thermogenetically activated *Tdc2+* octopaminergic neurons (*Tdc2-Gal4* \rightarrow UAS-*TrpA1*) under starvation (N=10). (B) Evolution of running speeds during vinegar stimulation over ten trials for controls and the experimental group. (C) Boxplot comparison for average running speeds during odor stimulation for controls and *Tdc2+* activated starved flies. (D) Boxplot comparison for average running speeds in the first trial prior to odor delivery for controls and *Tdc2+* activated starved flies. (E) Boxplot comparison for average first running bout times after odor onset of controls and experimental *Tdc2-Gal4* \rightarrow UAS-*TrpA1* flies. (F) Boxplot for average absolute turning speeds during the stimulation periods of controls and experimental *Tdc2-Gal4* \rightarrow UAS-*TrpA1* flies.

Activation of OA+ neurons in fed flies did not generate a significant reduction in speed during odor stimulation as fed flies rarely engaged in sustained odor tracking (Figure 32).

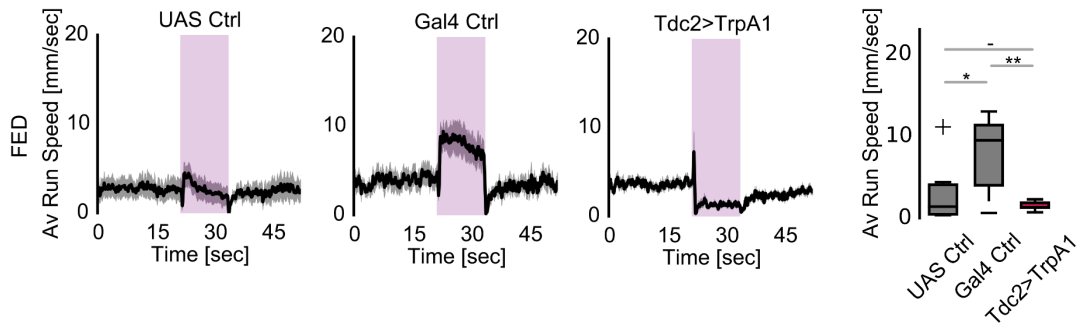


Figure 32 Chronic activation of Tdc2+ neurons in vinegar tracking of fed flies

Left. Average running speeds of UAS (\rightarrow UAS-*TrpA1*) and Gal4 (*Tdc2-Gal4* \rightarrow) fed control flies in comparison to fed flies with thermogenetically activated Tdc2+ octopaminergic neurons (*Tdc2-Gal4* \rightarrow UAS-*TrpA1*) (N=8/9/9). Right. Boxplot comparison for average running speeds during odor stimulation for controls and Tdc2+ activated fed flies.

Olfactory responses are odor concentration-dependent (Galizia, 2014). The OA activation phenotype observed so far could be due to broadening aversive response window of the flies. Consequently, I also probed OA mediated arrest in 1% and 5% vinegar concentrations (Figure 33). These flies reiterated stopping behavior under such low concentrations, as in 20% vinegar exposure (Figure 31).

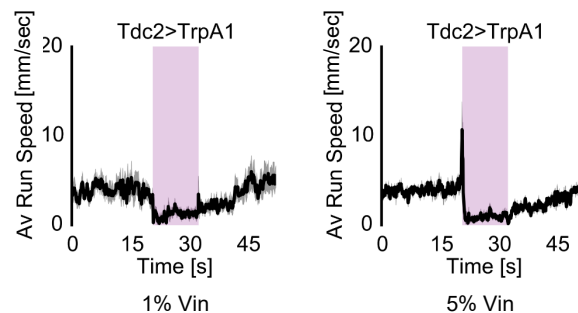


Figure 33 Chronic activation of Tdc2+ neurons in lower concentration tracking of starved flies

Left. Average running speed over ten trials for starved *Tdc2-Gal4* \rightarrow UAS-*TrpA1* flies under 1% vinegar odor presentation (N=4). Right. Average running speed over ten trials for starved *Tdc2-Gal4* \rightarrow UAS-*TrpA1* flies under 5% vinegar odor presentation (N=4).

Lastly, air only responses were found to be no different from the controls (Figure 34). This suggests stimulus valence is significant for OA induced arrest.

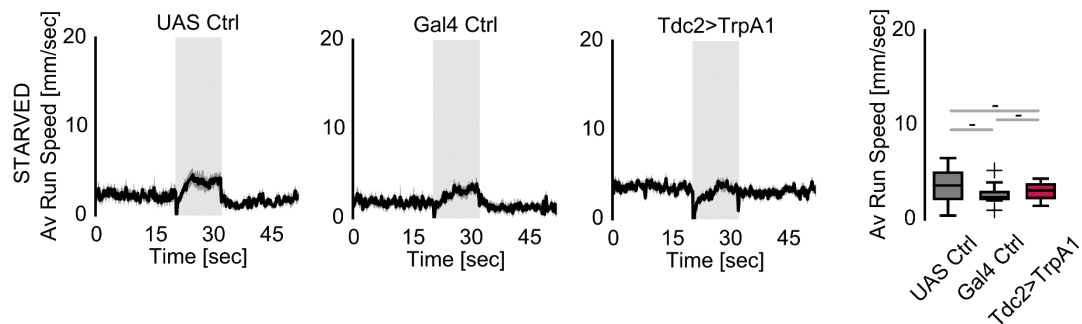


Figure 34 Chronic activation of Tdc2+ neurons during air stimulation of starved flies

Left. Average running speeds of UAS (\rightarrow UAS-*TrpA1*) and Gal4 (*Tdc2-Gal4*>-) starved control flies and starved flies with thermogenetically activated Tdc2+ octopaminergic neurons (*Tdc2-Gal4*>UAS-*TrpA1*) under air only delivery (N=10). Right. Boxplot comparison for average running speeds during air stimulation for controls and Tdc2+ activated starved flies.

Could the arrest caused by depolarizing OA+ neurons might be a by-product of non-olfactory processes? Octopamine can be a culprit of inducing aggression, rendering flies smell-blind, promoting seizures. To address such issues, the project student I supervised Lisa Marie Frisch, who performed 4-arm behavioral arena

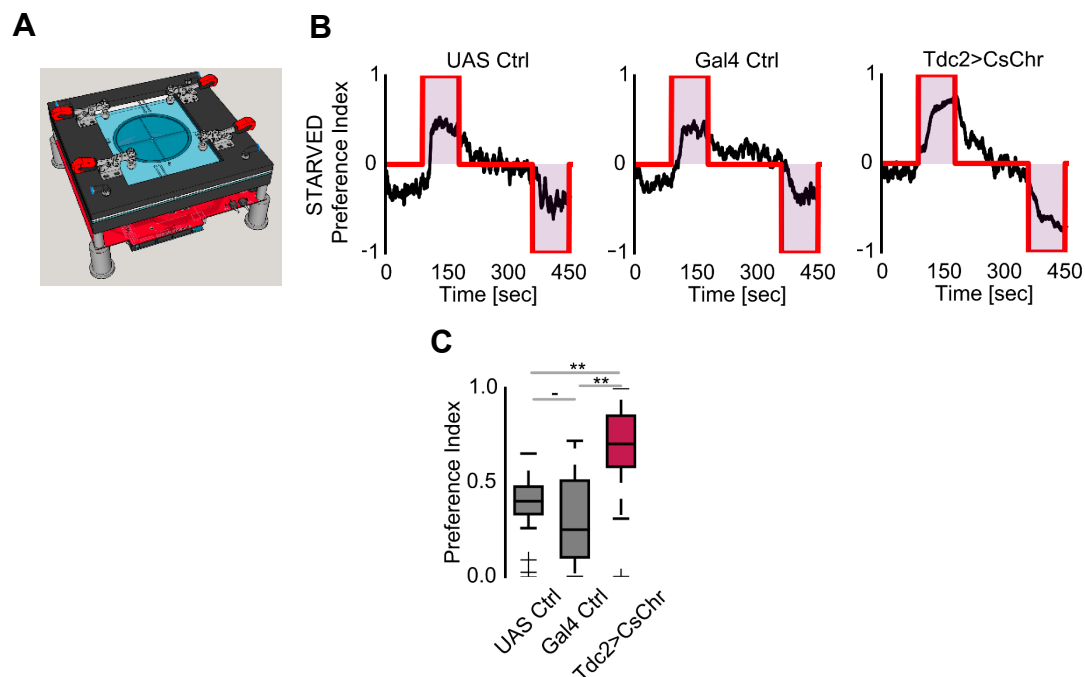


Figure 35 Optogenetic activation of Tdc2+ neurons in the arena assay

(A) Combined olfactory and optogenetics arena. (B) Average preference index over time for starved UAS (\rightarrow UAS-*CsChr*) and Gal4 (*Tdc2*>-) control and experimental flies (*Tdc2*>UAS-*CsChr*) under concurrent odor and optogenetic presentation. Stimuli were represented first in quadrant 1 and 3, then in reciprocal quadrant (2 and 4). Fly accumulation in quadrant 1 and 3 corresponded to positive preference indices results, whereas quadrant 2 and 4 negative preference indices results (N=16). (C) Boxplot comparison for average side-corrected preference index under simultaneous odor and optogenetic stimulation for controls and *Tdc2*>UAS-*CsChr* starved flies. Performed by Lisa M. Frisch.

experiments (Figure 35.A). When opposing quadrant pairs received simultaneous odor and optogenetic stimulation, freely walking *Tdc2-Gal4>UAS-CsChr* and the control flies accumulated in these quarters (Figure 35.B). Activation of OA led to flies amassed in higher numbers for respective quadrants than the controls (Figure 35.C). We did not observe an increased instance of seizures or aggression (Data not shown). This result supports the proposal that OA+ depolarization causes the switch from exploration to exploitation.

To our knowledge, only one functional evidence was available in the literature that OA neurons respond to gustatory stimuli in the SEZ region (Andrews et al., 2014). When Jean-Francois De Backer imaged OA neurons in SEZ with *Tdc2-Gal4>UAS-GCaMP6f* in an *in vivo* preparation (Figure 36), he observed reliable yet transient calcium signals from starved flies (Figure 36.E). This calcium activity was higher than peak amplitude observed in fed flies (Figure 36.F). The magnitude of starved fly responses was comparable to previously observed *Tdc2* calcium activity profile (Andrews et al., 2014). However, it is worth to note that behavioral data suggested a persistent OA activity (Figure 27 and Figure 28). Is this disagreement due to technical limitations of imaging octopaminergic neuronal activity in the SEZ or a faithful reflection of OA neuron response dynamics? This is currently an open question.

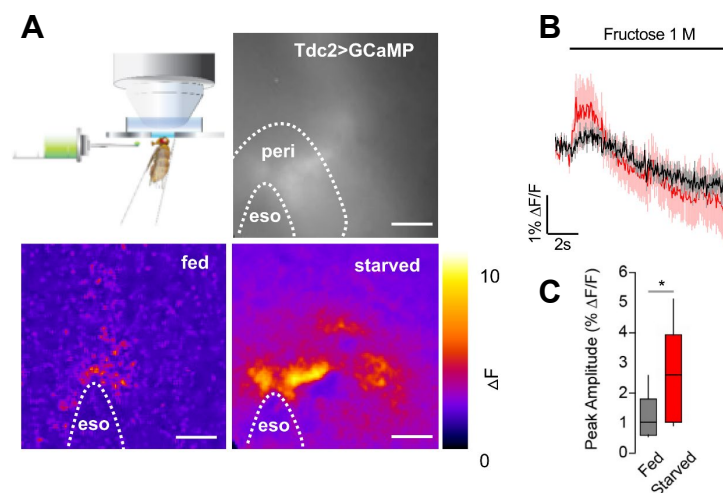


Figure 36 Calcium imaging of *Tdc2* neurons in SEZ *in vivo*

(A) Upper left. Schematics of *in vivo* SEZ imaging during feeding 1 molar fructose. Representative true baseline and pseudocolored *Tdc2>GCaMP6f* signal images recorded in flies. (B) Calcium signal traces of *Tdc2>UAS-GCaMP6f* line monitored in SEZ upon fructose feeding *in vivo*. (C) Comparison of GCaMP activity in fed and starved flies (N=10/9). Performed by Jean-Francois De Backer.

Taken together, this plethora of Tdc2+ neuronal activation experiments acknowledged OA activity in a sustained fashion prevented flies from responding to repeated vinegar plumes. Collectively with anatomical and functional evidence, I conclude that OA neurons facilitate the sequence transition in foraging.

4.5.3 Octopaminergic Neurons are Modulators of Odor Responses

Since I have established the sufficiency of OA+ neurons in sequence transition, I further questioned whether OA is necessary for processing olfactory information.

Tβh mutants cannot synthesize octopamine from tyramine. When I compared *Tβh* null and heterozygous mutants, null mutants lacking OA failed to track vinegar and were significantly slower during stimulation phase (Figure 37.A). Lack of octopamine did not alter absolute turning (Figure 37.B).

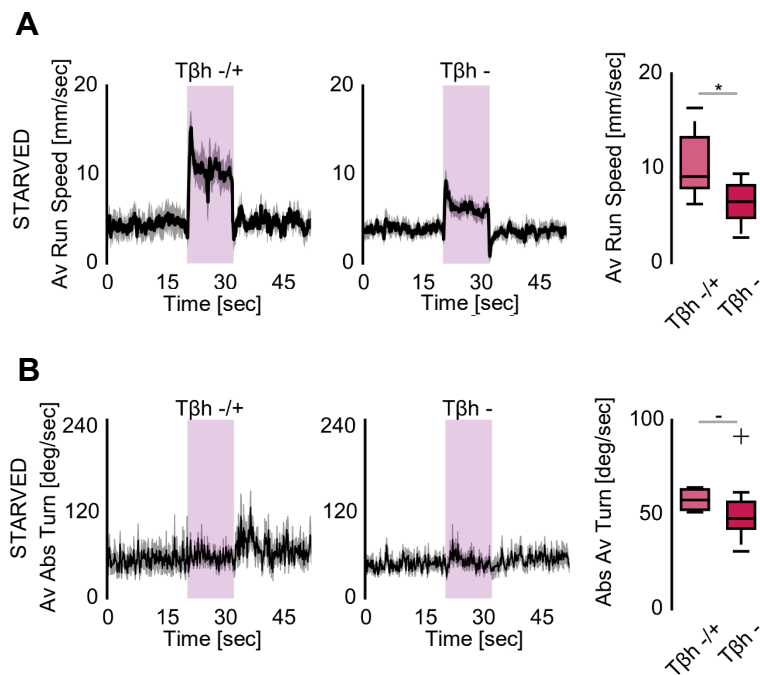


Figure 37 Tyramine β hydroxylase mutants during persistent odor tracking

(A) Average running speeds for ten trials of *Tβh* heterozygous (left, N=5) and null (right, N=8) mutant starved flies over time during vinegar stimulation. (B) Average absolute turning speeds for ten trials of *Tβh* heterozygous and null mutant starved flies over time during vinegar stimulation.

Similarly, blocking the activity of Tdc2 labeled OA+ neurons significantly reduced vinegar response in comparison to controls (Figure 38.A,B, UAS control from Figure 17). As in *Tβh* mutants, turning behavior was not changed by lack of input from OA neurons (Figure 38.C,D). I found out blocking OA+ neuron activity only in the central nervous system recapitulates previous OA loss-of-function phenotypes (Figure 38.E).

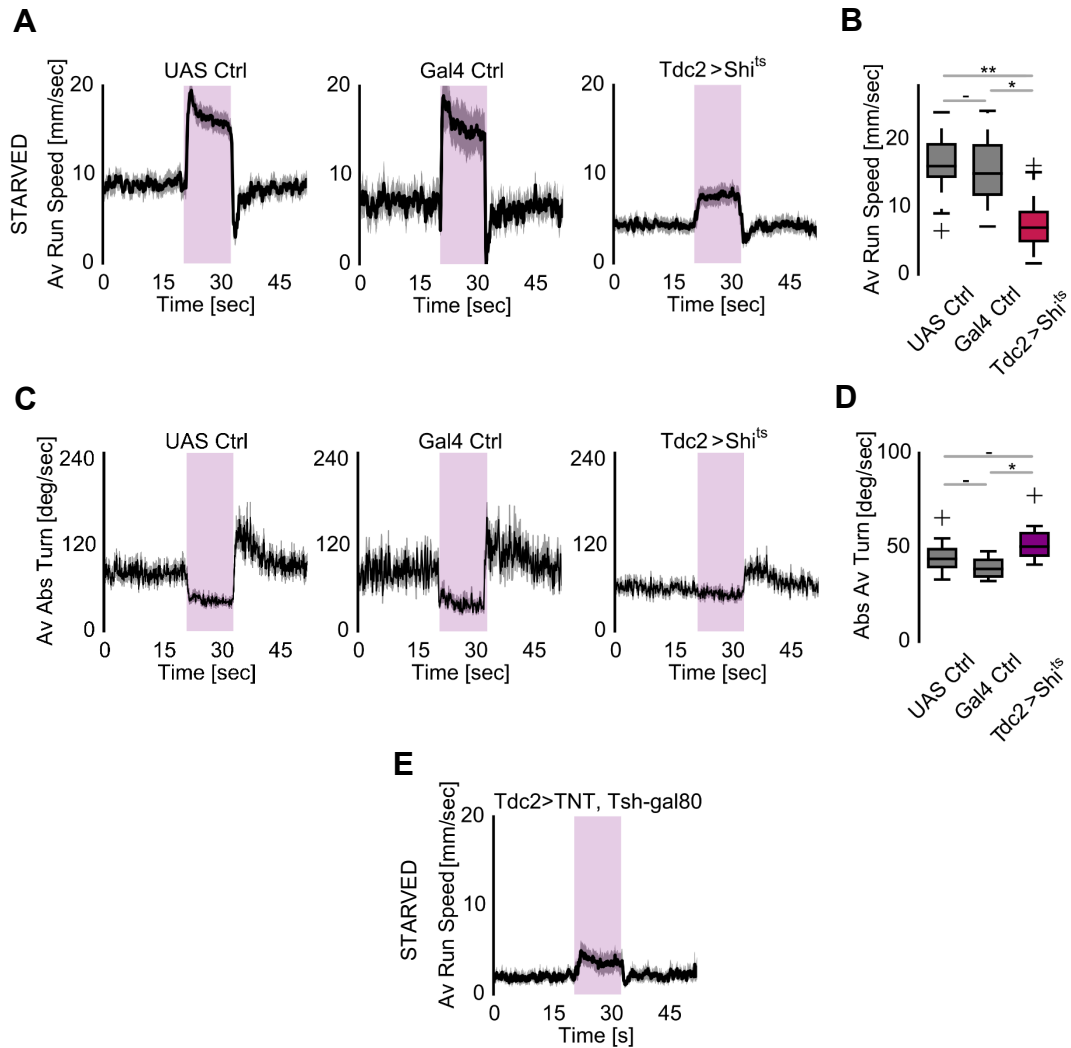


Figure 38 Blocking synaptic release from Tdc2+ neurons in vinegar approach

(A) Average running speeds of UAS (\rightarrow UAS-Shi^{ts1}) and Gal4 (*Tdc2-Gal4*>-) starved control flies, in comparison to starved flies with synaptically blocked octopaminergic neurons (*Tdc2-Gal4*>UAS-Shi^{ts1}) over time during vinegar stimulation for ten trials (N=18/6/18). (B) Boxplot for average running speeds during the odor stimulation periods of controls and *Tdc2-Gal4*>UAS-Shi^{ts1} flies. (C) Average absolute turning speeds of starved control and *Tdc2-Gal4*>UAS-Shi^{ts1} over time during vinegar stimulation for ten trials. (D) Boxplot for average absolute turning speeds during the odor stimulation periods of controls and *Tdc2*>UAS-Shi^{ts1} flies. (E) Average running speeds of starved flies (*Tdc2-Gal4*>UAS-TNT, *Tsh-gal80*), of which octopaminergic activity was blocked only in the central nervous system, over time (N=7).

According to these experiments, octopaminergic neurons in the brain are required for odor tracking. Considering that OA neurons are high in number, possibly, activation and blocking of all Tdc2+ OA neurons favor different subsets.

4.5.4 Octopamine and NPF as Possible Partners

Octopamine has been previously attributed to playing a role in linking metabolism and hunger state for flies. This link can be the focal point in the understanding the phenotypes observed through manipulating octopaminergic neuron activity, especially loss-of-function results. Significant players in asserting internal state for fly olfaction are *sNPF* and *NPF* signaling pathways (Sayin et al., 2018). Would interfering with *sNPF-R* or *NPF-R* expression specifically in Tdc2+ neurons modulate persistent odor tracking?

To achieve cell-specificity, I targeted either *sNPF-R* or *NPF-R* mRNAs through RNA interference (Figure 39). *sNPF-R* knockdown in Tdc2 neurons did not have a visible outcome (Figure 39.A). We employed the two RNAi available lines for *NPF-R* in our stock. *Tdc2-Gal4>UAS-NPF-R (KK)* flies were indistinguishable from the controls (Figure 39.B), whereas *Tdc2-Gal4>UAS-NPF-R (TRiP)* flies were significantly faster in odor tracking during vinegar presentation (Figure 39.C). Discrepancies in RNA interference phenotypes can be expected due to transgenic line efficiency and target specificity. These results provide preliminary evidence that OA and *NPF* signaling might interact. However, additional analyses of RNAi specificity and alternative mutant alleles are necessary for stronger claims at the moment.

Considering that *NPF* neuromodulation might have an impact on OA neurons, I decided to investigate the role of *NPF* in the spherical treadmill paradigm.

When *NPF* signaling was blocked with Shi^{ts}, there was a minor, but a significant rise in vinegar tracking speed after outlier removal in the experimental group (Figure 40). *NPF* plays a role in promoting odor responses in fed flies when artificially activated (Beshel and Zhong, 2013). Activation of *NPF* in satiated flies did not result in persistent vinegar tracking (Figure 41.A). On the contrary, during

NPF activation in fed flies, fly forward run profile under vinegar exposure, to some extent, paralleled *Tdc2*⁺ activation (Figure 41.A-C). Preliminary experiments with activation in starved flies of *NPF* neurons did not produce phenotype (Figure 41.D).

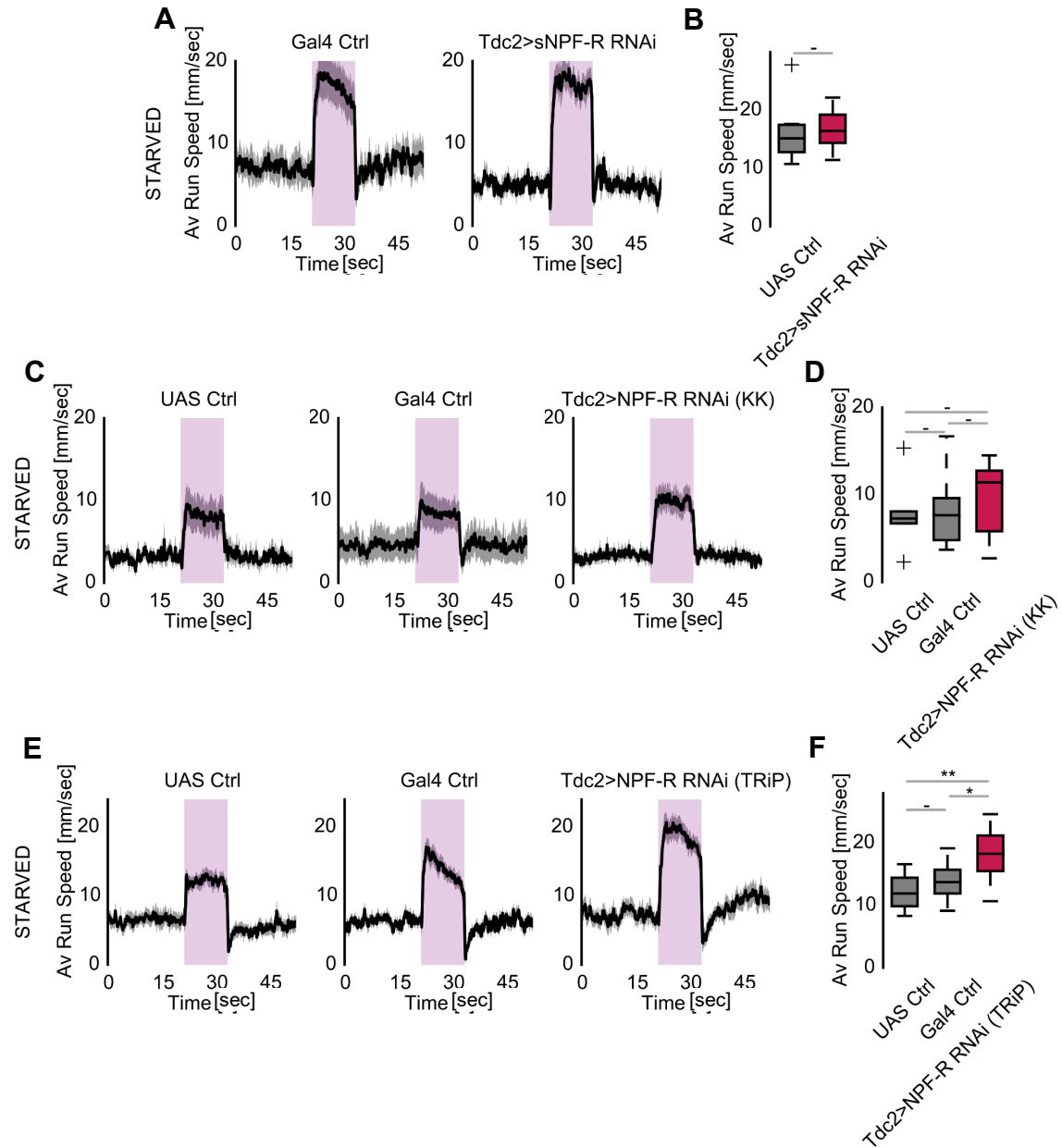


Figure 39 Knockdown of *sNPF-R* and *NPF-R* receptors in *Tdc2*⁺ neurons during persistence

(A) Average running speeds of starved Gal4 control (*Tdc2-Gal4*^{>-}) and octopaminergic *sNPF-R* receptor knockdown (*Tdc2-Gal4*[>]*UAS-sNPF-R RNAi*) flies over ten trials (N=6). Right. Boxplot for average running speeds during the odor stimulation periods of controls and experimental flies. (B) Average running speeds of starved Gal4 control (*Tdc2-Gal4*^{>-}) and octopaminergic *NPF-R* receptor knockdown (*Tdc2-Gal4*[>]*UAS-NPF-R RNAi KK*) flies over ten trials (N=6/5/10). Right. Boxplot for average running speeds during the odor stimulation periods of controls and experimental flies. (C) Average running speeds of starved Gal4 control (*Tdc2-Gal4*^{>-}) and octopaminergic *NPF-R* receptor knockdown (*Tdc2-Gal4*[>]*UAS-NPF-R RNAi TRiP*) flies over ten trials (N=10). (D) Boxplot for average running speeds during the odor stimulation periods of controls and experimental flies.

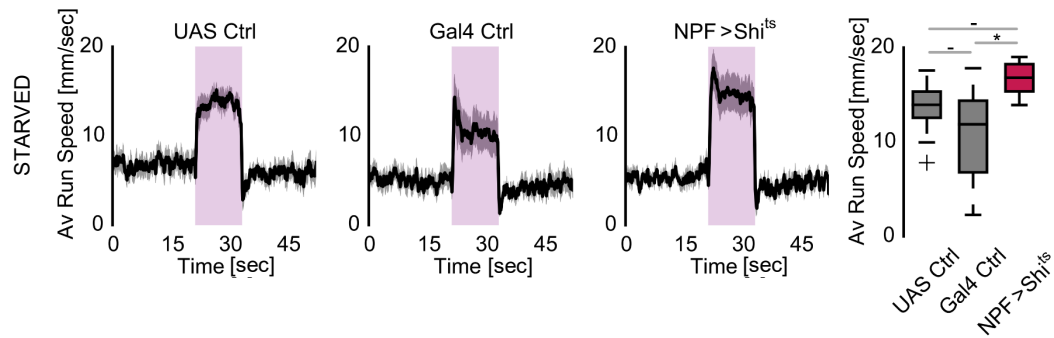


Figure 40 Blocking synaptic output from *NPF* neurons in vinegar tracking in starved flies

Left. Average running speeds of UAS (\rightarrow UAS-*Shi^{ts1}*) and Gal4 (*NPF-Gal4*>-) starved control flies, in comparison to starved flies with synaptically blocked octopaminergic neurons (*NPF-Gal4*>UAS-*Shi^{ts1}*) over time during vinegar stimulation for ten trials (N=9/7/8). Right. Boxplot for average running speeds during the odor stimulation periods of controls and *NPF-Gal4*>UAS-*Shi^{ts1}* flies after removal of an outlier. The outlier removal was performed according to Iglewicz and Hoaglin's robust test for multiple outliers with a cut-off at Z-score 3.5

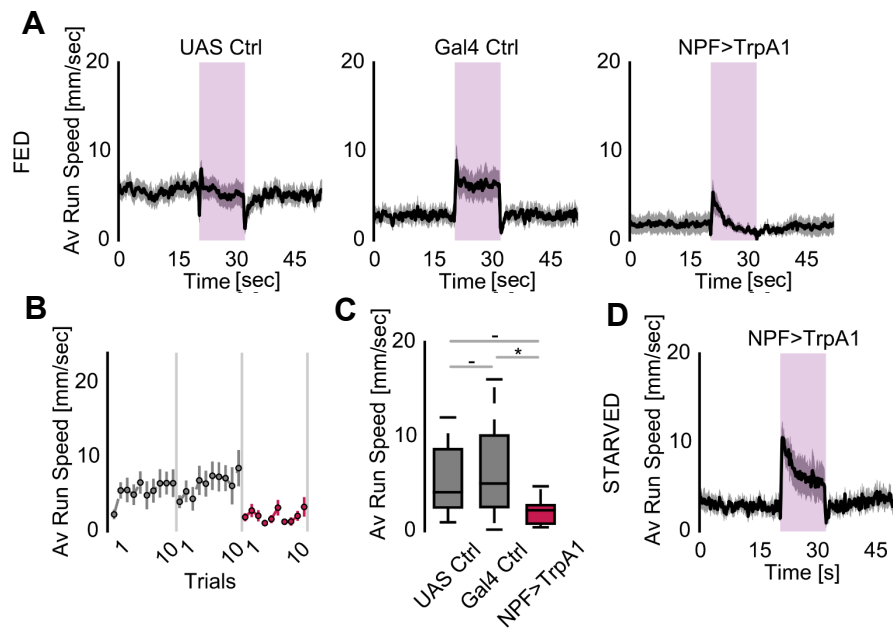


Figure 41 Artificial activation of *NPF* neurons during vinegar tracking

(A) Average running speeds of UAS (\rightarrow UAS-*TrpA1*) and Gal4 (*NPF-Gal4*>-) fed control flies in comparison to fed flies with chronic *NPF*+ neurons activated (*NPF-Gal4*>UAS-*TrpA1*) over time (N=10). (B) Evolution of running speeds in odor presentation over ten trials for controls and the experimental group. (C) Boxplot comparison for average running speeds during odor stimulation for fed control flies and *NPF*+ activated fed flies. (D) Average running speed of starved *NPF-Gal4*>UAS-*TrpA1* over time (N=6).

In conclusion, these results might suggest that the possibility of an interaction between *OA* and *NPF* signaling. Such an interaction might indicate a deeper coupling of separate motivational mechanisms. Considering broad expression patterns of both *Tdc2* and *NPF* drivers and the weak phenotype effects, however, stand as a word of caution.

4.6 Specific OANs Suppress Olfaction

4.6.1 Characterization of VPM3 and VPM4 neurons

Since *Tdc2-gal4* neurons label more than 100 neurons in the fly brain (Busch et al., 2009), it was imperative to narrow down the targeted neuron profile. For this purpose, we screened a small selection of candidate lines including two split-Gal4 lines available from Janelia collection. VPM3 and VPM4 neurons were conceived to be ideal candidates since they connect SEZ and higher brain centers, and for the sparsity of the split-Gal4 lines. MB22B harbored VPM3 and VPM4 neurons, while MB113C labeled only VPM4 neurons (Aso et al., 2014a) (Figure 42. A-B'). Both

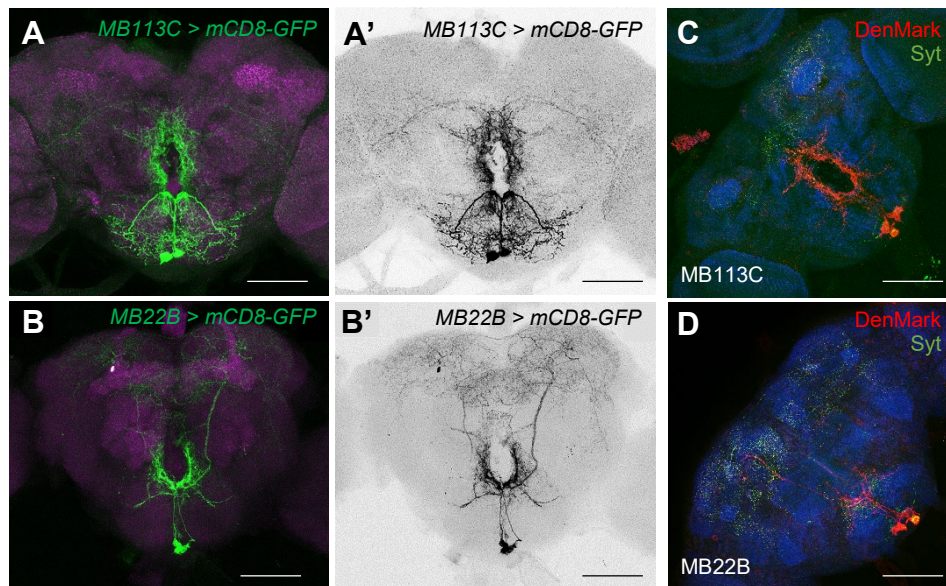


Figure 42 Morphological immunohistochemistry analyses of VPM neurons

(A-B') Expression patterns of split-Gal4 lines MB22B and MB113 were visualized with mCD8-GFP (*MB22B>UAS-mCD8-GFP* and *MB113C>UAS-mCD8-GFP*, green/black). The background neuropile staining was anti-*N-Cad* (magenta/grey). (C-D) Polarity analyses of split-Gal4 lines MB22B and MB113 (*MB22B>UAS-DenMark*, *UAS-syt-GFP* and *MB113C>UAS-DenMark* (red), *UAS-syt-GFP* (green)). The background neuropile staining was anti-*N-Cad* (blue). Data by Anja Friedrich.

neurons innervate various regions in the protocerebrum (Busch et al., 2009). However, their neuronal polarity was yet to be determined. Anja Friedrich confirmed the earlier hypotheses (Figure 42.C, D). Both VPM neurons had their dendritic regions branched in SEZ and sent their axons to protocerebrum.

For VPM, Anja Friedrich also verified that these neurons are indeed octopaminergic (Figure 43.A-A''). Furthermore, we have not observed any evidence for retention of octopamine-precursor tyramine in these cells (Figure 43.B-B'').

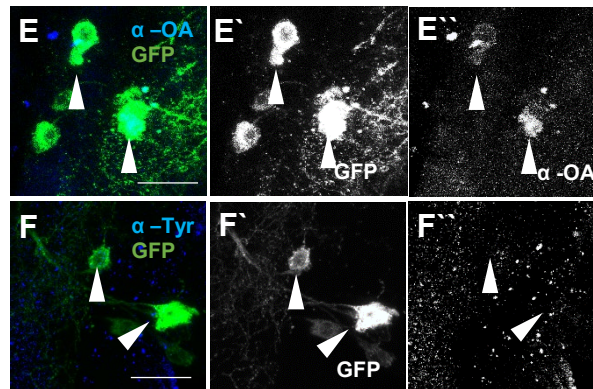


Figure 43 Octopamine and tyramine stainings of VPM4 neuron.

Co-localization analyses of VPM4 (*MB113C>UAS-mCD8-GFP*) and anti-octopamine (A-A'') and anti-tyramine (B-B'') signals. Data by Anja Friedrich.

Consequently, the morphology of VPMs indeed seemed suitable for our hypotheses: VPMs connect primary taste relay SEZ to olfactory center MB. Additionally, the distinct polarity of VPMs suggested this connection from SEZ to MB is a linear trajectory, to confer sequential antagonism.

4.6.2 VPMs Phenocopy *Tdc2* Activation

Would manipulating a single VPM neuron replicate the broad activation of 100+ OA neurons in the brain? To address this, I optogenetically activated VPM3 and VPM4 for neurons using MB22B and MB113C split-Gal4 lines in starved flies (Figure 44). Upon depolarization of VPM neurons, both experimental groups showed reduced odor tracking (Figure 44.A, C). The withdrawal from vinegar was immediate and observed even in the first trial (Figure 44.B). This effect was not due to any observed motor defect as the fly speed of all genotypes were comparable before odor and optogenetic stimulation (Figure 44.D).

Since octopaminergic neurons are required for associative learning (Burke et al., 2012; Huetteroth et al., 2015), I analyzed how concurrent exposure to VPM activity altered later vinegar responses (Figure 44.E). After normalizing ‘odor only’ running speed to the first trial ‘odor only’ phase response, flies showed no apparent

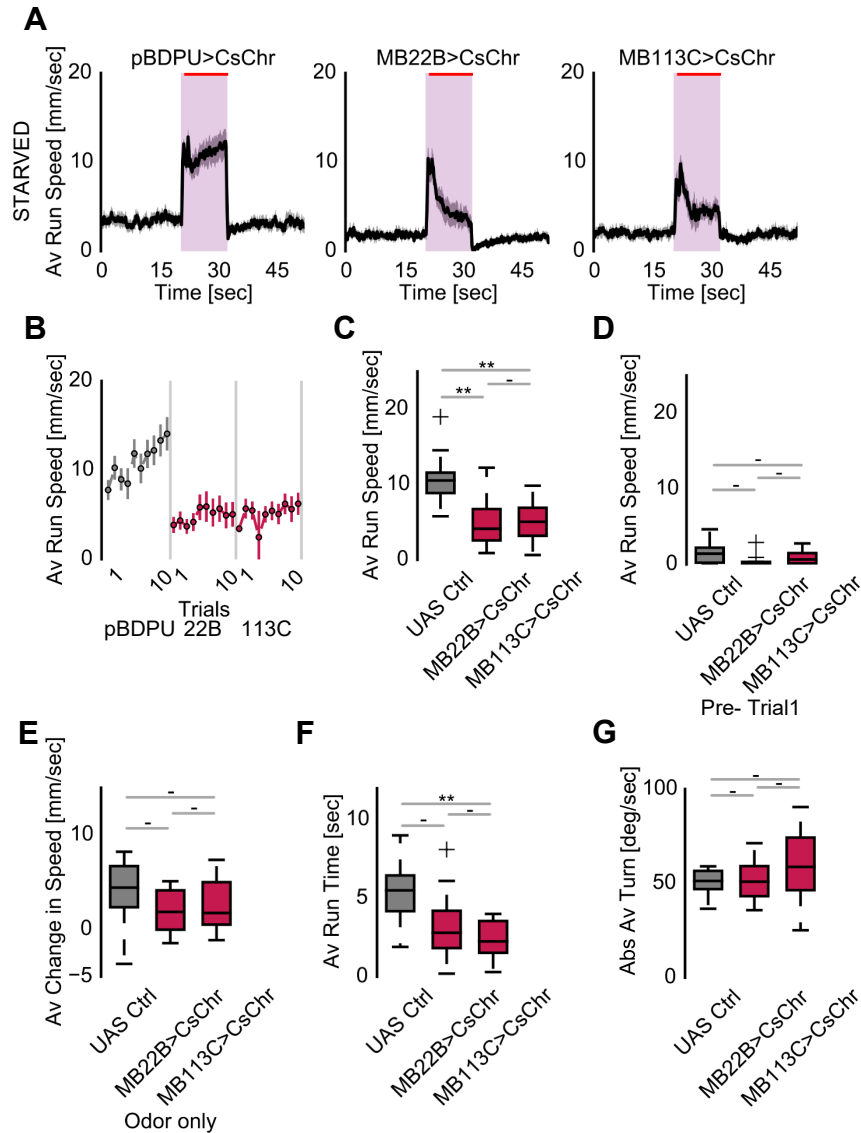


Figure 44 Acute activation of OA+ MB split-Gal4 lines

(A) Average running speeds of *UAS* control (*pBDP-Gal4U>UAS-CsChr*) and octopaminergic split-Gal4 (*MB22B-Gal4>UAS-CsChr* for VPM3 and VPM4, *MB113C-Gal4>UAS-CsChr* for VPM4 only) flies over a timeframe of single trial for ten trials under starvation (N=10). (B) Evolution of running speeds during concurrent vinegar exposure and optogenetic manipulation over ten trials for controls and *MB22B-Gal4>UAS-CsChr* and *MB113C-Gal4>UAS-CsChr* flies. (C) Boxplot for average running speeds during concurrent vinegar exposure and optogenetic manipulation over ten trials for controls and *MB22B-Gal4>UAS-CsChr* and *MB113C-Gal4>UAS-CsChr* flies. (D) Boxplot for average running speeds in pre-stimulation periods for controls and split-Gal4 lines. (E) Boxplot for average change in running speeds during odor only phase for the control and *MB22B-Gal4>UAS-CsChr* and *MB113C-Gal4>UAS-CsChr* flies. Subsequent trials were normalized to trial 1 response. (F) Boxplot comparison for average initial running bout times after optogenetic onset. (G) Boxplot for average absolute turning speeds during stimulation periods.

reduction in vinegar response. Only, the acute activity of VPM neurons led to reduced tracking. *MB113C-Gal4>UAS-CsChr* flies also had shorter run times (Figure 44.F). Manipulation of VPM did not moderate turning behavior during vinegar exposure (Figure 44.G).

To rule out the expression of MB22B-Gal4 and MB113-Gal4, along with UAS-CsChr, might cause changes in the baseline running or introduce motor defects, I tested starved *MB22B-Gal4>UAS-CsChr* and *MB113C-Gal4>UAS-CsChr* flies in the absence of any optogenetic stimulation. These flies performed comparably to the controls (Figure 45).

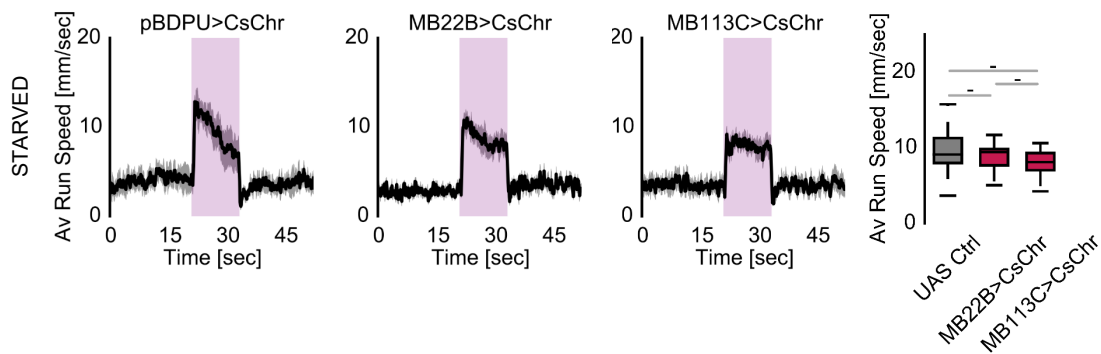


Figure 45 CsChrimson expressing OA+ MB split-Gal4 flies in vinegar only approach

Left. Average running speeds of UAS control (*pBDP-Gal4U>UAS-CsChr*) and octopaminergic split-Gal4 (*MB22B>UAS-CsChr* for VPM3 and VPM4, *MB113C>UAS-CsChr* for VPM4 only) flies over a timeframe of single trial for ten trials under starvation in the absence of optogenetic stimuli (N=6). Right. Boxplot for average running speeds in vinegar only exposure.

Chronic thermogenetic activation of both VPMs (Figure 46) and only VPM4 (Figure 47) neurons recapitulated acute activation phenotypes. VPM activation reduced running speed (Figure 46.B, C and Figure 47.B, C) without motor defects observed (Figure 46.D and Figure 47.D). In contrast to chronic activation of Tdc2 neurons, however, VPM activation alone produced lower basal speeds (Figure 46.A and Figure 47.A).

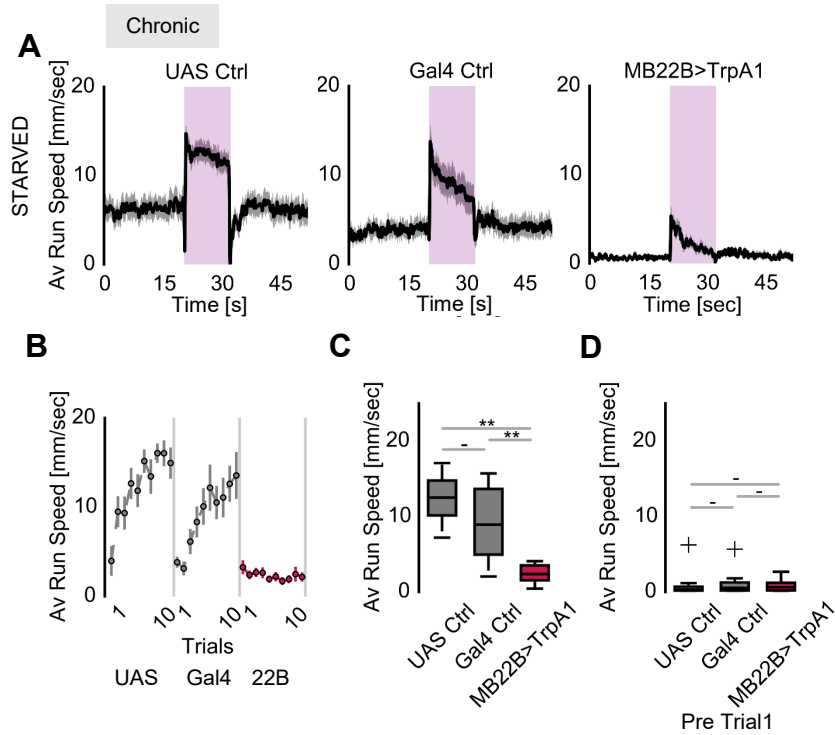


Figure 46 Chronic activation of VPM3 and VPM4 neurons in starved flies

(A) Average running speeds of UAS (\rightarrow UAS-*TrpA1*) and Gal4 (*MB22B-Gal4*>) control flies and MB22B flies (*MB22B-Gal4*>UAS-*TrpA1*) during chronic activation under starvation (N=10). (B) Evolution of running speeds during odor application over ten trials for controls and the *MB22B-Gal4*>UAS-*TrpA1* group. (C) Boxplot comparison for average running speeds during odor application for controls and *MB22B-Gal4*>UAS-*TrpA1* group. (D) Boxplot comparison for average running speeds in the first trial prior to odor delivery.

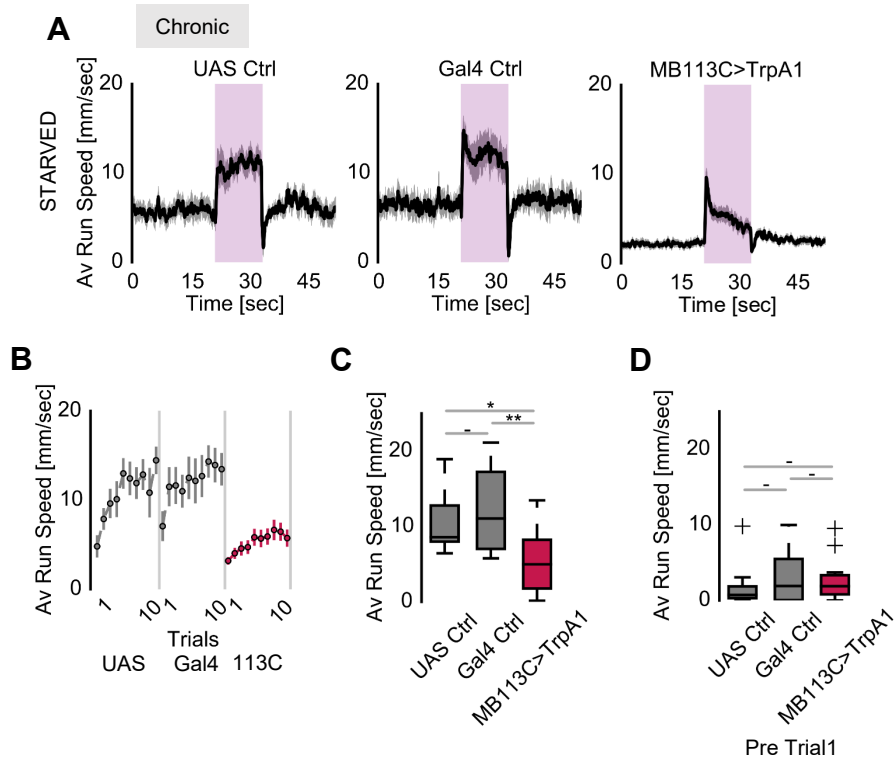


Figure 47 Chronic activation of only VPM4

Continued from previous page

(A) Average running speeds of UAS (->UAS-*TrpA1*) and Gal4 (*MB113C-Gal4>*) control flies and MB113C flies (*MB113C -Gal4>UAS-TrpA1*) during chronic activation under starvation (N=9/10/29). (B) Evolution of running speeds during odor application over ten trials for controls and the *MB22B-Gal4>UAS-TrpA1* group. (C) Boxplot comparison for average running speeds during odor application for controls and *MB113C -Gal4>UAS-TrpA1* group. (D) Boxplot comparison for average running speeds in the first trial prior to odor delivery.

These chronic and acute activation experiments clearly indicate that octopaminergic VPM4 neurons, as the common denominator of MB22B and MB113C lines, alone are sufficient to reproduce activation of *Tdc2* phenotypes and suppress persistent tracking.

4.6.3 VPMs are not Necessary for Olfaction

Are VPM neurons essential for the perception of olfaction? In contrast to comprehensive blocking of *Tdc2*+ octopaminergic synaptic activity (Figure 38), lack

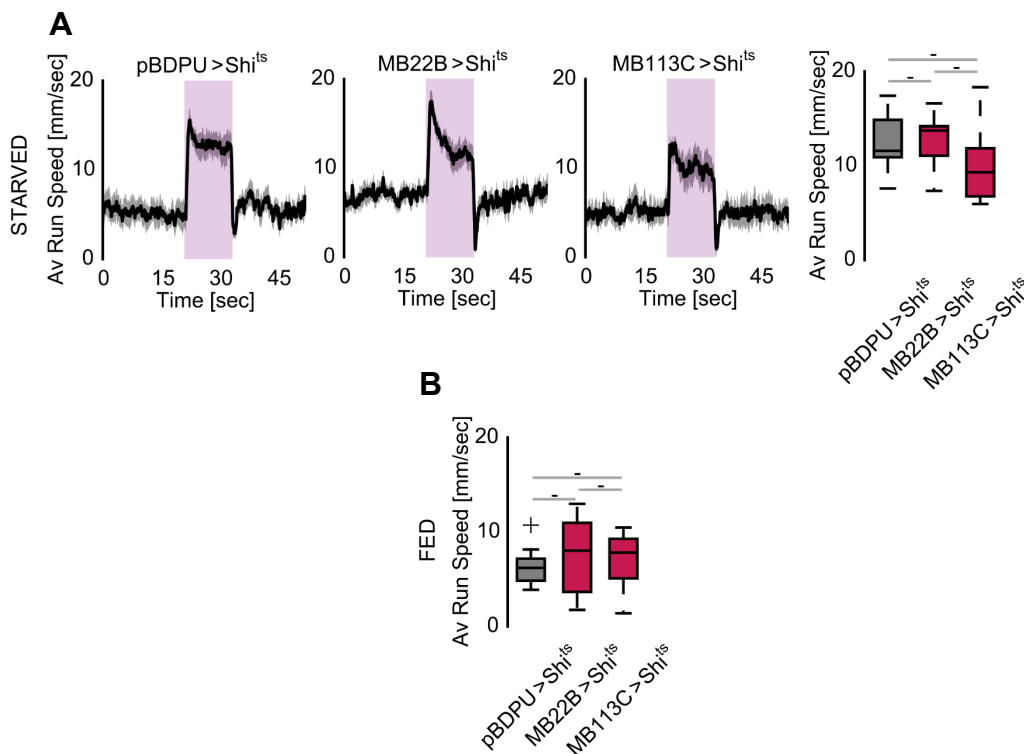


Figure 48 Blocking VPM activity in starved and fed flies

(A) Left. Average running speeds of control (*pBDP-Gal4U>UAS-Shi^{ts1}*) with experimental groups (*MB22B>UAS-Shi^{ts1}* and *MB113C>UAS-Shi^{ts1}*) for starved flies, during vinegar exposure for ten trials (N=7/8/8). Right. Boxplot for average running speeds. (B) Boxplot for average running speed for *pBDP-Gal4U>UAS-Shi^{ts1}* with experimental groups *pBDP-Gal4U>UAS-Shi^{ts1}*, *MB22B>UAS-Shi^{ts1}* and *MB113C>UAS-Shi^{ts1}* fed flies (N=10).

of input from VPM neurons did not induce any modulation of vinegar responses in both fed and starved flies (Figure 48.A-D). In conclusion, indeed, octopaminergic VPM neuron poses to be the connection between olfaction and gustation, but not a canonical part of the olfactory circuitry *per se*.

4.6.4 Manipulations of other OA+ SEZ neurons

In addition to VPM neurons, octopaminergic neurons in SEZ includes several morphologically distinct subgroups (Busch et al., 2009). We had access to another split-Gal4 which labeled VUMa2 and several other OA+ neurons, distinct from VPM3 and VPM4 (The line is referred to as VUMa2-Gal4 from now on.) VUMa2 activation, both chronic and acute, led to similar phenotypes (Figure 49). On average, flies were slower when this OA+ subset of neurons was activated artificially (Figure 49.A, B, C). Lack of VUMa2 did not alter olfactory behavior (Figure 50).

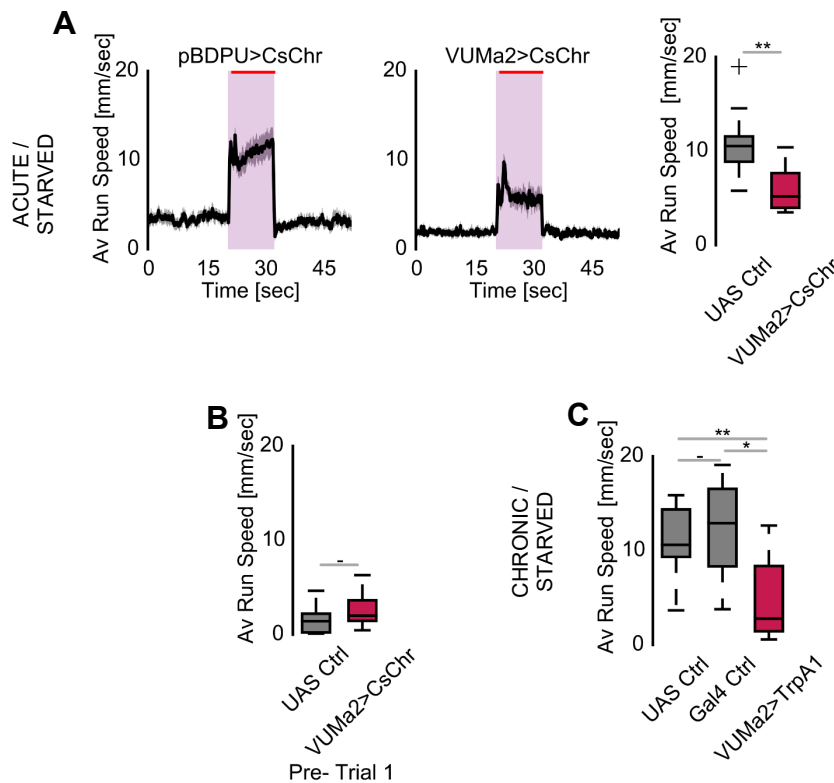


Figure 49 Acute and chronic activation of OA+ VUMa2 for starved flies

(A) Left. Average running speeds of optogenetic activation of UAS (*pBDP-Gal4U>UAS-CsChr*) and VUM2a labeled flies (*VUMa2-Gal4>UAS-CsChr*) for ten trials under starvation (N=10). Right. Boxplot for average running speeds during the stimulation periods of controls and VUM2a activated flies. (B) Boxplot for average running speeds in pre-stimulation periods for chronic activation. (C) Chronic thermogenetic activation for controls (*->TrpA1* and *VUMa2-Gal4>-*) and *VUMa2-Gal4>UAS-TrpA1* starved flies (N=9/9/10).

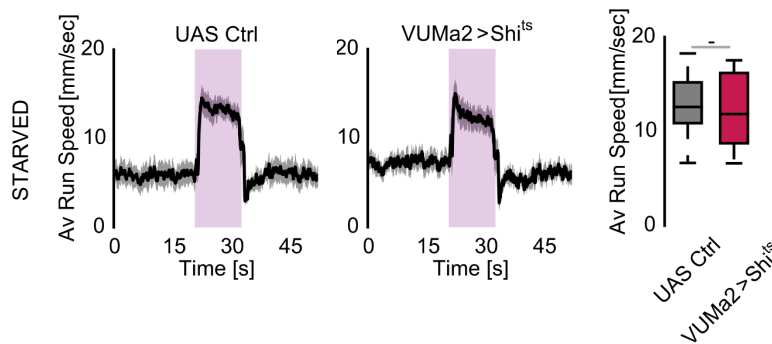


Figure 50 Blocking VUMa2 output during vinegar approach

Left. Average running speeds of hungry UAS control flies ($\rightarrow UAS-Shi^{ts1}$), hungry flies with synaptically blocked VUMa2 octopaminergic ($VUMa2 > Shi^{ts1}$) for ten trials (N=10). Right. Boxplot for average running speeds for UAS control and $VUMa2 > Shi^{ts1}$ flies.

These results propose that while there may be redundancy within SEZ OA neurons, further clarification is needed.

4.6.5 MVP2 and VPMs are connected

So far observed behavioral profiles upon MVP2 and VPM activation are exact opposites. While MVP2 promoted, VPM halted odor-search. Gross anatomical features of MVP2 and VPM, especially proximity in the mushroom body peduncle region, also postulates that these two neurons might be part of a bidirectional micro-circuit governing appetitive odor perception.

With a double labeling experiment, Anja Friedrich stained MVP2 (MB112) and VPM4 (GMR95A10-LexA) neurons with two different fluorescent proteins (Figure 51). It was possible to visualize both neurons in a single confocal plane at peduncle, hinting an anatomical connection between these two neurons. A stronger line of evidence emerged through partial connectomics (Figure 52). In an attempt to reconstruct mushroom body connectome, the groups led by G. Jefferis and D. Bock identified VPMs as direct pre-synaptic partners of MVP2, bypassing DAN and KCs in the peduncle (Figure 52.B, C). Both VPMs had dense synaptic innervations with MVP2. VPMs and MVP2 had a set of reciprocal connections (Figure 52.D). Further close inspection revealed that two physically distinct types of vesicles were present between VPM and MVP2 (Figure 52.E,F). This observation hints that VPM neurons could co-release two different neurotransmitters or neuromodulators.

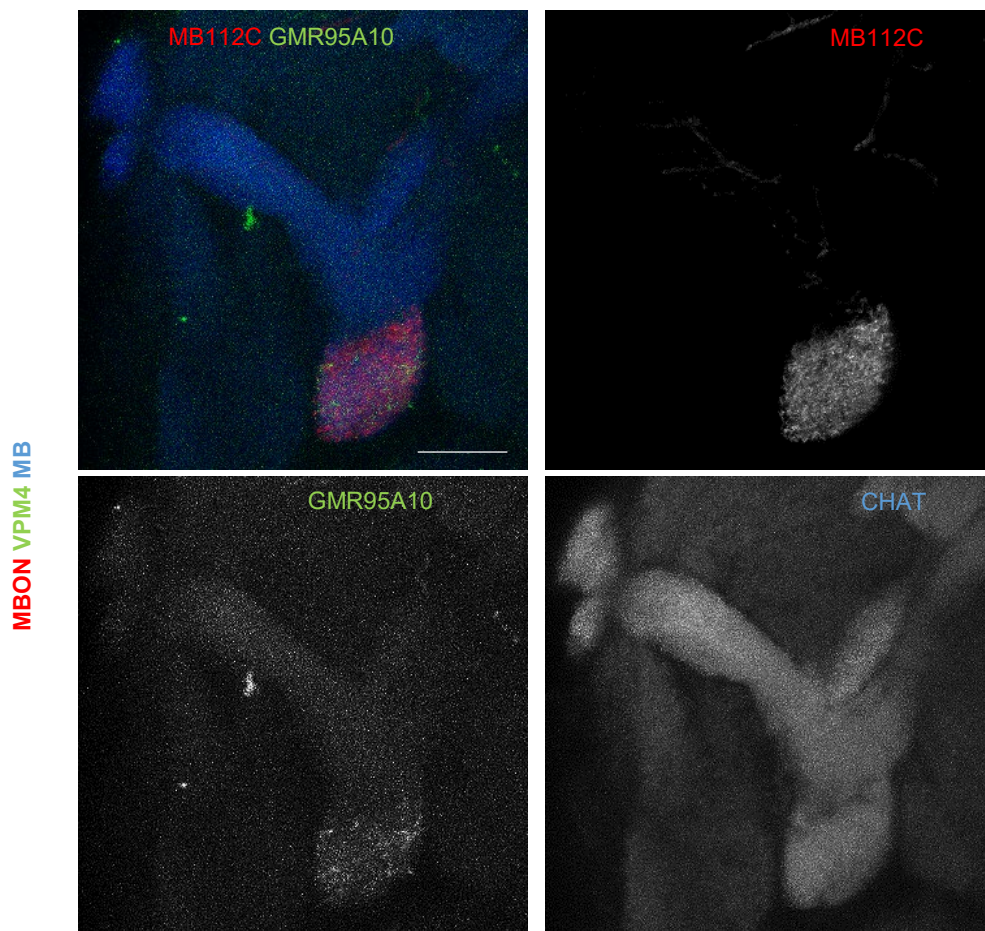


Figure 51 Double-labeling of VPM4 and MVP2 neurons

Expression patterns of MVP2 (*MB22B>UAS-mCD8-RFP*, red) and VPM4 (*GMR95A10-LexA>LexAop2-mCD8-GFP*, green) neurons in the peduncle region of mushroom body. The background neuropile staining for MB lobes was anti-CHAT (blue). Data by Anja Friedrich.

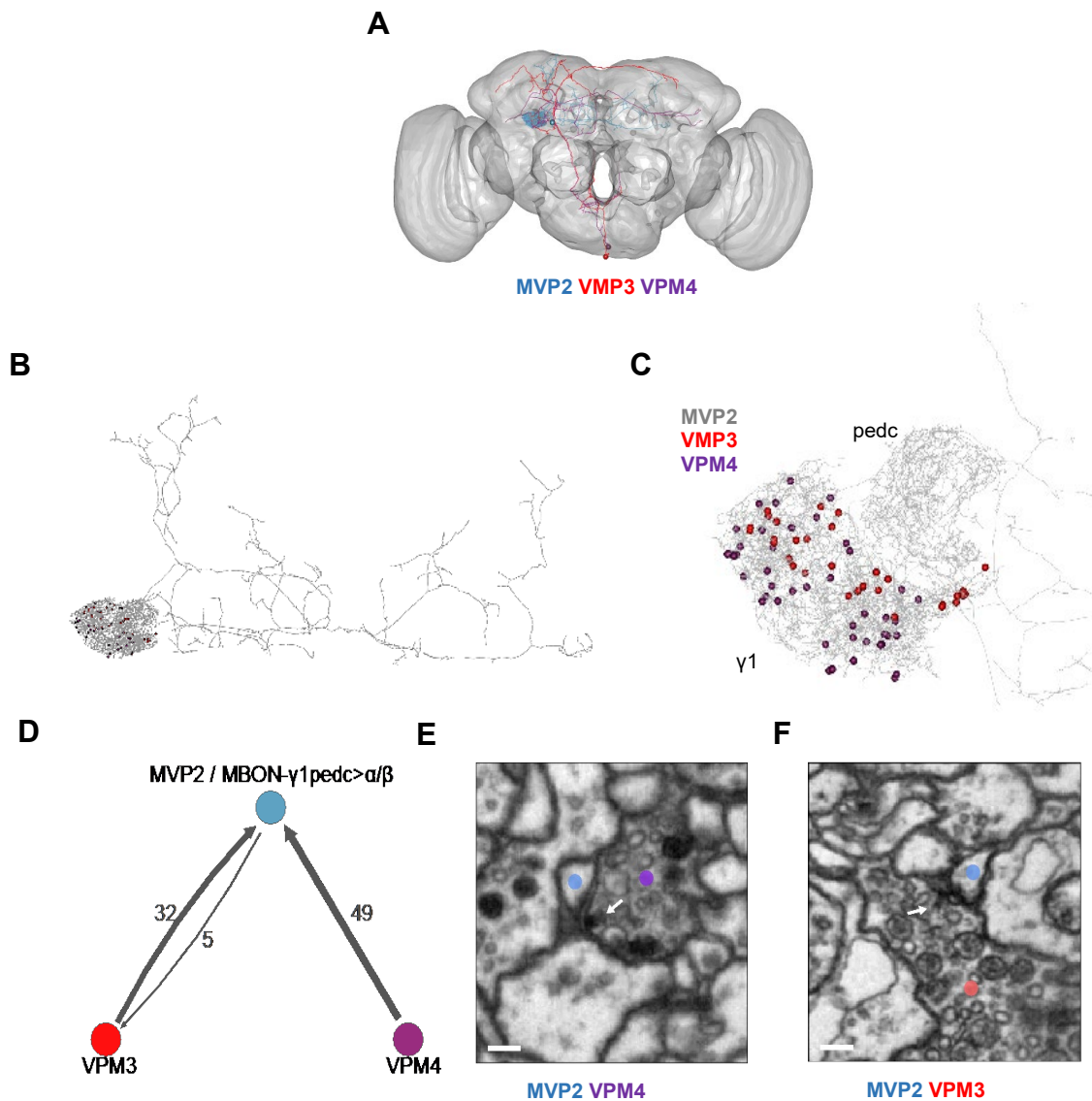


Figure 52 Connectome analyses of VPM and MVP2 neurons in MB peduncle

(A) Reconstructed trajectories of VPM3, VPM4 and MVP2 neurons. (B-C) Localization of VPM synaptic contacts in MVP2 dendrites. (D) Number of synapses traces between VPM and MVP2 neurons. (E) A representative section of VPM4 tracing in the peduncle. (F) A representative section of VPM3 tracing in the peduncle. Data by PS, AES, CBNF, SCS, SL, DB, MC, and GSXEJ.

In conclusion, we have provided strong evidence for how two behavioral modules, olfaction, and gustation, can be integrated directly at the synaptic level, by presenting connectomic and double labeling evidence between VPMs and MVP2.

4.6.5 VPMs mediated suppression of MVP2

From the perspective of odor tracking, olfaction and feeding produced opposite results. Artificial activation of MVP2 and VPM4 had contrary effects on vinegar approach. Lastly, the previous section established the direct connection between MVP2 and VPM4. However, anatomical connectivity provides limited information.

To probe functional connectivity, Jean-Francois De Backer expressed ATP-inducible P2X2 receptors in VPM4 neurons (*GMR95A-LexA>LexAop-P2X2*) and monitored GCaMP activity in MVP2 (*MB112C-Gal4>UAS-GCaMP*) (Figure 53). *In vivo*, the addition of ATP led to a significant and sustained reduction of MVP2 activity only in the presence of P2X2 expressing VPM4 neurons.

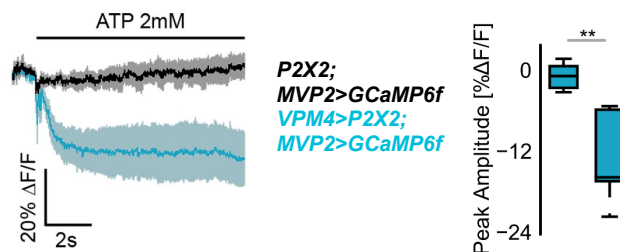


Figure 53 Functional connectivity between MVP2 and VPM4 *in vivo*

Left. Average calcium signal over time recorded from MVP2 neurons in the presence (*MB112C>UAS-GCaMP*, *GMR95A10-LexA>LexAop2-P2X2*, blue) and absence (*MB112C>UAS-GCaMP*, *->LexAop2-P2X2*, grey) of ATP induced VPM4 neuronal activation *in vivo* (N=5). Right. Boxplot comparison of calcium activity in MVP2 neurons at the onset of ATP application. Performed by Jean-Francois De Backer.

Anatomical and functional connectivity showed that MVP2 downstream of VPM4 neurons. As supportive evidence, I asked whether optogenetic activation of MVP2 neurons could rescue VPM4 driven inhibition. In this epistasis essay, I expressed CsChr in both neurons (Figure 54 and Figure 55). Simultaneous activation of MVP2 and VPM4 in fed (Figure 54) and starved flies (Figure 55)

repeated the pattern observed when only VPM4 was activated. It is plausible that the strong VPM4 driven inhibition (Figure 53) nullified artificial MVP2 depolarization.

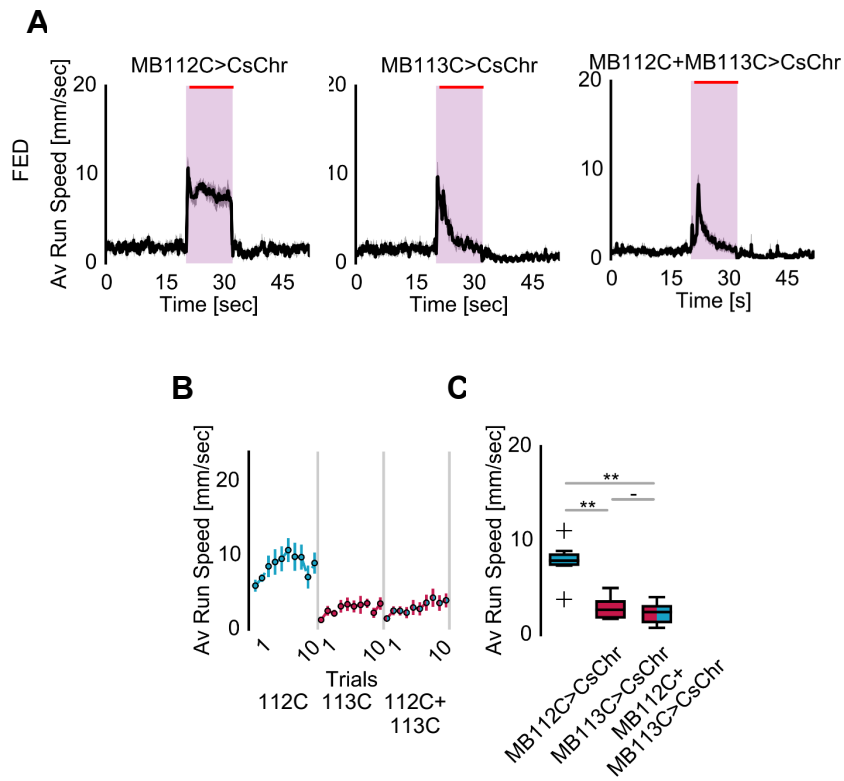


Figure 54 Epistasis analysis of MB112C and MB113C activation in fed flies

(A) Average running speeds of UAS control (*pBDP-Gal4U>UAS-CsChr*) and MB112C (*MB112C>UAS-CsChr*) and MB113C (*MB113C>UAS-CsChr*) starved flies in simultaneous odor and optogenetic stimulation experiments over a timeframe of single trial under starvation (N=7). (B) Evolution of average running speeds during optogenetic activation. (C) Boxplot for average running speeds during optogenetic activation.

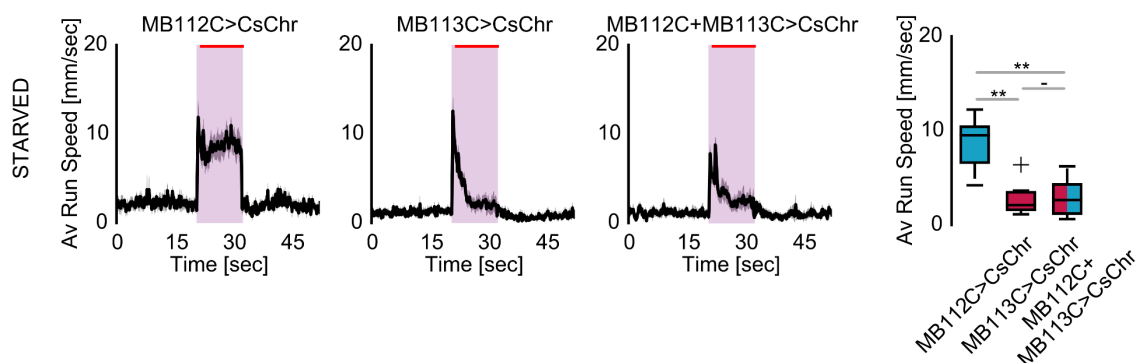


Figure 55 Epistasis analysis of MB112C and MB113C activation in starved flies

Left. Average running speeds of UAS control (*pBDP-Gal4U>UAS-CsChr*) and MB112C (*MB112C>UAS-CsChr*) and MB113C (*MB113C>UAS-CsChr*) starved flies in simultaneous odor and optogenetic stimulation experiments over a timeframe of single trial under starvation (N=7). Right. Boxplot for average running speeds during optogenetic activation.

Taken together, now I presented several lines of evidence for the interaction between octopaminergic VPM4 and mushroom body output neuron MVP2. The pre-synaptic partner VPM4 has abundant direct synaptic connections to MVP2. These connections were inhibitory. Epistasis experiments further reinforced the strength of VPM4 induced depression: even artificial activation of the post-synaptic partner MVP2 did not reconstitute odor attraction. Thus, an antagonistic transition of exploration to exploitation is represented by VPM4-MVP2 axis.

5 DISCUSSION

Although it is well known that flies are able to locate food over long distances, a complete understanding of how this is achieved is not understood. Such foraging behavior must be very challenging. For starved flies, olfaction plays a crucial role in this event (Sayin et al., 2018). Foraging ultimately translates into a dilemma, for *Drosophila melanogaster* and the rest of the animal kingdom alike: how would an animal sustain high energy cost behaviors when deprived of nutrients? How is this balance achieved in terms of motivational drivers? Furthermore, since the goal of foraging is exploiting food in the end, the transition from olfaction to feeding behaviors is not fully depicted. Would motivational circuits mediating olfactory behaviors conflict or reinforce other sensory decision-making circuits? With such aims, from a neurobiological point of view, I developed a novel behavioral assay to analyze single *Drosophila* olfactory behavior in high resolution using a spherical treadmill.

The initial experiments established that wild-type flies tracked vinegar persistently over ten trials, and avoided aversive odors in the spherical treadmill, under high arousal conditions (Figure 11-13). Persistence was only observed in food-deprived flies (Figure 14, 15). Flies, in the absence of input from a subset of dopaminergic neurons or lacking *Dop1R2* receptors, failed to perform vinegar tracking in a sustained fashion (Figure 17, 21). As a possible downstream target of dopaminergic modulation, a mushroom body output neuron, MVP2 was found to act as a motivational switch for hunger at the level of third-order neurons, and, when artificially activated, promoted odor-search in satiated flies (Figure 22-24).

To analyze how olfaction and feeding interacts, I depolarized gustatory neurons optogenetically and observed that olfaction and feeding are sequential antagonistic behaviors in the context of foraging (Figure 28). As an analog of norepinephrine, octopamine activation phenocopied the olfactory arrest (Figure 30,31). Additional experiments revealed that a single subset of octopaminergic neurons, VPM4, was sufficient to suppress olfaction (Figure 44, 46, 47). VPM4, with

its long projections starting from a region called SEZ (analog of the brainstem) to several major centers in the protocerebrum, was an ideal candidate to relay feeding information (Figure 42). Importantly, connectomics revealed that VPM4 and MVP2 were found directly connected, and this connection was functionally inhibitory (Figure 52-55). As a conclusion, while dopamine and MVP2 axis releases hunger dependent motivational drives for olfactory tracking, VPM4 directly depresses MVP2 to brake this behavior to enable switching from exploration to exploitation.

5.1 Flies Engage with Vinegar Persistently

To study behavior at higher resolution, I combined frontal, bilateral odor stimuli with the spherical treadmill built according to a blueprint designed for performing visual experiments (Seelig et al., 2010). In comparison to other olfactory treadmill assays for walking flies with unilateral odor delivery, I chose the bilateral, uniform concentration odor supply with the intention to present a higher salience stimulus. When odor concentrations vary less, and both antennae detect odor plumes simultaneously at a given time, such stimuli properties would signal immediate proximity of the odor source and might induce more robust behaviors. Indeed, in the experiments with the prototype of the setup, I challenged the flies with unilateral odor exposure (Figure 58, appendix). While flies engaged with the odor at the onset, they did not track the odor in a sustained manner. On the other hand, the bilateral stimulus did result in continuous tracking, depending on the hunger state (Figure 6-8, 14). This suggests fine spatiotemporal stimulus dynamics of odor plumes are taken into consideration by flies. Given this importance of stimulus dynamics to shape animal behavior, the next iteration of the spherical treadmill would be creating a true virtual reality for odors, in which unilateral and bilateral odor delivery modes work in combination. Such a protocol would crack odor approach behavior fully.

The closer look at this sustained behavior under bilateral vinegar sensation exposed a dynamic nature. Each passing trial, flies increased their running effort, expressed in speed increments (Figure 11). Meanwhile, I observed that turning behavior was reduced, indicating hungry flies were actively tracking vinegar (Figure

7). These observations solidified the claim that the behavior on the spherical treadmill was goal-driven, and not a by-product of an enhanced global arousal state which would be driven by starvation and higher ambient temperatures. Moreover, I found out that, independent of speed, further parameters could be extracted from the paradigm: while flies were faster in tracking vinegar, they also were more active (spend more time in odor-tracking as a fraction of the total stimulus period) and stopped later during odor exposure over trials (Figure 12, 13). Are these parameters encoded independently from speed at the level of neuronal computations? This novel assay can be exploited to posit such questions in the future.

5.2 Flies Avoid Repellent Odors on the Treadmill

It is well-established that flies are repelled by certain odors. Even a highly attractive food odor such as vinegar can be aversive in higher concentrations (Semmelhack and Wang, 2009). Flies were able to actively avoid odors such as benzaldehyde in tethered flight conditions (Wasserman et al., 2013). In contrast, few existing studies focused on single, walking animal paradigms for flies observed that repellent odor exposure led to a stop, not an active escape behavior (Borst and Heisenberg, 1982; Steck et al., 2012). These were followed by later proposals that aversion required, or at least augmented by collective behavior reinforcement (Ramdya et al., 2015). Here I showed that single *Drosophila melanogaster* flies do evade frontal CO₂ stimuli (Figure 9). Upon CO₂ plume, flies slowed down and engaged in escaped turns in either direction. What is the underlying factor for the apparent disagreement in the literature? I propose, ultimately the arousal levels are significant to the behavioral outcome in the presence of aversive odors. In comparison to the earlier studies, the higher ambient temperature in this paradigm I developed incentivized flies and lowered their behavioral thresholds. In low arousal conditions, flies might brace for impact and wait for the stimulus termination without committing costly escape behaviors.

Furthermore, since under CO₂ these flies did not accelerate, this results provided additional evidence that persistent odor tracking was dependent on odor valence.

5.3 The Mushroom Body Processes Innate Olfactory Attraction

In parallel to this doctoral thesis work, Laurence Lewis performed a silencing screen of lines that cover mushroom body output and modulatory neurons (Figure 22). MVP2 was found to be the most critical neuron for vinegar attraction. I confirmed this necessity also on the spherical treadmill and furthermore showed that MVP2 was sufficient to promote attraction in satiated flies (Figure 23, 24). These results indicate the latest addition to a list of results contradictory to the long-held view in the *Drosophila* neuroscience community that the MB was not necessary for innate olfactory behaviors. Earlier studies, in which MB was ablated chemically, flies without MB were indistinguishable from the controls (de Belle and Heisenberg, 1994). However, later on, the suppression of CO₂ aversion in hungry flies was found to be dependent on MB circuitry (Lewis et al., 2015). This indicated that indeed MB was able to partake in innate olfactory processing for aversive odors. Another study showed that activation of MVP2, a GABAergic inhibitory MBON, was able to suppress aversion to other innately aversive odors (Perisse et al., 2016). The fact that MVP2 showed highest neuronal activity for vinegar in a panel of odors hinted MVP2 could also shape innate attraction, an idea we confirmed with our experiments (Hige et al., 2015b).

While designated as a mushroom body output neuron MVP2 essentially is an intrinsic neuron. MVP2 axons innervate dendrites of two other MBONs, MBON- α 2sc and inhibitory M4/M6 cluster (Aso et al., 2014a). At least in aversive learning, MVP2 inhibits M4/M6 to enable attraction. For the same scenario, the axo-axonal connections between MVP2 and MBON- α 2sc did not alter the activity of post-synaptic partner (Perisse et al., 2016). Interestingly, MBON- α 2sc was the second hit in the T-maze screen performed by Laurence Lewis (Figure 22). Therefore, one could suggest that MVP2 and MBON- α 2sc, directly or indirectly, can work as a cohort during vinegar attraction. Since MVP2 was critical for attraction, yet its absence did not nullify persistence, MBON- α 2sc could be the next line to be tested on the spherical treadmill.

The lateral horn was postulated to be the sole secondary center for innate odor perception. This view has been challenged by recent work as discussed above. So, what are the respective roles of MB and LH in guiding innate olfactory behavior? Some proposals suggest that MB and LH have distinct roles: MB to categorize and LH to assign a value (Galizia, 2014). However, MB is indeed divided into two broad categories with opposite influences on valence coding (Aso et al., 2014b), while the LH appears to categorize odors (Frechter et al., 2018; Jeanne et al., 2018). Therefore, any clear functional distinction is currently premature without comprehensive systematic analyses. In this regard, the full characterization of MB and LH outputs beyond 'good vs. bad' are needed.

5.4 Persistence is not a By-Product.

Every novel paradigm developed requires scrutiny against by-products of the experimental setup. There are several components of the treadmill that can act as possible perpetuators of such artifacts. One of these factors is higher ambient temperature. Flies do not prefer temperatures as high as 30°C (Barbagallo and Garrity, 2015). Dehydration can quickly become life-threatening for such small animals. An additional factor would be the long experimental durations (~20 minutes for open-loop experiments) that would exacerbate temperature pressure on the animal. Without surprise, increasing the temperature from 25°C to 30°C altered the basal and stimulus-driven running speeds (Figure 6, 7). However, these cannot be the explanation for persistence. In contrast to the open-loop experiments with fixed length odor delivery, the closed-loop experiments were designed so that, flies were given a choice to track the odor on a straight path (Figure 15). Flies ran at higher speeds over time in these experiments as well. Importantly, although external pressures were intensifying, the increase in behavior was not a linear one. The longest runs were distributed over different trials (Figure 15.C). This fact also excludes generalized arousal and acclimatization on the treadmill as a significant factor for persistence. The higher, non-specific arousal and longer time spent on the ball do not translate into a better performance. ORCO mutants that are able to process only fractional olfactory information, satiated wild-type flies and starved wild-type flies that received only background air also showed only limited

improvements in their responses over time. Coupled to these arguments provided by the closed-loop experiments, these results depict that persistence is not a by-product, but it's driven by olfaction dependent motivational mechanisms.

5.5 Persistence Generators

I have established TH+ dopaminergic neurons are required for persistence (Figure 17, 20-21). What are the possible mechanisms of persistent odor tracking at the neuronal circuit level? Several mechanisms can be proposed: error signal, efference copy, negative drive suppression, and infotaxis.

Animals, even so-called simple organisms as insects, are able to integrate past events: learning and memory. Associative learning monitors coincidences of relevant external sensory inputs. In another variant, operant learning, flies can acquire the outcomes of their own actions: if a particular motor action, turning left, for instance, can be punished by repeated heat exposure and eventually flies will learn to avoid that behavior (Brembs, 2008). If such self-learning can take place, it is more than plausible that flies can monitor the outcome of their actions during goal-directed innate behaviors. Highly salient events such as food odor tracking should create strong feedbacks: absence of success would mean death. In the context of learning, animals were shown to generate reward prediction errors: after training, if there is a discrepancy between the expected and actual reward, this 'error' is encoded by the dopaminergic neurons (Schultz, 2016). As suggested above, if vinegar is a prediction for food presence in proximity, then its absence can be integrated as the error. Since higher odor concentration and continuous, unbroken plumes might indicate stronger immediacy, the error signal can be higher to drive even more persistent behavior.

Another hypothetical mechanism is that lack of reward can be a potent penalty. Such an absence can be engaging as a negative drive to develop persistence. The unpleasant, detrimental situations create motivational drives in animals to extinguish them. This is called negative drive suppression (Leib et al., 2017). As a subset of TH cluster, PPL1 dopaminergic circuits are the conduit for

punishment learning in flies. It's a possibility that effortful events such as persistent odor running are also encoded on these punishment learning circuits. In contrast to the error prediction hypothesis above, such dopaminergic circuits do not necessarily encode for the reward or the difference between the observed and the expected, but only responds to reward's absence.

Sensorimotor integration could be the driving force in the emergence of persistence. Odor-tracking can be subdivided into olfactory sensation and subsequent locomotion. An efference copy produced by odor tracking can underlie persistence. Efference copy is defined as a secondary internal signal generated in the nervous system to account their self-movement: changes in visual gaze upon eye/head movements for instance (Crapse and Sommer, 2008). Thus, efference copy is convenient to differentiate the external sensory world from the self. Yet, it might be useful to accommodate as a counter for how much effort has been spent. While sensory input remains constant (Figure 16), or degrade over time, an efference copy generator provides the accumulation of total effort spent over all the trials a fly goes through in the spherical treadmill. Subsequent summation of olfactory information and efference copy would result in persistence. This efference copy can emerge from the periphery (for example, central pattern generators in VNC) and then send to the central brain via ascending neurons as a dopaminergic input. Another route would be an efference copy formed in the central brain itself. Central complex is a neuropil that commands motor control and visual navigation, and it could be an ideal center to generate such signals. Furthermore, dopaminergic PPL1 neurons in MB seem to encode motor activity (Berry et al., 2015). Surprisingly, TH+ *DOPA* neurons that I found necessary for persistence also include the PPL1 cluster. Since MB is central to olfactory processing, it is a highly suitable locus for sensorimotor integration that generates persistence. It is not clear exactly what type of movement information is encoded in PPL1 *DOPA* neurons. Do they solely represent the behavioral state? Do they differentiate odor guided, goal-oriented behavior or other running behaviors? Is there an amplitude threshold for running speed, which would enable to discriminate low-speed exploration and high effort sprints? To answer these questions, clearly designed experiments are needed.

One of the proposed algorithms for odor research is called infotaxis: this computation relies on information collection through past events to predict the future location with the highest likelihood of containing the odor source. Infotaxis utilizes Bayesian statistics and were shown to guide robots to locate odor sources (Moraud and Martinez, 2010; Vergassola et al., 2007). To my knowledge, infotaxis has not been observed *in vivo*. Nevertheless, infotaxis proposes that analogous mechanisms might take place in insect brains. In the spherical treadmill, I presented the odor from the same location with respect to flies. Since no other directionality was presented, fly nervous system could have easily integrated the spatial evidence over time and concluded with increasing assertion that odor source was ahead. This will undoubtedly require short-term memory, which has also been traced in MB PPL1 cluster neurons.

5.6 MB Dependent Mechanistic Descriptions of Persistence

Once the role of TH+ DANs is recognized, given the prominence of MB in olfactory behavior, the next question to be asked is how MB could, in theory, exploit *DOPA* input to generate persistence. Detailed analysis of TH-gal4 reveals that there are two clusters of TH+ input to MB: PPL1 and lesser-known PPL2ab (Aso et al., 2012).

In a simple functional connectivity hypothesis, since both vertical MBONs and PPL1 DANs are required for persistence, PPL1 DANs are expected to boost MBON activity. However, the majority of evidence in the literature points out the exact opposite: during learning, physiological evidence points out that MBONs are dampened by PPL1 activity (Hige et al., 2015a). In a previous study, repeated familiar odor exposure inhibited MBON- α '3 compartment via the corresponding PPL1 activity (Hattori et al., 2017). Nonetheless, when Kenyon Cells were blocked chemically, the interaction between PPL1 DANs and MBONs are reversed to excitatory. Indeed, there exists a number of direct synapses between PPL1 DANs and MBONs (Eichler et al., 2017; Takemura et al., 2017). Also during relief learning, in which punishment precedes odor exposure, dopaminergic neurons can influence MBONs positively (Aso and Rubin, 2016; Gerber et al., 2014).

MVP2 is downstream at *NPF/PPL1-γ1pedc*, a microcircuit that gates olfactory appetitive motivation (Beshel and Zhong, 2013; Krashes et al., 2009). Two recent papers put forward the possibility that this circuit is recurrent: Lack of MVP2 activity impeded PPL1 dependent behaviors (Ueoka et al., 2017). From the perspective of persistence generation, such positive feedback would be valuable: MVP2 gates hunger state and reinforces PPL1 activity-based persistence.

Much less is known about the PPL2ab cluster of neurons. In one functional study, PPL2 activity was able to recover aging-induced decline of courtship male performance. Importantly PPL2ab activation was correlated with longer courtship duration (Kuo et al., 2015). Dopamine was also previously associated with courtship persistence (Crickmore and Vosshall, 2013). While inputs to PPL2ab neurons are unidentified, PPL2ab DANs project to MB input, Kenyon cells' dendrites. Does PPL2ab neuron respond to odors or retain neuronal activity over time to generate persistence? KCs can hold information on previous events in a sustained manner (Lüdke et al., 2018). These suggest that PPL2ab and KC neurons together can maintain persistence and drive relevant MBONs.

Whether PPL1 or PPL2ab, I have presented substantial evidence that vinegar induced persistence relies on dopamine receptor *Dop1R2* signaling (Figure 21). Flies lacking *Dop1R2* performed worse over trials and could not maintain a persistent odor response. *Dop1R2* is essential for forgetting associative memories (Himmelreich et al., 2017). Whether a similar mechanism is also involved for persistence is not known at this stage. Removal of the *Dop1R2* receptor from PPL1 and PPL2ab candidate targets would allow a crucial experiment. Lastly, while running responses of *Dop1R1* null mutants were not changed, these flies retained higher baseline running, possibly suggesting that *Dop1R1* and *R2* signaling antagonize each other, as in learning (Figure 20, 21) (Davis and Zhong, 2017).

5.7 Sequence Transitions are Flexible

One of the core functions of nervous systems is action selection. At a given time, countless possibilities may exist, it is imperative to select optimum behavioral

choices for immediate and long-term survival. Foraging is a multi-step, complex behavior for animals. In flies, nutrient deprivation facilitates an increase in basal locomotion and lower sensory receptor thresholds (Yang et al., 2015; Yu et al., 2016). Upon encountering a food patch, exploration ceases, gustation and ingestion follow (Thoma et al., 2017). To understand how these transitions occur in a mechanistically manner, I decided to combine olfactory delivery with optogenetic activation of gustatory sensory neurons. Indeed, activation of gustatory receptors led to break away from olfactory tracking (Figure 28).

The sequence changes, however, are not strict. I found that activation of Gr5a+ neurons, one of the significant external sugar sensors, only briefly stopped olfactory tracking (Figure 28.A, D). Subsequent to initial onset response to activation, these flies resumed odor tracking and accelerated faster in comparison to Gr43a+ neuronal activation. While we have to take into account that Gr5a+ neurons were reported to go under habituation under sustained activation via another channelrhodopsin, the literature also supports our interpretation (Lin et al., 2013). Brief sugar presentation leads to the induction of local search in starved animals (Murata et al., 2017). It's likely that external sugar sensation alone is pleasant. However, it fails to satisfy a hungry fly's final goal: nutrient intake. On the other hand, Gr43a neuron fulfills this role as an internal nutrient sensor. Therefore, post-ingestion information, that is represented by activation of Gr43a, did indeed result in prolonged suppression of odor tracking (Figure 28.A-C). Do neurons that express other internal nutrient sensors also prevent odor tracking in this manner? Ultimately, these manipulations show that transition from olfaction to gustation and ingestion is not a linear, deterministic transition.

5.8 VPMs Exert Control on Behavioral Transitions

Action selection must involve inhibition between possible scenarios. The aberrant absence of inhibitory mechanisms is proposed to be an underlying factor of impulsive conditions (Bari and Robbins, 2013). Unsurprisingly, inhibition, as a central mechanism, requires significant energy expenditure in the brain (Buzsáki et

al., 2007). In flies, inhibition has proposed to guide forming sequentially antagonistic behavioral executions (Seeds et al., 2014).

In this study, I have observed that persistent odor-induced olfactory tracking is arrested by octopaminergic neuronal activity, reminiscent of gustatory neuron activation (Figure 30, 31). Furthermore, I was able to pinpoint this behavioral switch to a single subtype of OANs: VPM4 (Figure 44, 46-47). The activation of Tdc2+ OANs or VPM4 alone was sufficient to brake persistence immediately. This brake mechanism involved hyperpolarization of MVP2 neurons, a necessary neuron for odor approach, by VPM4 (Figure 53).

Another scenario of how VPMs control olfaction could be through inducing an internal state switch: activating VPMs might confer fed state to hungry animals. A closer look at the behavior of fed flies shows that they did not stop upon vinegar application (Figure 14, 15). Simply they maintained their basal running speed and did not engage odor plume. On the contrary, activation of broad Tdc2+ and narrow VPM4 neurons led to a stop behavior (Figure 30-31,44,47). These results show that these OANs indeed help sequence transitions.

5.9 Mechanisms of OAN Mediated Inhibition of MVP2 activity

Since octopamine and tyramine can induce opposite neuromodulatory effects, and share the same biochemical pathway for production, Anja Friedrich stained VPM4 neurons with antibodies against for neuromodulators. We did not observe any strong tyramine labeling in these neurons (Figure 43) and confirmed the earlier studies that this subtype of neurons is indeed octopaminergic (Busch et al., 2009). The interaction between presynaptic VPM4 and postsynaptic MVP2 neurons are inhibitory (Figure 53). Recently, there has been only one other study showing that OA could dampen the postsynaptic neuron (LeDue et al., 2016). OA signaling relies on G-coupled receptors for modulation (Evans and Maqueira, 2005). A number of different OA receptors are characterized in the fly brain, in particular for MB (El-Kholy et al., 2015). Ultimately, the modulatory sign for neuromodulation depends on which G-protein is involved downstream in the

signaling pathway for the post-synaptic neuron. Highly likely, this depression on neuronal activity is underlined by Gi subunit dependent signaling (Hamm, 1998).

It is important to note that, while VPM4 is octopaminergic, the culprit can be another neuromodulator. The closer look at the synapses between VPM4 and MVP2 showed that there are two morphologically distinct sets of vesicles at the pre-synaptic site (Figure 52.E). Co-release of octopamine and an inhibitory neuromodulator could occur, or depending on the activation profile of VPM4, the pre-synaptic neurons can release different modulators at a given time. Preliminary immunohistochemistry work by Anja Friedrich revealed that VPM4 could harbor glutamatergic signaling (Data not shown). Glutamate has been reported as an inhibitory actor (Liu and Wilson, 2013). Further experiments are needed to be done to flesh out whether OA or glutamate takes charge on inhibitory neuromodulation on MVP2.

5.10 VPM Post-Synaptic Targets are Diverse

For the first time in the literature, Anja Friedrich analyzed the polarity of VPM3 and VPM4 neurons (Figure 42). Confirming our hypotheses, these neurons had clear bi-polar morphology: their dendrites were located exclusively in the ventral brain, mostly in SEZ, whereas their projections were to be found only in the protocerebrum. These projections were indeed very extensive. VPM3 covered superior protocerebrum, fan-shaped body, noduli, and MB lobes; and VPM4 innervated ventrolateral protocerebrum, inferior protocerebrum, superior protocerebrum and MB lobes (Busch et al., 2009). What is the functional meaning of this broad innervation? One possibility is that VPMs mediate coordination and control of several brain regions, in particular, with regard to feeding-related behaviors.

In this study, I primarily focused on the relation between olfaction and feeding, the interaction between VPMs and MVP2. Lack of MVP2 activity resulted in reduced odor tracking. However, VPM4 activity in some cases led to complete stop behavior (Figure 54, 55). Where does the discrepancy arise? Since MVP2 is

part of the highly-interconnected MB network, it's possible that MVP2 shares some level of redundancy with other MB output neurons. In theory, VPM4 could inhibit several MBONs directly and influence MB network in multiple locations. Alternately, VPM dependent arrest phenotype relies on another locus in the protocerebrum. Blocking of MVP2 by VPM4 tunes down the motivational mechanisms for odor-induced running and, in a dissociated pathway, VPM4 executes a motor command for immediate stop. Only full electron microscopy reconstruction would reveal the extent of VPM4's influence.

5.11 VPM4 Might Receive Tarsal Input

In order to strengthen our hypothesis that VPMs bridge olfaction and feeding, my colleague Jean-Francois de Backer performed calcium imaging during fructose feeding *in vivo* using the *Tdc2-Gal4* line. Basal calcium indicator GCaMP levels in *MB113C-Gal4>UAS-GCaMP* flies were inadequate to locate VPM4 neurons. With *Tdc2-Gal4*, we were successful to observe a significant calcium signal in starved flies (Figure 36). The observed signal amplitude was comparable to another study where *Tdc2+* neurons were monitored for another gustatory input of Gr32a sensory neurons in the context of aggression (Andrews et al., 2014). However, in our hands, the transient signal did not recapitulate the duration of behavioral manipulations (12 seconds). Possible technical challenges (GCaMP dynamics, MB113C expression strength, VPM4 properties) might explain the lack of sustained response from VPM4. Despite this discrepancy in temporal scale, a recent study described VPM4 activation strengthened feeding behaviors. It is important to reiterate, the activation of gustatory receptors and VPM4 neurons followed a very similar pattern (Figure 28, 44). Coupled to these facts that SEZ, where VPM4 have extended dendrites, receives dense taste information, I can claim VPM4 has a role in taste processing. One highly likely source of input to VPM4 is ascending tarsal neurons that relay gustatory information to SEZ from the legs (Thoma et al., 2016). Legs would be the first appendage to encounter food patches during locomotion. Then, tarsal input would likely be the fastest route to facilitate the immediate arrest of olfactory induced attraction.

5.12 VPMs Do Not Regulate Olfactory Learning

It's important to note that, octopamine's role in learning has been extensively reported. Mainly, octopamine is required for reward presentation during positive association formation (Burke et al., 2012; Huetteroth et al., 2015). Nonetheless, in parallel to such reward neuronal circuits, any positive feedback instruments must be available for innate behaviors as well. Monitoring outcome of one's actions is indispensable. Yet, VPMs were insufficient to form short-term associations (Burke et al., 2012). Similarly, in my hands, the prior pairing of vinegar and VPM activation did not alter future odor responses to the odor (Figure 44.E). Connectomic data also reinforce this observation: VPMs innervated directly dendritic region of MVP2 while bypassing KCs and DANs. KC-DAN axis onto mushroom body output neurons is the primary pipeline for learning-induced changes (Owald and Waddell, 2015). VPMs do not interact with these canonical learning circuits. Therefore, my work and previous studies establish VPMs do not lead to olfactory learning.

5.13 Broad Manipulations of Tdc2+ OANs Have Opposite Effects

Chronic or acute activation of Tdc2+ OANs with different effector proteins and blocking synaptic output from the same set of neurons created seemingly similar phenotypes: reduction of running speed during repeated vinegar exposure (Figure 30, 31, 38). Furthermore, *Tβh* mutants with reduced OA production supported the Tdc2 driven loss-of-function phenotype (Figure 37). How was this conflicting set of results possible? However, closer looking of the running speed traces revealed subtle differences. Activation of Tdc2+ OANs would lead to immediate stopping behavior (decelerating from basal speed to 0 mm / sec at the onset) (Figure 30-33). This is interpreted as switching from exploration to exploitation. On the other hand, blocking OANs also resulted in slower running speeds (Figure 37-38). A possible explanation would be the following: the global of lack OA release equates to a lack of motivational drive for behaviors that need energy expenditure. To bolster the fact that these seemingly similar phenotypes were indeed precisely opposite, it was decided to use 4-arm olfactometer assay. In this paradigm, in comparison to tethered flies on the spherical treadmill, the test

animals were able to move unhindered and make spatial decisions to enter odor quadrants (Figure 35). Unsurprisingly, Lisa Marie Frisch performed these experiments, and we saw that simultaneous activation of OANs and odor application indeed led to an accumulation of flies. In the case of reduced motivational drives, animals would have dispersed in the circular arena, a scenario we did not observe. Therefore, we can surely claim that activation and inhibition of OANs produce distinct phenotypes.

Furthermore, it should be noted that Tdc2 line covers more than 100 neurons (Busch et al., 2009). Separate manipulations can favor different subsets from the parental Tdc2+ pool. Consequently, interpretations using broader lines should be always accompanied by additional sets of evidence. For example, functional imaging would narrow down participating neurons at a given behavior. A substitute approach would be utilization intersectional genetics, transgenic lines targeting distinct single subsets of neurons, as I did in this study. A narrower manipulation would surely enable a tighter correlation between neuronal activity and behavior.

5.14 OAN Diversity in SEZ

SEZ is rich in octopaminergic input and contains a number of OAN clusters. However, sparse transgenic targeting is not yet publicly available. Yet, in addition to VPMs, I tested an additional split-gal4 line that targets an additional OAN in this region: VUMa2. The acute and chronic depolarization of this neuron during odor exposure phenocopied broader octopaminergic neuron and specific VPM activation (Figure 49). *Drosophila* VUM neurons mediate feeding control (Zhang et al., 2013). Similar to VPMs, VUMa2 has long-distance projections in the fly CNS (at LH and MB calyx regions). As a result, it's possible to assume that VPMs and VUMa2 share some level of functional redundancy. Another plausible scenario is that VPM and VUM neurons interact functionally. However, it must be noted that VUMa2-Gal4 line has not been morphologically characterized and possibly harbors further neurons, including VPMs (personal communication, Yoshinari Aso). Nevertheless, this emphasizes the morphological diversity and abundance of octopaminergic neurons in the SEZ region. A systematic functional analysis is critical for our comprehensive

understanding of these neurons. Further expansion of split-gal4 library for OANs would be instrumental in this goal. Such systematic view also shed light in resolving diversity of norepinephrine in mammalian locus coeruleus. Locus coeruleus is highly similar to SEZ in term of gross anatomy and the emergence of norepinephrinergic input to distal regions from this location (Sara and Bouret, 2012).

5.15 Possible Tdc2 and NPF Signaling Convergence

Previous studies showed that insulin and AKH signaling exert influence OANs for enhanced locomotion under starvation (Yang et al., 2015; Yu et al., 2016). It is possible that neuronal computations that reconcile internal state and energy expenditure can exist in several distinct circuits. In this regard, I conducted several preliminary experiments that are known to relay hunger state. In the spherical treadmill, removing the *sNPF* receptor from Tdc2+ neurons did not alter odor approach (Figure 39.A, B). Perturbing *NPF* receptor via TRiP class RNA interference, however, boosted odor tracking (Figure 39.E, F). It should be noted that another RNAi line, KK class, did not recapitulate this (Figure 39.C, D). The particular RNA interference lines might have differential efficiency against the target mRNA. Therefore, additional experiments, analyses of mRNA *NPF-R* in Tdc2 neurons levels for these two RNAi lines, must be performed. Nevertheless, blocking *NPF* neuron activity also slightly strengthened odor tracking and activation of *NPF* neurons partially reduced vinegar response (Figure 40). Earlier studies showed that activation of *NPF* in the brain reduces motivational thresholds and leads to an increase in odor preference (Beshel and Zhong, 2013). One scenario would suggest that neuromodulator *NPF* acts on locomotion promoting Tdc2 neurons, inhibits them to bias flies towards exploiting the current local environment.

6 CONCLUSIONS AND FUTURE DIRECTIONS

The doctoral thesis provided extensive evidence for how nutrient deprived animals, faced with demise, act persistently to track laminar food odor plumes to acquire food. This is true despite the lack of an expected reward. In this novel behavioral paradigm, starved flies were presented with repeated vinegar exposure and found to increase their responses over time. The absence of input from TH+ dopaminergic neuromodulatory neurons and dopamine receptor *Dop1R2* obliterated persistence. Moreover, this tracking behavior was dependent on olfaction and gated by internal hunger state. Hunger state was incorporated at the level of the mushroom body; a single mushroom body output neuron, MVP2, was necessary and sufficient to govern *Drosophila* behavior accordingly. Fascinatingly, connectomic evidence demonstrated MVP2 was a direct target of octopaminergic VPM4 neuron. VPM4, in coordination with feeding, mediated a brake on olfactory persistence via inhibiting MVP2, thus ensuring that once the reward is reached, it can be exploited (Figure 56).

This study posits several interesting questions for future studies. Once the role of dopamine has been established for persistence generation, the outstanding question concerns the nature of information encoded in TH+ dopaminergic neurons. Out of the possible scenarios offered above (section 5.5), to find out what leads to persistence would ultimately require physiological studies in behaving flies. For instance, if persistence relies on error signals, TH+ neurons would respond to vinegar exposure even before the animal engages in odor tracking. During tracking, the error signal would increase with each vinegar exposure until a food patch encounter. In the case of accomplishing the goal, the dopaminergic activity would resettle at the basal level. Moreover, persistence encoding would generalize to other odors that guide goal-directed behaviors, and amplitude of dopamine signaling would indicate the predictive power of a given odor to achieve the goal.

The second avenue of research would be a comprehensive characterization of octopaminergic neurons in SEZ. Once the intersectional genetics provides

sufficient coverage to target all *OA+* neurons, at single subtype resolution, in this region of the fly brain, their functional diversity would surely provide a template for understanding mammalian locus coeruleus. A combination of behavioral screens and physiological observations would unravel their role in neuromodulation of coordinating behaviors such as olfaction, feeding, and aggression. Identification of their targets, via trans-synaptic labeling or connectomics, would also be significant to understand the function of these octopaminergic neurons.

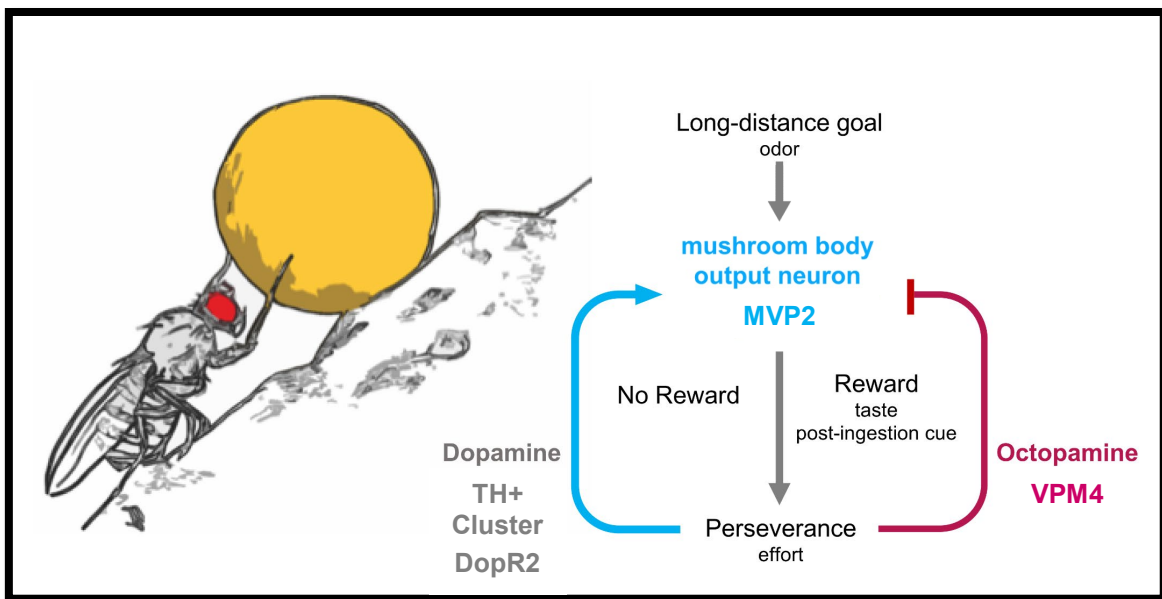


Figure 56 Summary

7 REFERENCES

- Andrews, J.C., Fernández, M.P., Yu, Q., Leary, G.P., Leung, A.K., Kavanaugh, M.P., Kravitz, E.A., and Certel, S.J. (2014). Octopamine neuromodulation regulates *gr32a*-linked aggression and courtship pathways in *Drosophila* males. *PLoS Genet.* 10, e1004356.
- Aso, Y., and Rubin, G.M. (2016). Dopaminergic neurons write and update memories with cell-type-specific rules. *Elife* 5.
- Aso, Y., Herb, A., Ogueta, M., Siwanowicz, I., Templier, T., Friedrich, A.B., Ito, K., Scholz, H., and Tanimoto, H. (2012). Three Dopamine Pathways Induce Aversive Odor Memories with Different Stability. *PLoS Genet.* 8, e1002768.
- Aso, Y., Hattori, D., Yu, Y., Johnston, R.M., Iyer, N.A., Ngo, T.-T., Dionne, H., Abbott, L., Axel, R., Tanimoto, H., et al. (2014a). The neuronal architecture of the mushroom body provides a logic for associative learning. *Elife* 3, e04577.
- Aso, Y., Sitaraman, D., Ichinose, T., Kaun, K.R., Vogt, K., Belliart-Guérin, G., Plaçais, P.Y., Robie, A.A., Yamagata, N., Schnaitmann, C., et al. (2014b). Mushroom body output neurons encode valence and guide memory-based action selection in *Drosophila*. *Elife* 3, e04580.
- Bachmann, A., and Knust, E. (2008). The Use of P-Element Transposons to Generate Transgenic Flies. In *Methods in Molecular Biology* (Clifton, N.J.), pp. 61–77.
- Badel, L., Ohta, K., Tsuchimoto, Y., and Kazama, H. (2016). Decoding of Context-Dependent Olfactory Behavior in *Drosophila*. *Neuron* 91, 155–167.
- Bahl, A., Ammer, G., Schilling, T., and Borst, A. (2013). Object tracking in motion-blind flies. *Nat. Neurosci.* 16, 730–738.
- Baines, R.A., Uhler, J.P., Thompson, A., Sweeney, S.T., and Bate, M. (2001). Altered electrical properties in *Drosophila* neurons developing without synaptic transmission. *J. Neurosci.* 21, 1523–1531.
- Barbagallo, B., and Garrity, P.A. (2015). Temperature sensation in *Drosophila*. *Curr. Opin. Neurobiol.* 34, 8–13.
- Bargmann, C.I. (2012). Beyond the connectome: How neuromodulators shape neural circuits. *BioEssays* 34, 458–465.
- Bari, A., and Robbins, T.W. (2013). Inhibition and impulsivity: Behavioral and neural basis of response control. *Prog. Neurobiol.* 108, 44–79.
- Barnstedt, O., Oswald, D., Felsenberg, J., Brain, R., Moszynski, J.-P., Talbot, C.B., Perrat, P.N., and Waddell, S. (2016). Memory-Relevant Mushroom Body Output Synapses Are Cholinergic. *Neuron* 89, 1237–1247.
- de Belle, J.S., and Heisenberg, M. (1994). Associative odor learning in *Drosophila* abolished by chemical ablation of mushroom bodies. *Science* 263, 692–695.
- Benton, R., Vannice, K.S., Gomez-Diaz, C., and Vossell, L.B. (2009). Variant

- Ionotropic Glutamate Receptors as Chemosensory Receptors in *Drosophila*. *Cell* **136**, 149–162.
- Berck, M.E., Khandelwal, A., Claus, L., Hernandez-Nunez, L., Si, G., Tabone, C.J., Li, F., Truman, J.W., Fetter, R.D., Louis, M., et al. (2016). The wiring diagram of a glomerular olfactory system. *Elife* **5**.
- Berridge, K.C. (2004). Motivation concepts in behavioral neuroscience. *Physiol. Behav.* **81**, 179–209.
- Berry, J.A., Cervantes-Sandoval, I., Nicholas, E.P., and Davis, R.L. (2012). Dopamine is required for learning and forgetting in *Drosophila*. *Neuron* **74**, 530–542.
- Berry, J.A., Cervantes-Sandoval, I., Chakraborty, M., and Davis, R.L. (2015). Sleep Facilitates Memory by Blocking Dopamine Neuron-Mediated Forgetting. *Cell* **161**, 1656–1667.
- Beshel, J., and Zhong, Y. (2013). Graded Encoding of Food Odor Value in the *Drosophila* Brain. *J. Neurosci.* **33**, 15693–15704.
- Beshel, J., Dubnau, J., and Zhong, Y. (2017). A Leptin Analog Locally Produced in the Brain Acts via a Conserved Neural Circuit to Modulate Obesity-Linked Behaviors in *Drosophila*. *Cell Metab.* **25**, 208–217.
- Bischof, J., Maeda, R.K., Hediger, M., Karch, F., and Basler, K. (2007). An optimized transgenesis system for *Drosophila* using germ-line-specific phiC31 integrases. *Proc. Natl. Acad. Sci. U. S. A.* **104**, 3312–3317.
- Block, E., Jang, S., Matsunami, H., Sekharan, S., Dethier, B., Ertem, M.Z., Gundala, S., Pan, Y., Li, S., Li, Z., et al. (2015). Implausibility of the vibrational theory of olfaction. *Proc. Natl. Acad. Sci. U. S. A.* **112**, E2766–74.
- Borst, A., and Heisenberg, M. (1982). Osmotropotaxis in *Drosophila melanogaster*. *J. Comp. Physiol. ? A* **147**, 479–484.
- Bouzaiane, E., Trannoy, S., Scheunemann, L., Plaçais, P.-Y., and Preat, T. (2015). Two independent mushroom body output circuits retrieve the six discrete components of *Drosophila* aversive memory. *Cell Rep.* **11**, 1280–1292.
- Bräcker, L.B., Siju, K.P., Varela, N., Aso, Y., Zhang, M., Hein, I., Vasconcelos, M.L., and Grunwald Kadow, I.C. (2013). Essential Role of the Mushroom Body in Context-Dependent CO₂ Avoidance in *Drosophila*. *Curr. Biol.* **23**, 1228–1234.
- Brand, A.H., and Perrimon, N. (1993). Targeted gene expression as a means of altering cell fates and generating dominant phenotypes. *Development* **118**, 401–415.
- Brembs, B. (2008). Operant learning of *Drosophila* at the torque meter. *J. Vis. Exp.*
- Brembs, B., Christiansen, F., Pfluger, H.J., and Duch, C. (2007). Flight Initiation and Maintenance Deficits in Flies with Genetically Altered Biogenic Amine Levels. *J. Neurosci.* **27**, 11122–11131.
- van Breugel, F., and Dickinson, M. (2014). Plume-Tracking Behavior of Flying *Drosophila* Emerges from a Set of Distinct Sensory-Motor Reflexes. *Curr. Biol.* **24**, 274–286.
- de Bruyne, M., Clyne, P.J., and Carlson, J.R. (1999). Odor coding in a model

- olfactory organ: the *Drosophila* maxillary palp. *J. Neurosci.* 19, 4520–4532.
- Burke, C.J., Huetteroth, W., Oswald, D., Perisse, E., Krashes, M.J., Das, G., Gohl, D., Silies, M., Certel, S., and Waddell, S. (2012). Layered reward signalling through octopamine and dopamine in *Drosophila*. *Nature* 492, 433–437.
- Busch, S., Selcho, M., Ito, K., and Tanimoto, H. (2009). A map of octopaminergic neurons in the *Drosophila* brain. *J. Comp. Neurol.* 513, 643–667.
- Butcher, N.J., Friedrich, A.B., Lu, Z., Tanimoto, H., and Meinertzhagen, I.A. (2012). Different classes of input and output neurons reveal new features in microglomeruli of the adult *Drosophila* mushroom body calyx. *J. Comp. Neurol.* 520, 2185–2201.
- Buzsáki, G., Kaila, K., and Raichle, M. (2007). Inhibition and brain work. *Neuron* 56, 771–783.
- Campbell, R.A.A., Honegger, K.S., Qin, H., Li, W., Demir, E., and Turner, G.C. (2013). Imaging a population code for odor identity in the *Drosophila* mushroom body. *J. Neurosci.* 33, 10568–10581.
- Cao, G., Platasa, J., Pieribone, V.A., Raccuglia, D., Kunst, M., and Nitabach, M.N. (2013). Genetically Targeted Optical Electrophysiology in Intact Neural Circuits. *Cell* 154, 904–913.
- Caron, S.J.C., Ruta, V., Abbott, L.F., and Axel, R. (2013). Random convergence of olfactory inputs in the *Drosophila* mushroom body. *Nature* 497, 113–117.
- Cervantes-Sandoval, I., Phan, A., Chakraborty, M., and Davis, R.L. (2017). Reciprocal synapses between mushroom body and dopamine neurons form a positive feedback loop required for learning.
- Cho, W., Heberlein, U., and Wolf, F.W. (2004). Habituation of an odorant-induced startle response in *Drosophila*. *Genes, Brain Behav.* 3, 127–137.
- Claridge-Chang, A., Roorda, R.D., Vrontou, E., Sjulson, L., Li, H., Hirsh, J., and Miesenböck, G. (2009). Writing Memories with Light-Addressable Reinforcement Circuitry. *Cell* 139, 405–415.
- Clemens, J.C., Worby, C.A., Simonson-Leff, N., Muda, M., Maehama, T., Hemmings, B.A., and Dixon, J.E. (2000). Use of double-stranded RNA interference in *Drosophila* cell lines to dissect signal transduction pathways. *Proc. Natl. Acad. Sci. U. S. A.* 97, 6499–6503.
- Clyne, J.D., and Miesenböck, G. (2008). Sex-Specific Control and Tuning of the Pattern Generator for Courtship Song in *Drosophila*. *Cell* 133, 354–363.
- Clyne, P.J., Warr, C.G., Freeman, M.R., Lessing, D., Kim, J., and Carlson, J.R. (1999). A novel family of divergent seven-transmembrane proteins: candidate odorant receptors in *Drosophila*. *Neuron* 22, 327–338.
- Cohn, R., Morante, I., and Ruta, V. (2015). Coordinated and Compartmentalized Neuromodulation Shapes Sensory Processing in *Drosophila*. *Cell* 163, 1742–1755.
- Cole, S.H., Carney, G.E., McClung, C.A., Willard, S.S., Taylor, B.J., and Hirsh, J. (2005). Two functional but noncomplementing *Drosophila* tyrosine decarboxylase genes: distinct roles for neural tyramine and octopamine in female fertility. *J. Biol. Chem.* 280, 14948–14955.

- Corrales-Carvajal, V.M., Faisal, A.A., and Ribeiro, C. (2016). Internal states drive nutrient homeostasis by modulating exploration-exploitation trade-off. *Elife* 5.
- Coyne, J.A., Bryant, S.H., and Turelli, M. (1987). Long-Distance Migration of *Drosophila*. 2. Presence in Desolate Sites and Dispersal Near a Desert Oasis. *Am. Nat.* 129, 847–861.
- Crapse, T.B., and Sommer, M.A. (2008). Corollary discharge across the animal kingdom. *Nat. Rev. Neurosci.* 9, 587–600.
- Crickmore, M.A., and Vosshall, L.B. (2013). Opposing dopaminergic and GABAergic neurons control the duration and persistence of copulation in *Drosophila*. *Cell* 155, 881–893.
- Crittenden, J.R., Skoulakis, E.M., Han, K.A., Kalderon, D., and Davis, R.L. Tripartite mushroom body architecture revealed by antigenic markers. *Learn. Mem.* 5, 38–51.
- Crocker, A., Shahidullah, M., Levitan, I.B., and Sehgal, A. (2010). Identification of a neural circuit that underlies the effects of octopamine on sleep:wake behavior. *Neuron* 65, 670–681.
- Dahanukar, A., Lei, Y.-T., Kwon, J.Y., and Carlson, J.R. (2007). Two Gr Genes Underlie Sugar Reception in *Drosophila*. *Neuron* 56, 503–516.
- Das, S., Sadanandappa, M.K., Dervan, A., Larkin, A., Lee, J.A., Sudhakaran, I.P., Priya, R., Heidari, R., Holohan, E.E., Pimentel, A., et al. (2011). Plasticity of local GABAergic interneurons drives olfactory habituation. *Proc. Natl. Acad. Sci. U. S. A.* 108, E646-54.
- DasGupta, S., Ferreira, C.H., and Miesenbock, G. (2014). FoxP influences the speed and accuracy of a perceptual decision in *Drosophila*. *Science* (80-). 344, 901–904.
- Davis, R.L., and Zhong, Y. (2017). The Biology of Forgetting-A Perspective. *Neuron* 95, 490–503.
- Dethier, V.G. (Vincent G. (1976). *The hungry fly: a physiological study of the behavior associated with feeding* (Harvard University Press).
- Duistermars, B.J., Chow, D.M., and Frye, M.A. (2009). Flies Require Bilateral Sensory Input to Track Odor Gradients in Flight. *Curr. Biol.* 19, 1774–1775.
- Dus, M., Ai, M., and Suh, G.S.B. (2013). Taste-independent nutrient selection is mediated by a brain-specific Na⁺/solute co-transporter in *Drosophila*. *Nat. Neurosci.* 16, 526–528.
- Eichler, K., Li, F., Litwin-Kumar, A., Park, Y., Andrade, I., Schneider-Mizell, C.M., Saumweber, T., Huser, A., Eschbach, C., Gerber, B., et al. (2017). The complete connectome of a learning and memory centre in an insect brain. *Nature* 548, 175–182.
- El-Kholy, S., Stephano, F., Li, Y., Bhandari, A., Fink, C., and Roeder, T. (2015). Expression analysis of octopamine and tyramine receptors in *Drosophila*. *Cell Tissue Res.* 361, 669–684.
- Evans, P.D., and Maqueira, B. (2005). Insect octopamine receptors: a new classification scheme based on studies of cloned *Drosophila* G-protein coupled receptors. *Invertebr. Neurosci.* 5, 111–118.

- Farhan, A., Gulati, J., Große-Wilde, E., Vogel, H., Hansson, B.S., and Knaden, M. (2013). The CCHamide 1 receptor modulates sensory perception and olfactory behavior in starved *Drosophila*. *Sci. Rep.* 3, 2765.
- Ferrario, C.R., Labouèbe, G., Liu, S., Nieh, E.H., Routh, V.H., Xu, S., and O'Connor, E.C. (2016). Homeostasis Meets Motivation in the Battle to Control Food Intake. *J. Neurosci.* 36, 11469–11481.
- Fiala, A., Spall, T., Diegelmann, S., Eisermann, B., Sachse, S., Devaud, J.-M., Buchner, E., and Galizia, C.G. (2002). Genetically expressed cameleon in *Drosophila melanogaster* is used to visualize olfactory information in projection neurons. *Curr. Biol.* 12, 1877–1884.
- Fishilevich, E., and Vosshall, L.B. (2005). Genetic and Functional Subdivision of the *Drosophila* Antennal Lobe. *Curr. Biol.* 15, 1548–1553.
- Fox, L.E., Soll, D.R., and Wu, C.F. (2006). Coordination and modulation of locomotion pattern generators in *Drosophila* larvae: effects of altered biogenic amine levels by the tyramine beta hydroxylase mutation. *J. Neurosci.* 26, 1486–1498.
- Frank, D.D., Jouandet, G.C., Kearney, P.J., Macpherson, L.J., and Gallio, M. (2015). Temperature representation in the *Drosophila* brain. *Nature* 519, 358–361.
- Frechter, S., Bates, A.S., Tootoonian, S., Dolan, M.-J., Manton, J.D., Jamasb, A., Kohl, J., Bock, D., and Jefferis, G.S.X.E. (2018). Functional and Anatomical Specificity in a Higher Olfactory Centre. *BioRxiv* 336982.
- Fujii, S., Yavuz, A., Slone, J., Jagge, C., Song, X., and Amrein, H. (2015). *Drosophila* sugar receptors in sweet taste perception, olfaction, and internal nutrient sensing. *Curr. Biol.* 25, 621–627.
- Galili, D.S., Dylla, K.V., Lüdke, A., Friedrich, A.B., Yamagata, N., Wong, J.Y.H., Ho, C.H., Szyszka, P., and Tanimoto, H. (2014). Converging Circuits Mediate Temperature and Shock Aversive Olfactory Conditioning in *Drosophila*. *Curr. Biol.* 24, 1712–1722.
- Galizia, C.G. (2014). Olfactory coding in the insect brain: data and conjectures. *Eur. J. Neurosci.* 39, 1784–1795.
- Gaudry, Q., Hong, E.J., Kain, J., de Bivort, B.L., and Wilson, R.I. (2012). Asymmetric neurotransmitter release enables rapid odour lateralization in *Drosophila*. *Nature* 493, 424–428.
- Gerber, B., Yarali, A., Diegelmann, S., Wotjak, C.T., Pauli, P., and Fendt, M. (2014). Pain-relief learning in flies, rats, and man: basic research and applied perspectives. *Learn. Mem.* 21, 232–252.
- Goldman, A.L., Van der Goes van Naters, W., Lessing, D., Warr, C.G., and Carlson, J.R. (2005). Coexpression of Two Functional Odor Receptors in One Neuron. *Neuron* 45, 661–666.
- Gordon, M.D., and Scott, K. (2009). Motor Control in a *Drosophila* Taste Circuit. *Neuron* 61, 373–384.
- Groschner, L.N., Chan Wah Hak, L., Bogacz, R., DasGupta, S., and Miesenböck, G. (2018). Dendritic Integration of Sensory Evidence in Perceptual Decision-Making. *Cell* 173, 894–905.e13.

- Gruntman, E., and Turner, G.C. (2013). Integration of the olfactory code across dendritic claws of single mushroom body neurons. *Nat. Neurosci.* 16, 1821–1829.
- Grunwald Kadow, I.C. (2019). State-dependent plasticity of innate behavior in fruit flies. *Curr. Opin. Neurobiol.* 54, 60–65.
- Gu, H., and O'Dowd, D.K. (2006). Cholinergic synaptic transmission in adult *Drosophila* Kenyon cells in situ. *J. Neurosci.* 26, 265–272.
- Hallem, E.A., and Carlson, J.R. (2006). Coding of Odors by a Receptor Repertoire. *Cell* 125, 143–160.
- Hamada, F.N., Rosenzweig, M., Kang, K., Pulver, S.R., Ghezzi, A., Jegla, T.J., and Garrity, P.A. (2008). An internal thermal sensor controlling temperature preference in *Drosophila*. *Nature* 454, 217–220.
- Hamm, H.E. (1998). The many faces of G protein signaling. *J. Biol. Chem.* 273, 669–672.
- Hammer, M., and Menzel, R (1998). Multiple sites of associative odor learning as revealed by local brain microinjections of octopamine in honeybees. *Learn. Mem.* 5, 146–156.
- Harris, D.T., Kallman, B.R., Mullaney, B.C., and Scott, K. (2015). Representations of Taste Modality in the *Drosophila* Brain. *Neuron* 86, 1449–1460.
- Hattori, D., Aso, Y., Swartz, K.J., Rubin, G.M., Abbott, L.F., and Axel, R. (2017). Representations of Novelty and Familiarity in a Mushroom Body Compartment. *Cell* 169, 956–969.e17.
- Heisenberg, M. (2003). Mushroom body memoir: from maps to models. *Nat. Rev. Neurosci.* 4, 266–275.
- Hige, T., Aso, Y., Modi, M.N., Rubin, G.M., and Turner, G.C. (2015a). Heterosynaptic Plasticity Underlies Aversive Olfactory Learning in *Drosophila*. *Neuron* 88, 985–998.
- Hige, T., Aso, Y., Rubin, G.M., and Turner, G.C. (2015b). Plasticity-driven individualization of olfactory coding in mushroom body output neurons. *Nature* 526, 258–262.
- Himmelreich, S., Masuho, I., Berry, J.A., MacMullen, C., Skamangas, N.K., Martemyanov, K.A., and Davis, R.L. (2017). Dopamine Receptor DAMB Signals via Gq to Mediate Forgetting in *Drosophila*. *Cell Rep.* 21, 2074–2081.
- Honegger, K.S., Campbell, R.A.A., and Turner, G.C. (2011). Cellular-resolution population imaging reveals robust sparse coding in the *Drosophila* mushroom body. *J. Neurosci.* 31, 11772–11785.
- Hong, E.J., and Wilson, R.I. (2015). Simultaneous Encoding of Odors by Channels with Diverse Sensitivity to Inhibition. *Neuron* 85, 573–589.
- Huetteroth, W., Perisse, E., Lin, S., Klappenbach, M., Burke, C., and Waddell, S. (2015). Sweet taste and nutrient value subdivide rewarding dopaminergic neurons in *Drosophila*. *Curr. Biol.* 25, 751–758.
- Hussain, A., Zhang, M., Üçpınar, H.K., Svensson, T., Quillery, E., Gompel, N., Ignell, R., and Grunwald Kadow, I.C. (2016). Ionotropic Chemosensory

- Receptors Mediate the Taste and Smell of Polyamines. *PLOS Biol.* **14**, e1002454.
- Ikemoto, S., Yang, C., and Tan, A. (2015). Basal ganglia circuit loops, dopamine and motivation: A review and enquiry. *Behav. Brain Res.* **290**, 17–31.
- Inagaki, H.K., Jung, Y., Hoopfer, E.D., Wong, A.M., Mishra, N., Lin, J.Y., Tsien, R.Y., and Anderson, D.J. (2014). Optogenetic control of *Drosophila* using a red-shifted channelrhodopsin reveals experience-dependent influences on courtship. *Nat. Methods* **11**, 325–332.
- Ito, I., Ong, R.C., Raman, B., and Stopfer, M. (2008). Sparse odor representation and olfactory learning. *Nat. Neurosci.* **11**, 1177–1184.
- Jeanne, J.M., Fişek, M., and Wilson, R.I. (2018). The Organization of Projections from Olfactory Glomeruli onto Higher-Order Neurons. *Neuron* **98**, 1198–1213.e6.
- Jefferis, G.S.X.E., Potter, C.J., Chan, A.M., Marin, E.C., Rohlifing, T., Maurer, C.R., and Luo, L. (2007). Comprehensive Maps of *Drosophila* Higher Olfactory Centers: Spatially Segregated Fruit and Pheromone Representation. *Cell* **128**, 1187–1203.
- Jiao, Y., Moon, S.J., Wang, X., Ren, Q., and Montell, C. (2008). Gr64f Is Required in Combination with Other Gustatory Receptors for Sugar Detection in *Drosophila*. *Curr. Biol.* **18**, 1797–1801.
- Joiner, W.J., Crocker, A., White, B.H., and Sehgal, A. (2006). Sleep in *Drosophila* is regulated by adult mushroom bodies. *Nature* **441**, 757–760.
- Jones, W.D., Cayirlioglu, P., Grunwald Kadow, I., and Vosshall, L.B. (2007). Two chemosensory receptors together mediate carbon dioxide detection in *Drosophila*. *Nature* **445**, 86–90.
- Joseph, R.M., and Carlson, J.R. (2015). *Drosophila* Chemoreceptors: A Molecular Interface Between the Chemical World and the Brain. *Trends Genet.* **31**, 683–695.
- Joseph, R.M., Sun, J.S., Tam, E., and Carlson, J.R. (2017). A receptor and neuron that activate a circuit limiting sucrose consumption. *Elife* **6**.
- Kain, P., and Dahanukar, A. (2015). Secondary taste neurons that convey sweet taste and starvation in the *Drosophila* brain. *Neuron* **85**, 819–832.
- Karaiskos, N., Wahle, P., Alles, J., Boltengagen, A., Ayoub, S., Kipar, C., Kocks, C., Rajewsky, N., and Zinzen, R.P. (2017). The *Drosophila* embryo at single-cell transcriptome resolution. *Science* eaan3235.
- Kaun, K.R., Azanchi, R., Maung, Z., Hirsh, J., and Heberlein, U. (2011). A *Drosophila* model for alcohol reward. *Nat. Neurosci.* **14**, 612–619.
- Kazama, H., and Wilson, R.I. (2008). Homeostatic matching and nonlinear amplification at identified central synapses. *Neuron* **58**, 401–413.
- Keene, A.C., and Masek, P. (2012). Optogenetic induction of aversive taste memory. *Neuroscience* **222**, 173–180.
- Keleman, K., Vrontou, E., Krüttner, S., Yu, J.Y., Kurtovic-Kozaric, A., and Dickson, B.J. (2012). Dopamine neurons modulate pheromone responses in *Drosophila* courtship learning. *Nature* **489**, 145–149.

- Kim, I.S., and Dickinson, M.H. (2017). Idiothetic Path Integration in the Fruit Fly *Drosophila melanogaster*. *Curr. Biol.* 27, 2227–2238.e3.
- Kim, H., Kirkhart, C., and Scott, K. (2017). Long-range projection neurons in the taste circuit of *Drosophila*. *Elife* 6.
- Kim, Y.-C., Lee, H.-G., and Han, K.-A. (2007). D1 Dopamine Receptor dDA1 Is Required in the Mushroom Body Neurons for Aversive and Appetitive Learning in *Drosophila*. *J. Neurosci.* 27, 7640–7647.
- Kirkhart, C., and Scott, K. (2015). Gustatory Learning and Processing in the *Drosophila* Mushroom Bodies. *J. Neurosci.* 35, 5950–5958.
- Kitamoto, T. (2001). Conditional modification of behavior in *Drosophila* by targeted expression of a temperature-sensitive *shibire* allele in defined neurons. *J. Neurobiol.* 47, 81–92.
- Klapoetke, N.C., Murata, Y., Kim, S.S., Pulver, S.R., Birdsey-Benson, A., Cho, Y.K., Morimoto, T.K., Chuong, A.S., Carpenter, E.J., Tian, Z., et al. (2014). Independent optical excitation of distinct neural populations. *Nat. Methods* 11, 338–346.
- Knaden, M., Strutz, A., Ahsan, J., Sachse, S., and Hansson, B.S. (2012). Spatial representation of odorant valence in an insect brain. *Cell Rep.* 1, 392–399.
- Ko, K.I., Root, C.M., Lindsay, S.A., Zaninovich, O.A., Shepherd, A.K., Wasserman, S.A., Kim, S.M., and Wang, J.W. (2015). Starvation promotes concerted modulation of appetitive olfactory behavior via parallel neuromodulatory circuits. *Elife* 4.
- Koon, A.C., Ashley, J., Barria, R., DasGupta, S., Brain, R., Waddell, S., Alkema, M.J., and Budnik, V. (2011). Autoregulatory and paracrine control of synaptic and behavioral plasticity by octopaminergic signaling. *Nat. Neurosci.* 14, 190–199.
- Krashes, M.J., DasGupta, S., Vreede, A., White, B., Armstrong, J.D., and Waddell, S. (2009). A Neural Circuit Mechanism Integrating Motivational State with Memory Expression in *Drosophila*. *Cell* 139, 416–427.
- Kuo, S.-Y., Wu, C.-L., Hsieh, M.-Y., Lin, C.-T., Wen, R.-K., Chen, L.-C., Chen, Y.-H., Yu, Y.-W., Wang, H.-D., Su, Y.-J., et al. (2015). PPL2ab neurons restore sexual responses in aged *Drosophila* males through dopamine. *Nat. Commun.* 6, 7490.
- Lai, S.-L., and Lee, T. (2006). Genetic mosaic with dual binary transcriptional systems in *Drosophila*. *Nat. Neurosci.* 9, 703–709.
- Landayan, D., Feldman, D.S., and Wolf, F.W. (2018). Satiation state-dependent dopaminergic control of foraging in *Drosophila*. *Sci. Rep.* 8, 5777.
- Larderet, I., Fritsch, P.M., Gendre, N., Neagu-Maier, G.L., Fetter, R.D., Schneider-Mizell, C.M., Truman, J.W., Zlatić, M., Cardona, A., and Sprecher, S.G. (2017). Organization of the *Drosophila* larval visual circuit. *Elife* 6.
- Larsson, M.C., Domingos, A.I., Jones, W.D., Chiappe, M.E., Amrein, H., and Vosshall, L.B. (2004). Or83b encodes a broadly expressed odorant receptor essential for *Drosophila* olfaction. *Neuron* 43, 703–714.
- LeDue, E.E., Mann, K., Koch, E., Chu, B., Dakin, R., Gordon, M.D., Scully, A., Carlson, J.W., Wan, K.H., Lavery, T.R., et al. (2016). Starvation-Induced

- Depotential of Bitter Taste in *Drosophila*. *Curr. Biol.* 26, 2854–2861.
- Lee, G., and Park, J.H. (2004). Hemolymph sugar homeostasis and starvation-induced hyperactivity affected by genetic manipulations of the adipokinetic hormone-encoding gene in *Drosophila melanogaster*. *Genetics* 167, 311–323.
- Leib, D.E., Zimmerman, C.A., Poormoghaddam, A., Huey, E.L., Ahn, J.S., Lin, Y.-C., Tan, C.L., Chen, Y., and Knight, Z.A. (2017). The Forebrain Thirst Circuit Drives Drinking through Negative Reinforcement. *Neuron* 96, 1272–1281.e4.
- Lewis, L.P.C.P.C., Siju, K.P.P., Aso, Y., Friedrich, A.B.B., Bulteel, A.J.B.J.B., Rubin, G.M.M., and Grunwald Kadow, I.C. (2015). A Higher Brain Circuit for Immediate Integration of Conflicting Sensory Information in *Drosophila*. *Curr. Biol.* 25, 2203–2214.
- Li, Y., Tiedemann, L., von Frieling, J., Nolte, S., El-Kholy, S., Stephano, F., Gelhaus, C., Bruchhaus, I., Fink, C., and Roeder, T. (2017). The Role of Monoaminergic Neurotransmission for Metabolic Control in the Fruit Fly *Drosophila Melanogaster*. *Front. Syst. Neurosci.* 11, 60.
- Li, Y.Y., Hoffmann, J., Li, Y.Y., Stephano, F., Bruchhaus, I., Fink, C., and Roeder, T. (2016). Octopamine controls starvation resistance, life span and metabolic traits in *Drosophila*. *Sci. Rep.* 6, 35359.
- Liang, L., Li, Y., Potter, C.J., Yizhar, O., Deisseroth, K., Tsien, R.W., and Luo, L. (2013). GABAergic projection neurons route selective olfactory inputs to specific higher-order neurons. *Neuron* 79, 917–931.
- Liman, E.R., Zhang, Y.V., and Montell, C. (2014). Peripheral Coding of Taste. *Neuron* 81, 984–1000.
- Lin, A.C., Bygrave, A.M., de Calignon, A., Lee, T., and Miesenböck, G. (2014a). Sparse, decorrelated odor coding in the mushroom body enhances learned odor discrimination. *Nat. Neurosci.* 17, 559–568.
- Lin, J.Y., Knutsen, P.M., Muller, A., Kleinfeld, D., and Tsien, R.Y. (2013). ReaChR: a red-shifted variant of channelrhodopsin enables deep transcranial optogenetic excitation. *Nat. Neurosci.* 16, 1499–1508.
- Lin, S., Oswald, D., Chandra, V., Talbot, C., Huetteroth, W., and Waddell, S. (2014b). Neural correlates of water reward in thirsty *Drosophila*. *Nat. Neurosci.* 17, 1536–1542.
- Lindsley, D.L., and Zimm, G.G. (1992). *The Genome of Drosophila melanogaster*. (Elsevier Science).
- Liu, W.W., and Wilson, R.I. (2013). Glutamate is an inhibitory neurotransmitter in the *Drosophila* olfactory system. *Proc. Natl. Acad. Sci.* 110, 10294–10299.
- Liu, C., Plaçais, P.-Y., Yamagata, N., Pfeiffer, B.D., Aso, Y., Friedrich, A.B., Siwanowicz, I., Rubin, G.M., Preat, T., and Tanimoto, H. (2012). A subset of dopamine neurons signals reward for odour memory in *Drosophila*. *Nature* 488, 512–516.
- Lorenz, K., and Leyhausen, P. (1973). *Motivation of human and animal behavior; an ethological view* (Van Nostrand Reinhold Co).
- Luan, H., Peabody, N.C., Vinson, C.R., and White, B.H. (2006). Refined spatial

- manipulation of neuronal function by combinatorial restriction of transgene expression. *Neuron* 52, 425–436.
- Lüdke, A., Raiser, G., Nehrkorn, J., Herz, A.V.M., Galizia, C.G., and Szyszka, P. (2018). Calcium in Kenyon Cell Somata as a Substrate for an Olfactory Sensory Memory in *Drosophila*. *Front. Cell. Neurosci.* 12, 128.
- Luo, J., Lushchak, O. V, Goergen, P., Williams, M.J., and Nassel, D.R. (2014). *Drosophila* insulin-producing cells are differentially modulated by serotonin and octopamine receptors and affect social behavior. *PLoS One* 9, e99732.
- Ma, Z., Stork, T., Bergles, D.E., and Freeman, M.R. (2016). Neuromodulators signal through astrocytes to alter neural circuit activity and behaviour. *Nature* 539, 428–432.
- Majid, A., and Kruspe, N. (2018). Hunter-Gatherer Olfaction Is Special. *Curr. Biol.* 28, 409–413.e2.
- Major, G., and Tank, D. (2004). Persistent neural activity: prevalence and mechanisms. *Curr. Opin. Neurobiol.* 14, 675–684.
- Mann, K., Gordon, M.D., and Scott, K. (2013). A Pair of Interneurons Influences the Choice between Feeding and Locomotion in *Drosophila*. *Neuron* 79, 754–765.
- Mann, K., Gallen, C.L., and Clandinin, T.R. (2017). Whole-Brain Calcium Imaging Reveals an Intrinsic Functional Network in *Drosophila*. *Curr. Biol.* 27, 2389–2396.e4.
- Manzo, A., Silies, M., Gohl, D.M., and Scott, K. (2012). Motor neurons controlling fluid ingestion in *Drosophila*. *Proc. Natl. Acad. Sci. U. S. A.* 109, 6307–6312.
- Marella, S., Mann, K., and Scott, K. (2012). Dopaminergic Modulation of Sucrose Acceptance Behavior in *Drosophila*. *Neuron* 73, 941–950.
- Marin, E.C., Jefferis, G.S.X., Komiyama, T., Zhu, H., and Luo, L. (2002). Representation of the Glomerular Olfactory Map in the *Drosophila* Brain. *Cell* 109, 243–255.
- Martelli, C., Pech, U., Kobbenbring, S., Pauls, D., Bahl, B., Sommer, M.V., Pooryasin, A., Barth, J., Arias, C.W.P., Vassiliou, C., et al. (2017). SIFamide Translates Hunger Signals into Appetitive and Feeding Behavior in *Drosophila*. *Cell Rep.* 20, 464–478.
- Mason, G.J., and Bateson, M. (2009). Motivation and the Organization of Behaviour. *Ethol. Domest. Anim.* 38–56.
- Matsuda, H., Yamada, T., Yoshida, M., and Nishimura, T. (2015). Flies without trehalose. *J. Biol. Chem.* 290, 1244–1255.
- Miyamoto, T., and Amrein, H. (2014). Diverse roles for the *Drosophila* fructose sensor Gr43a. *Fly (Austin)*. 8, 19–25.
- Miyamoto, T., Slone, J., Song, X., and Amrein, H. (2012). A fructose receptor functions as a nutrient sensor in the *Drosophila* brain. *Cell* 151, 1113–1125.
- Mlodzik, M., and Hiromi, Y. (1992). Enhancer Trap Method in *Drosophila*: Its Application to Neurobiology. *Methods Neurosci.* 9, 397–414.
- Mohammad, F., Stewart, J.C., Ott, S., Chlebikova, K., Chua, J.Y., Koh, T.-W., Ho, J., and Claridge-Chang, A. (2017). Optogenetic inhibition of behavior with

- anion channelrhodopsins. *Nat. Methods* **14**, 271–274.
- Monastirioti, M., Linn, C.E., and White, K. (1996). Characterization of *Drosophila* Tyramine α -hydroxylase gene and isolation of mutant flies lacking octopamine. *J. Neurosci.* **16**, 3900–3911.
- Morad, E., and Martinez, D. (2010). Effectiveness and robustness of robot infotaxis for searching in dilute conditions. *Front. Neurobot.* **4**, 1.
- Murata, S., Brockmann, A., and Tanimura, T. (2017). Pharyngeal stimulation with sugar triggers local searching behavior in *Drosophila*. *J. Exp. Biol.* **220**, 3231–3237.
- Nagel, K.I., and Wilson, R.I. (2011). Biophysical mechanisms underlying olfactory receptor neuron dynamics. *Nat. Neurosci.* **14**, 208–216.
- Nagel, K.I., and Wilson, R.I. (2016). Mechanisms Underlying Population Response Dynamics in Inhibitory Interneurons of the *Drosophila* Antennal Lobe. *J. Neurosci.* **36**, 4325–4338.
- Nitabach, M.N., Wu, Y., Sheeba, V., Lemon, W.C., Strumbos, J., Zelensky, P.K., White, B.H., and Holmes, T.C. (2006). Electrical hyperexcitation of lateral ventral pacemaker neurons desynchronizes downstream circadian oscillators in the fly circadian circuit and induces multiple behavioral periods. *J. Neurosci.* **26**, 479–489.
- Ohhara, Y., Kayashima, Y., Hayashi, Y., Kobayashi, S., and Yamakawa-Kobayashi, K. (2012). Expression of β -adrenergic-like Octopamine Receptors during *Drosophila* Development. *Zoolog. Sci.* **29**, 83–89.
- Olsen, S.R., Bhandawat, V., and Wilson, R.I. (2010). Divisive Normalization in Olfactory Population Codes. *Neuron* **66**, 287–299.
- Ormerod, K.G., Hadden, J.K., Deady, L.D., Mercier, A.J., and Krans, J.L. (2013). Action of octopamine and tyramine on muscles of *Drosophila melanogaster* larvae. *J. Neurophysiol.* **110**, 1984–1996.
- Owald, D., and Waddell, S. (2015). Olfactory learning skews mushroom body output pathways to steer behavioral choice in *Drosophila*. *Curr. Opin. Neurobiol.* **35**, 178–184.
- Owald, D., Felsenberg, J., Talbot, C.B., Das, G., Perisse, E., Huetteroth, W., and Waddell, S. (2015). Activity of defined mushroom body output neurons underlies learned olfactory behavior in *Drosophila*. *Neuron* **86**, 417–427.
- Parnas, M., Lin, A.C., Huetteroth, W., and Miesenböck, G. (2013). Odor discrimination in *Drosophila*: from neural population codes to behavior. *Neuron* **79**, 932–944.
- Perisse, E., Oswald, D., Barnstedt, O., Talbot, C.B.B., Huetteroth, W., and Waddell, S. (2016). Aversive Learning and Appetitive Motivation Toggle Feed-Forward Inhibition in the *Drosophila* Mushroom Body. *Neuron* **90**, 1086–1099.
- Pfeiffer, B.D., Ngo, T.-T.B., Hibbard, K.L., Murphy, C., Jenett, A., Truman, J.W., and Rubin, G.M. (2010). Refinement of Tools for Targeted Gene Expression in *Drosophila*. *Genetics* **186**, 735–755.
- Pitman, J.L., McGill, J.J., Keegan, K.P., and Allada, R. (2006). A dynamic role for the mushroom bodies in promoting sleep in *Drosophila*. *Nature* **441**, 753–

- Pool, A.-H., Kvello, P., Mann, K., Cheung, S.K., Gordon, M.D., Wang, L., and Scott, K. (2014). Four GABAergic interneurons impose feeding restraint in *Drosophila*. *Neuron* 83, 164–177.
- Potter, C.J., and Luo, L. (2011). Using the Q system in *Drosophila melanogaster*. *Nat. Protoc.* 6, 1105–1120.
- Qi, Y.-X., Xu, G., Gu, G., Mao, F., Ye, G.-Y., Liu, W., and Huang, J. (2017). A new *Drosophila* octopamine receptor responds to serotonin. *Insect Biochem. Mol. Biol.* 90, 61–70.
- Ramdyia, P., Lichocki, P., Cruchet, S., Frisch, L., Tse, W., Floreano, D., and Benton, R. (2015). Mechanosensory interactions drive collective behaviour in *Drosophila*. *Nature* 519, 233–236.
- Rezával, C., Nojima, T., Neville, M.C., Lin, A.C., and Goodwin, S.F. (2014). Sexually dimorphic octopaminergic neurons modulate female postmating behaviors in *Drosophila*. *Curr. Biol.* 24, 725–730.
- Riemensperger, T., Völler, T., Stock, P., Buchner, E., and Fiala, A. (2005). Punishment prediction by dopaminergic neurons in *Drosophila*. *Curr. Biol.* 15, 1953–1960.
- Rodrigues, V. (1988). Spatial coding of olfactory information in the antennal lobe of *Drosophila melanogaster*. *Brain Res.* 453, 299–307.
- Root, C.M., Ko, K.I., Jafari, A., and Wang, J.W. (2011). Presynaptic facilitation by neuropeptide signaling mediates odor-driven food search. *Cell* 145, 133–144.
- Ryglewski, S., Duch, C., and Altenhein, B. (2017). Tyramine Actions on *Drosophila* Flight Behavior Are Affected by a Glial Dehydrogenase/Reductase. *Front. Syst. Neurosci.* 11, 68.
- Sachse, S., Rueckert, E., Keller, A., Okada, R., Tanaka, N.K., Ito, K., and Vosshall, L.B. (2007). Activity-Dependent Plasticity in an Olfactory Circuit. *Neuron* 56, 838–850.
- Sara, S.J., and Bouret, S. (2012). Orienting and Reorienting: The Locus Coeruleus Mediates Cognition through Arousal. *Neuron* 76, 130–141.
- Saraswati, S., Fox, L.E., Soll, D.R., and Wu, C.F. (2004). Tyramine and octopamine have opposite effects on the locomotion of *Drosophila* larvae. *J. Neurobiol.* 58, 425–441.
- Sato, K., Tanaka, K., and Touhara, K. (2011). Sugar-regulated cation channel formed by an insect gustatory receptor. *Proc. Natl. Acad. Sci. U. S. A.* 108, 11680–11685.
- Sayin, S., Boehm, A.C., Kobler, J.M., De Backer, J.-F., and Grunwald Kadow, I.C. (2018). Internal State Dependent Odor Processing and Perception-The Role of Neuromodulation in the Fly Olfactory System. *Front. Cell. Neurosci.* 12, 11.
- Schneider, A., Ruppert, M., Hendrich, O., Giang, T., Ogueta, M., Hampel, S., Vollbach, M., Büschges, A., and Scholz, H. (2012). Neuronal Basis of Innate Olfactory Attraction to Ethanol in *Drosophila*. *PLoS One* 7, 1–12.

- Schroll, C., Riemensperger, T., Bucher, D., Ehmer, J., V?ller, T., Erbguth, K., Gerber, B., Hendel, T., Nagel, G., Buchner, E., et al. (2006). Light-Induced Activation of Distinct Modulatory Neurons Triggers Appetitive or Aversive Learning in *Drosophila* Larvae. *Curr. Biol.* 16, 1741–1747.
- Schultz, W. (2016). Dopamine reward prediction error coding. *Dialogues Clin. Neurosci.* 18, 23–32.
- Schulze, A., Gomez-Marin, A., Rajendran, V.G., Lott, G., Musy, M., Ahammad, P., Deogade, A., Sharpe, J., Riedl, J., Jarriault, D., et al. (2015). Dynamical feature extraction at the sensory periphery guides chemotaxis. *Elife* 4, e06694.
- Schwaerzel, M., Monastirioti, M., Scholz, H., Friggi-Grelin, F., Birman, S., and Heisenberg, M. (2003). Dopamine and octopamine differentiate between aversive and appetitive olfactory memories in *Drosophila*. *J. Neurosci.* 23, 10495–10502.
- Seeds, A.M., Ravbar, P., Chung, P., Hampel, S., Midgley, F.M., Mensh, B.D., and Simpson, J.H. (2014). A suppression hierarchy among competing motor programs drives sequential grooming in *Drosophila*. *Elife* 3, e02951.
- Seelig, J.D., Chiappe, M.E., Lott, G.K., Dutta, A., Osborne, J.E., Reiser, M.B., and Jayaraman, V. (2010). Two-photon calcium imaging from head-fixed *Drosophila* during optomotor walking behavior. *Nat. Methods* 7, 535.
- Selcho, M., Pauls, D., El Jundi, B., Stocker, R.F., and Thum, A.S. (2012). The Role of octopamine and tyramine in *Drosophila* larval locomotion. *J. Comp. Neurol.* 520, 3764–3785.
- Semmelhack, J.L., and Wang, J.W. (2009). Select *Drosophila* glomeruli mediate innate olfactory attraction and aversion. *Nature* 459, 218–223.
- Shang, Y., Claridge-Chang, A., Sjulson, L., Pypaert, M., and Miesenböck, G. (2007). Excitatory Local Circuits and Their Implications for Olfactory Processing in the Fly Antennal Lobe. *Cell* 128, 601–612.
- Sitaraman, D., Aso, Y., Rubin, G.M., and Nitabach, M.N. (2015). Control of Sleep by Dopaminergic Inputs to the *Drosophila* Mushroom Body. *Front. Neural Circuits* 9, 73.
- Steck, K., Veit, D., Grandy, R., Badia, S.B. i, Mathews, Z., Verschure, P., Hansson, B.S., and Knaden, M. (2012). A high-throughput behavioral paradigm for *Drosophila* olfaction - The Flywalk. *Sci. Rep.* 2, 361.
- Stephenson, R., and Metcalfe, N. (2013). *Drosophila melanogaster*: a fly through its history and current use. *J. R. Coll. Physicians Edinb.* 43, 70–75.
- Stocker, R.F., Lienhard, M.C., Borst, A., and Fischbach, K.F. (1990). Neuronal architecture of the antennal lobe in *Drosophila melanogaster*. *Cell Tissue Res.* 262, 9–34.
- Strutz, A., Soelter, J., Baschwitz, A., Farhan, A., Grabe, V., Rybak, J., Knaden, M., Schmuker, M., Hansson, B.S., and Sachse, S. (2014). Decoding odor quality and intensity in the *Drosophila* brain. *Elife* 3, e04147.
- Su, C.-Y., Menuz, K., Reiser, J., and Carlson, J.R. (2012). Non-synaptic inhibition between grouped neurons in an olfactory circuit. *Nature* 492, 66–71.
- Suh, G.S.B., Wong, A.M., Hergarden, A.C., Wang, J.W., Simon, A.F., Benzer, S.,

- Axel, R., and Anderson, D.J. (2004). A single population of olfactory sensory neurons mediates an innate avoidance behaviour in *Drosophila*. *Nature* **431**, 854–859.
- Suster, M.L., Seugnet, L., Bate, M., and Sokolowski, M.B. (2004). Refining GAL4-driven transgene expression in *Drosophila* with a GAL80 enhancer-trap. *Genesis* **39**, 240–245.
- Sweeney, S.T., Broadie, K., Keane, J., Niemann, H., and O’Kane, C.J. (1995). Targeted expression of tetanus toxin light chain in *Drosophila* specifically eliminates synaptic transmission and causes behavioral defects. *Neuron* **14**, 341–351.
- Szyszkka, P., Gerkin, R.C., Galizia, C.G., and Smith, B.H. (2014). High-speed odor transduction and pulse tracking by insect olfactory receptor neurons. *Proc. Natl. Acad. Sci. U. S. A.* **111**, 16925–16930.
- Takemura, S.S., Aso, Y., Hige, T., Wong, A., Lu, Z., Xu, C.S., Rivlin, P.K., Hess, H., Zhao, T., Parag, T., et al. (2017). A connectome of a learning and memory center in the adult *Drosophila* brain. *Elife* **6**, e26975.
- Talay, M., Richman, E.B., Snell, N.J., Hartmann, G.G., Fisher, J.D., Sorkaç, A., Santoyo, J.F., Chou-Freed, C., Nair, N., Johnson, M., et al. (2017). Transsynaptic Mapping of Second-Order Taste Neurons in Flies by trans-Tango. *Neuron* **96**, 783–795.e4.
- Tanaka, N.K., Tanimoto, H., and Ito, K. (2008). Neuronal assemblies of the *Drosophila* mushroom body. *J. Comp. Neurol.* **508**, 711–755.
- Theodosiou, N.A., and Xu, T. (1998). Use of FLP/FRT System to Study *Drosophila* Development. *Methods* **14**, 355–365.
- Thoma, V., Knapek, S., Arai, S., Hartl, M., Kohsaka, H., Sirigrivatanawong, P., Abe, A., Hashimoto, K., and Tanimoto, H. (2016). Functional dissociation in sweet taste receptor neurons between and within taste organs of *Drosophila*. *Nat. Commun.* **7**, 10678.
- Thoma, V., Kobayashi, K., and Tanimoto, H. (2017). The Role of the Gustatory System in the Coordination of Feeding. *Eneuro* **4**, ENEURO.0324-17.2017.
- Thorne, N., Chromey, C., Bray, S., and Amrein, H. (2004). Taste Perception and Coding in *Drosophila*. *Curr. Biol.* **14**, 1065–1079.
- Tomchik, S.M. (2013). Dopaminergic neurons encode a distributed, asymmetric representation of temperature in *Drosophila*. *J. Neurosci.* **33**, 2166–76a.
- Tsao, C.-H., Chen, C.-C., Lin, C.-H., Yang, H.-Y., and Lin, S. (2018). *Drosophila* mushroom bodies integrate hunger and satiety signals to control innate food-seeking behavior. *Elife* **7**.
- Turin, L. (1996). A Spectroscopic Mechanism for Primary Olfactory Reception. *Chem. Senses* **21**, 773–791.
- Turner, S.L., and Ray, A. (2009). Modification of CO₂ avoidance behaviour in *Drosophila* by inhibitory odorants. *Nature* **461**, 277–281.
- Twick, I., Lee, J.A., and Ramaswami, M. (2014). Olfactory Habituation in *Drosophila*—Odor Encoding and its Plasticity in the Antennal Lobe. In *Progress in Brain Research*, pp. 3–38.

- Ueoka, Y., Hiroi, M., Abe, T., and Tabata, T. (2017). Suppression of a single pair of mushroom body output neurons in *Drosophila* triggers aversive associations. *FEBS Open Bio* 7, 562–576.
- Vergassola, M., Villerman, E., and Shraiman, B.I. (2007). 'Infotaxis' as a strategy for searching without gradients. *Nature* 445, 406–409.
- Vogt, K., Schnaitmann, C., Dylla, K. V, Knapek, S., Aso, Y., Rubin, G.M., and Tanimoto, H. (2014). Shared mushroom body circuits underlie visual and olfactory memories in *Drosophila*. *Elife* 3.
- Vogt, K., Aso, Y., Hige, T., Knapek, S., Ichinose, T., Friedrich, A.B., Turner, G.C., Rubin, G.M., and Tanimoto, H. (2016). Direct neural pathways convey distinct visual information to *Drosophila* mushroom bodies. *Elife* 5.
- Vosshall, L.B., Amrein, H., Morozov, P.S., Rzhetsky, A., and Axel, R. (1999). A spatial map of olfactory receptor expression in the *Drosophila* antenna. *Cell* 96, 725–736.
- Vosshall, L.B., Wong, A.M., and Axel, R. (2000). An olfactory sensory map in the fly brain. *Cell* 102, 147–159.
- Wang, J.W., Wong, A.M., Flores, J., Vosshall, L.B., and Axel, R. (2003). Two-photon calcium imaging reveals an odor-evoked map of activity in the fly brain. *Cell* 112, 271–282.
- Wang, Q.P., Lin, Y.Q., Zhang, L., Wilson, Y.A., Oyston, L.J., Cotterell, J., Qi, Y., Khuong, T.M., Bakhshi, N., Planchenault, Y., et al. (2016). Sucralose Promotes Food Intake through NPY and a Neuronal Fasting Response. *Cell Metab.* 24, 75–90.
- Wasserman, S., Salomon, A., and Frye, M.A. (2013). *Drosophila* tracks carbon dioxide in flight. *Curr. Biol.* 23, 301–306.
- Wilson, R.I. (2005). Role of GABAergic Inhibition in Shaping Odor-Evoked Spatiotemporal Patterns in the *Drosophila* Antennal Lobe. *J. Neurosci.* 25, 9069–9079.
- Wolf, R., Wittig, T., Liu, L., Wustmann, G., Eyding, D., and Heisenberg, M. (1998). *Drosophila* mushroom bodies are dispensable for visual, tactile, and motor learning. *Learn. Mem.* 5, 166–178.
- Wong, A.M., Wang, J.W., and Axel, R. (2002). Spatial Representation of the Glomerular Map in the *Drosophila* Protocerebrum. *Cell* 109, 229–241.
- Wu, C.-L., Shih, M.-F.M., Lee, P.-T., and Chiang, A.-S. (2013). An octopamine-mushroom body circuit modulates the formation of anesthesia-resistant memory in *Drosophila*. *Curr. Biol.* 23, 2346–2354.
- Yaksi, E., and Wilson, R.I. (2010). Electrical Coupling between Olfactory Glomeruli. *Neuron* 67, 1034–1047.
- Yang, Z., Yu, Y., Zhang, V., Tian, Y., Qi, W., Wang, L., Lao, K., Surani, M., Lowell, B., and David, J. (2015). Octopamine mediates starvation-induced hyperactivity in adult *Drosophila*. *Proc. Natl. Acad. Sci.* 112, 5219–5224.
- Yao, Z., Macara, A.M., Lelito, K.R., Minosyan, T.Y., and Shafer, O.T. (2012). Analysis of functional neuronal connectivity in the *Drosophila* brain. *J. Neurophysiol.* 108, 684–696.

- Yapici, N., Cohn, R., Schusterreiter, C., Ruta, V., and Vosshall, L.B. (2016). A Taste Circuit that Regulates Ingestion by Integrating Food and Hunger Signals. *Cell* 165, 715–729.
- Yasuyama, K., Kitamoto, T., and Salvaterra, P.M. (1995). Localization of choline acetyltransferase-expressing neurons in the larval visual system of *Drosophila melanogaster*. *Cell Tissue Res.* 282, 193–202.
- Youn, H., Kirkhart, C., Chia, J., and Scott, K. (2018). A subset of octopaminergic neurons that promotes feeding initiation in *Drosophila melanogaster*. *PLoS One* 13, e0198362.
- Yu, Y., Huang, R., Ye, J., Zhang, V., Wu, C., Cheng, G., Jia, J., and Wang, L. (2016). Regulation of starvation-induced hyperactivity by insulin and glucagon signaling in adult *Drosophila*. *Elife* 5, e15693.
- Zhang, T., Branch, A., and Shen, P. (2013). Octopamine-mediated circuit mechanism underlying controlled appetite for palatable food in *Drosophila*. *Proc. Natl. Acad. Sci. U. S. A.* 110, 15431–15436.
- Zheng, Z., Lauritzen, J.S., Perlman, E., Robinson, C.G., Nichols, M., Milkie, D., Torrens, O., Price, J., Fisher, C.B., Sharifi, N., et al. (2017). A Complete Electron Microscopy Volume Of The Brain Of Adult *Drosophila melanogaster*. *BioRxiv* 140905.
- Zhou, C., Rao, Y., and Rao, Y. (2008). A subset of octopaminergic neurons are important for *Drosophila* aggression. *Nat. Neurosci.* 11, 1059–1067.

8 APPENDIX

Fly Lines		
D.mel/Canton-S	Bloomington DSC	Flybase: FBst0064349
D.mel/Dop1R1 ^{attP}	Gift from Vanessa Ruta	N/A
D.mel/Dop1R2 ^{attP}	Keleman et al., 2012	FlyBase: FBal0283280
D.mel/GMR58E02-Gal4	Bloomington DSC	FlyBase: FBst0041347
D.mel/GMR64C08-Gal4	Bloomington DSC	FlyBase: FBst0039299
D.mel/GMR95A10-LexA	Bloomington DSC	FlyBase: FBst0061633
D.mel/Gr43a-Gal4	Miyamoto et al., 2012	Flybase: FBti0168340
D.mel/Gr5a-Gal4	Bloomington DSC	Flybase: FBst0057592
D.mel/LexAop2-mCD8-GFP	Bloomington DSC	FlyBase: FBst0056182
D.mel/LexAop-P2X2	Bloomington DSC	FlyBase: FBst0076030
D.mel/MB22B	Janelia RC	FlyBase: FBst0068298
D.mel/MB112C	Janelia RC	FlyBase: FBst0068263
D.mel/MB113C	Janelia RC	FlyBase: FBst0068264
D.mel/NPF RNAi (KK)	Vienna DRC	Flybase: FBst0025939
D.mel/NPF RNAi (TRiP)	Bloomington DSC	Flybase: FBst0479482
D.mel/NPF-Gal4	Bloomington DSC	Flybase: FBst0025681
D.mel/ORCO-Gal4	Bloomington DSC	Flybase: FBst0023292
D.mel/pBDP-Gal4U	Bloomington DSC	Flybase: FBst0068384
D.mel/sNPF-R- NAI	Vienna DRC	Flybase: FBst0471482
D.mel/Tdc2-Gal4	Bloomington DSC	FlyBase: FBst0009313
D.mel/TH-Gal4	Bloomington DSC	FlyBase: FBst0008848
D.mel/Tsh-Gal80	Clyne and Miesenbock, 2008	Flybase: FBti0114123
D.mel/Tβh ^{M18}	Bloomington DSC	FlyBase: FBal0061578
D.mel/UAS-CsChrimson	Bloomington DSC	FlyBase: FBst0055134
D.mel/UAS-DenMark	Bloomington DSC	FlyBase: FBst0033062
D.mel/UAS-dTrpA1	Bloomington DSC	FlyBase: FBst0026264
D.mel/UAS-GCaMP3	Bloomington DSC	Flybase: FBst0032116
D.mel/UAS-GCaMP6f	Bloomington DSC	FlyBase: FBst0042747
D.mel/UAS-mCD8-GFP	Bloomington DSC	FlyBase: FBst0030001
D.mel/UAS-Shibire ^{ts1}	Bloomington DSC	FlyBase: FBst0044222
D.mel/UAS-syt-GFP	Bloomington DSC	FlyBase: FBst0006926
D.mel/UAS-TNT	Bloomington DSC	Flybase: FBst0028997
D.mel/VUMa2-Gal4	Gift from Yoshinori Aso	N/A
D.mel/w ¹¹¹⁸	Bloomington DSC	Flybase: FBst0003605

Table 1 Fly Lines

Antibodies		
Anti-Mouse Alexa488	Molecular Probes	AB_221544
Anti-Mouse Alexa633	Molecular Probes	AB_141431
Anti-Rabbit Alexa568	Molecular Probes	AB_141416
Anti-Rabbit Alexa633	Molecular Probes	AB_2535731
Anti-Rat Alexa568	Molecular Probes	AB_141874
Mouse monoclonal anti-ChAT	Yasuyama et al., 1995	N/A
Mouse monoclonal anti-OA	Jena Bioscience	AB_2315000
Rabbit polyclonal anti-dsRed	Clontech	AB_10013483
Rabbit polyclonal anti-Tyr	Millipore	AB_11215460
Rat monoclonal anti-GFP [3H9]	Chromotek	AB_10773374
Rat monoclonal anti-Ncadherin	DSHB	AB_528121

Table 2 List of antibodies

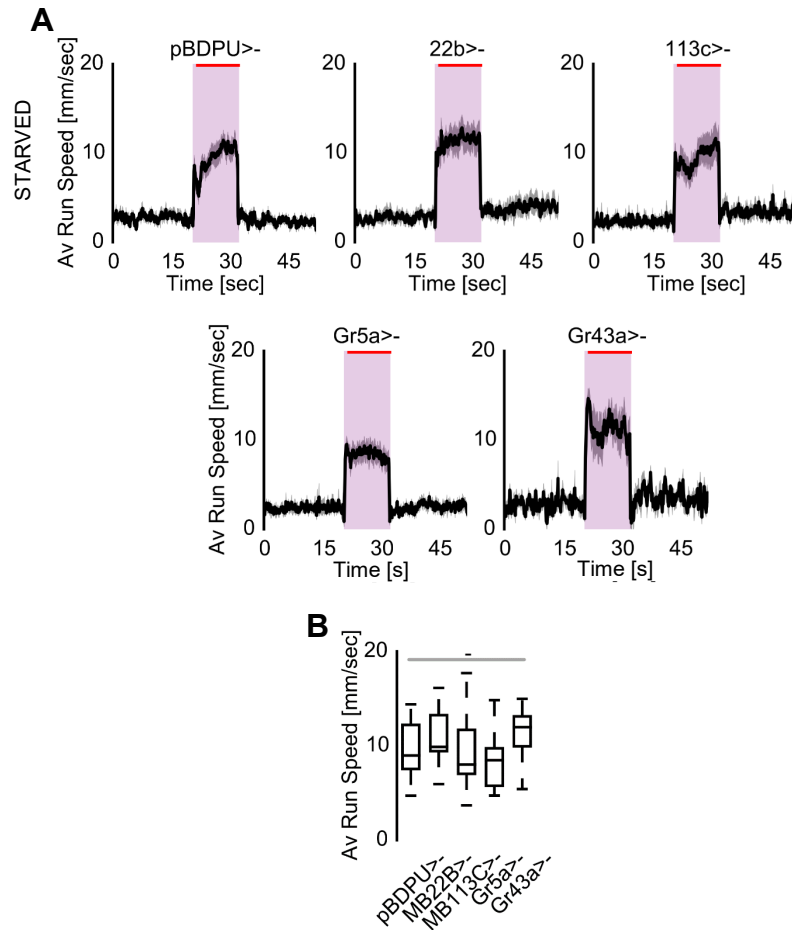


Figure 57 Common starved Gal4 controls used in the study

(A) Average running speeds of UAS (*pBDP-Gal4U>UAS-CsChr*) and Gal4 (*MB22b>-*, *MB113C>-*, *Gr5a>-*, *Gr43a>-*) controls during optogenetic treadmill paradigm under starvation (N=10/10/10/10/4). (B) Boxplot for average running speeds of UAS and Gal4 control lines during optogenetic activation.

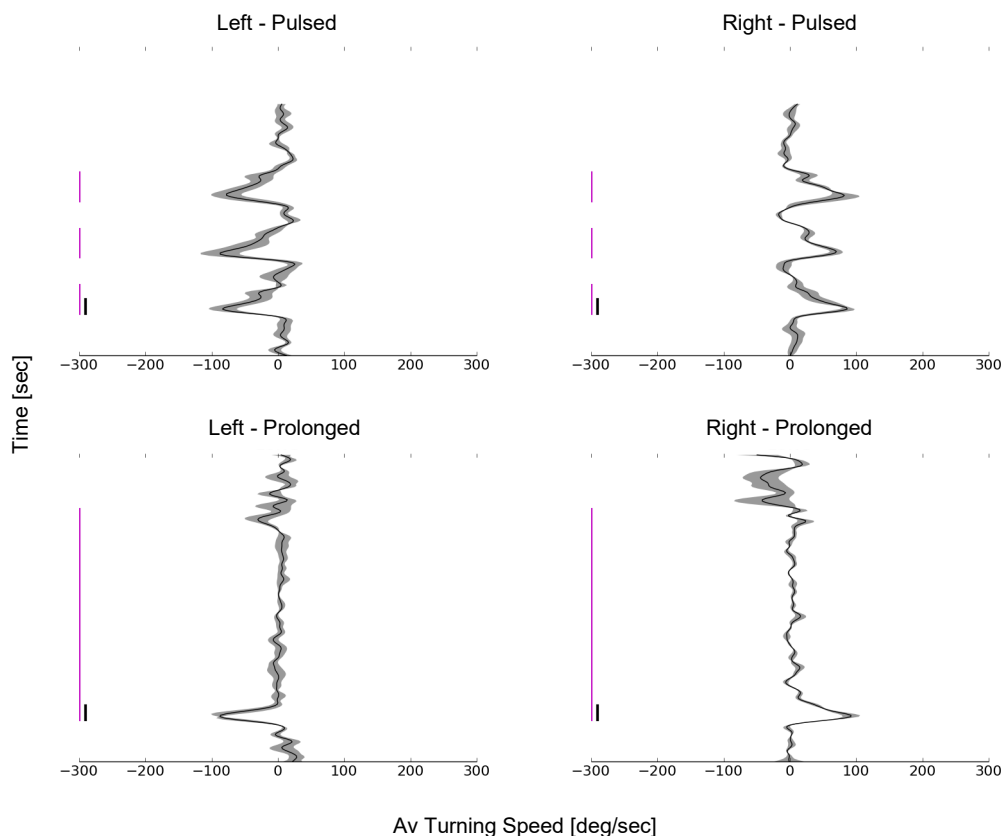


Figure 58 Unilateral odor presentation for wild-type flies

Laminar vinegar flow (20%, 100 ml/min) was directed to either left or right antennae. In each experiment, non-stimulus antennae received compensatory pressured air at the same volume. The odor presentation was repeated for 8 trials for one direction and then switched to the other antenna. No considerable difference was observed depending on which antenna was stimulated before. The odor duration was 2 seconds for pulsed (3 flies, 24 hours starved), and 15 seconds for prolonged exposure (3 flies, 24 hours starved). These flies did not exhibit persistence under prolonged stimuli.

CURRICULUM VITAE

EDUCATION

Marie Curie Initial Training Networks: FliACT ITN Fellow	2012 - 2015, Munich, DE
Ludwig-Maximilians-Universität München PhD Student, Biology	2014 - 2018, Munich, DE
Bogazici University MSc, Molecular Biology and Genetics	2009 - 2012, Istanbul, TR
Bogazici University BSc, Molecular Biology and Genetics	2005 - 2009, Istanbul, TR

RESEARCH EXPERIENCE

Max Planck Institute of Neurobiology	2012 - 2016, Munich, DE
TUM School of Life Sciences Weihenstephan	2017 - 2018, Freising, DE
Bogazici University	2009 - 2012, Istanbul, TR
Vlaams Instituut voor Biotechnologie	2008, Leuven, BE

PUBLICATIONS

A neural circuit arbitrates between perseverance and withdrawal in hungry *Drosophila*
Sercan Sayin, Jean-Francois De Backer, Laurence Lewis, K.P. Siju, Lisa-Marie Frisch, and Ilona C. Grunwald Kadow. *bioRxiv* 259119; *Cell*, in review

Internal State Dependent Odor Processing and Perception - The Role of Neuromodulation in the Fly Olfactory System
Frontiers in Cellular Neuroscience, 12, DOI=10.3389/fncel.2018.00011

CONFERENCES / MEETINGS

CSHL 2018: Neuronal Circuits	2018, New York, USA
Olfaction Symposium 2017: Neuronal Mechanisms of Odor-Guided Behavior	2017, Regensburg, DE
6 th Bernstein Sparks Workshop: Multi-modal Closed-loop Stimulation and Virtual Realities	2015, Tutzing, DE
Cell Symposia: Genes, Circuits and Behaviour	2013, Toronto, CA
7 th Forum of European Neuroscience	2010, Amsterdam, NL
21 th European Drosophila Research Conference	2009, Nice, FR
EMBO Young Investigators Meeting	2008, Istanbul, TR

Eidesstattliche Erklärung

Ich versichere hiermit an Eides statt, dass die vorgelegte Dissertation von mir selbständig und ohne unerlaubte Hilfe angefertigt ist.

Hiermit erkläre ich, dass die Dissertation nicht ganz oder in Wesentlichen Teilen einer anderen Prüfungskommission vorgelegt worden ist und dass ich mich anderweitig einer Doktorprüfung ohne Erfolg nicht unterzogen habe.

Sercan Sayin

München, den 14/01/2019